UNIVERSITY OF VENDA

SCHOOL OF ENVIRONMENTAL SCIENCES

DEPARTMENT OF MINING AND ENVIRONMENTAL GEOLOGY

GEOLOGY AND CHARACTERISATION OF COAL AT THE MUSHITHE COAL OCCURRENCE, SOUTPANSBERG COALFIELD, LIMPOPO PROVINCE, SOUTH AFRICA

BY

SEDZANI MUKATUNI

STUDENT NUMBER: 11617651

A MASTER'S DISSERTATION SUBMITTED TO THE DEPARTMENT OF MINING AND ENVIRONMENTAL GEOLOGY IN THE SCHOOL OF ENVIRONMENTAL SCIENCES, IN FULFILMENT OF THE REQUIREMENTS FOR THE DEGREE OF MASTER OF EARTH SCIENCES IN MINING AND ENVIRONMENTAL GEOLOGY

SIGNATURES

STUDENT: MR. S. MUKATUNI …….....

SUPERVISOR: PROF. J.S. OGOLA …….....

CO-SUPERVISOR: DR J.K. KIRUI ……..…….

MAY 2019

DECLARATION

I, Mukatuni Sedzani, declare that this dissertation is my own unaided work, except where otherwise acknowledged. It is being submitted for the degree of Master of Earth Sciences in Mining and Environmental Geology at the University of Venda, and it has not been submitted for any degree in any other University.

Signature	Date
…….	…….
Supervisor Signature	Date
…….	…….
Co-Supervisor Signature	Date
…….	…….

DEDICATION

This dissertation is dedicated to my parents, Mrs T.J. Maise and Mr T.D. Mukatuni as well as my siblings Lucky, Tshanduko and Rilwele for their unwavering support and inspiration. I also dedicate this work to my nephews Wandeme Mukatuni and Tshilidzi Tshisa.

ACKNOWLEDGEMENT

Firstly, I would like to thank my supervisor Prof. J.S. Ogola and co-supervisor Dr. J.K. Kirui for their support, patience and meticulous supervision. Without their suggestions and comments the accomplishment of this research would have been unmanageable.

I would like to thank the National Research Foundation (NRF) for funding this project.

I am grateful to the almighty God for sheltering me and bestowing in me the skills and understanding to pursue studies in geology up to this level.

I would also like to render my deep appreciation to the following people; P.G. Munyai, V.L. Netshimbupfe, K.L. Nephawe, E. Nemutanzhela, H.N. Phuvhe H. Masiagwala, K. Mukatuni, R.B. Mamphweli and P. Mudzanani for being supportive throughout the completion of this dissertation and offering suggestions that perpetuated success. In addition, I would like to thank Ravele Solly for his selfless camaraderie and assistance with fieldwork during the course of the dissertation.

Special thanks to my associates on the Mushithe Project: Mphanama Thangeni and Sidogi Ramaano for their assistance during fieldwork and at the laboratory as well as their support, encouragement and suggestions. Moreover, I would like to express gratitude to the Chief of Mushithe Village for allowing me to conduct this study on his land and equally providing aides to escort us to the field.

Last but not least, I would like to thank following staff members of the Department of Mining and Environmental Geology: Ms. Mundalamo, Mr. Muzerengi, Mr. Nengovhela and Mr. Nemapate for their support and encouragement throughout the study.

ABSTRACT

The Mushithe coal occurrence is situated approximately 16 km west of the Tshikondeni coal mine in the Tshipise-Pafuri sub-basin of the Soutpansberg coalfield in South Africa. The Soutpansberg Coalfield has received comparatively less attention compared to other more notable South African coalfields. There is as a consequence very limited information in the public domain applicable to the geology as well as quality of coal in this coalfield, as a result there is no known study focused exclusively on the Mushithe coal occurrence.

The aim of the study was to conduct detailed geological mapping of the Mushithe Deposit so as to ascertain the geological environment and petrological characteristics of rocks within the area. Further work involved coal sampling and analysis in order to establish coal quality and its physical and chemical characteristics.

Samples were collected using geological field mapping and channel sampling. Nine coal samples were collected from the coalbed and host rock, exposed along the Mbodi River, during geological field mapping using channel sampling. Furthermore, 92 rock samples were collected during geological field mapping of which 10 representative samples were selected for further analysis. X-ray fluorescence spectrometry was conducted on all selected samples. Proximate analysis and ultimate analyses, and calorimetry tests were undertaken on coal samples. Three samples were selected based on calorific value for maceral identification, mineral analyses and vitrinite reflectance using petrographic study.

Detailed geological mapping of the area around the Mushithe coal occurrence showed the geological setting of coal in this area. The following lithologies were identified in the study area: sandstone, mudstone, ironstone, calcrete, shale, quartzite, quartz vein with a general strike direction to the north-east. The host rocks including coal were intruded by dolerite dykes and this resulted in the devolatilization of coal.

The current study concluded that the Mushithe coal was formed in a wet swampy environment. This has been confirmed based on tissue preservation index (1.69) and

gelification index (2.35). Coal rank ranged from bituminous Rank C- B according to United Nations Economic Commission for Europe Coal Classification (UNECE) and samples were characterised by high ash (27.90%), high moisture (10.47%) and low sulphur (0.24%). Furthermore, coal was graded below grade D based on classification for use by ESKOM which consider any calorific value below 24.5 MJ/kg to be in this category. The coal is vitrinite rich (77.75 vol%) and low in Inertinite (22.25 vol%) and devoid of Liptinite and pseudovitrinite, thus it is of good coking quality. Geochemical analysis revealed that the coal was enriched in TiO_2 and Fe_2O_3 which was corroborated by the mineral matter which was mostly clay and pyrite. Comparatively, coal quality analysis revealed the calorific value of 14.26 MJ/kg and vitrinite reflectance between 0.94 %ROV to 1 %ROV which was less than that of the Tshikondeni Deposit but greater than that at Waterberg coalfield.

The study recommends further detailed exploration of coal in the area, applying such techniques such as geophysical exploration and borehole drilling leading to resource evaluation. Further studies are recommended to provide a better interpretation of the depositional environment of coal at Mushithe as well as the effect of devolatilaziton by a dolerite dyke.

Keywords: *Soutpansberg Coalfield, Mushithe coal occurrence, Bituminous coal, wet swampy environment, Devolatilization.*

TABLE OF CONTENT

DECLARATION i

DEDICATION ii

ACKNOWLEDGEMENT iii

ABSTRACT iv

TABLE OF CONTENT vi

LIST OF FIGURES x

LIST OF PLATES xiv

LIST OF TABLES xv

LIST OF ABBREVIATIONS AND ACRONYMS xvi

CHAPTER 1: INTRODUCTION 1

1.1 Background 1

1.2 Study area 2

1.2.1 Location 2

1.2.2 Climate 3

1.2.3 Topography and drainage 3

1.2.4 Soil and Vegetation 3

1.3 Problem statement 3

1.4 Justification 4

1.5 Research questions 4

1.6 Objectives 4

CHAPTER 2: LITERATURE REVIEW 6

2.1 Regional geology 6

2.1.1 Karoo Basin 6

2.1.2 Soutpansberg Group 8
2.1.3 Limpopo Mobile Belt 11
2.2 General overview of prominent South African Coalfields 14
2.2.1 Witbank Coalfield 15
2.2.2 Waterberg Coalfield 16
2.2.3 Highveld Coalfield 17
2.2.4 Soutpansberg coalfield 17
2.3 Coal formation and occurrence 19
2.4 Constituents of coal 22
2.4.1 Coal mineralogy 22
2.4.2 Major and trace elements of coal 23
2.4.3 Maceral composition 23
2.5 Physical properties of coal 25
CHAPTER 3: MATERIALS AND METHODS 28
3.1 Preliminary work 29
3.1.1 Desktop study 29
3.1.2 Reconnaissance survey 29
3.2 Fieldwork 29
3.2.1 Geological field mapping of Mushithe area 30
3.2.2 Coal sampling 31
3.3 Laboratory work 32
3.3.1 Sample preparation 33

3.3.2 Sample analysis 36
3.3.3 Petrographic study 36
3.3.4 Coal analysis 37
3.3.5 Whole rock geochemistry 39
CHAPTER 4: RESULTS AND DISCUSSION 41
4.1 Coal characterisation 41
4.1.1 Profile description 41
4.1.2 Proximate and ultimate analysis 43
4.1.3 Calorific value 49
4.1.4 Petrographic description of coal 52
4.1.5 Geochemical composition analysis of coal 60
4.1.6 Coal classification 65
4.1.7 Depositional environment of coal 66
4.2 Geological map 68
4.3 Description of rocks 71
4.4 Mineralogical analysis of rocks 86
4.5 Textural and grain size analysis 87
4.6 Whole rock geochemical analysis 89
4.6.1 Major oxides analysis 89
4.6.2 Trace element analysis 92
CHAPTER 5: CONCLUSIONS AND RECOMMENDATIONS 100
5.1 Conclusions 100

5.2 Recommendations 102

REFERENCES 103

APPENDICES

LIST OF FIGURES

Figure 1.1: Locality map of the study area. 2

Figure 2.1: Stratigraphic correlation of the Main Karoo Basin and the Northern sub-basins 7

Figure 2.2: Illustrative map showing the distribution of geological formations within the Soutpansberg Group 9

Figure 2.3: Simplified geological map of the Limpopo Mobile Belt 13

Figure 2.4 Coalfields of South Africa 15

Figure 2.5: Map illustrating metallurgical coal trends of the Soutpansberg coalfield. 19

Figure 3.1: Flowchart illustrating methods and procedures applied in the study. 28

Figure 3.2: Map indicating the traverses that were mapped in the study area 31

Figure 3.3: Coalbed image showing three profiles (A-C) delineated for channel sampling. 32

Figure 3.4: Thin section preparation equipment;A) Diamond saw; B) Bonding jig; C) Streuers Accutum-50 cutting machine; and D) Streuers RotoPol-35 polishing machines. 34

Figure 3.5: Laboratory equipment: A) Vacutec drying oven; and B) Restsch RS 200 milling machine used to prepare coal samples. 36

Figure 4.1: Stratigraphic section representing Mushithe coal seams. 42

Table 4.1: Results of proximate analysis (Wt. %) 44

Figure 4.2: Interpretation of proximate analysis for all samples. 45

Table 4.2: Results of ultimate coal analysis (Wt. %) 48

Figure 4.3: Interpretation of ultimate analysis for all coal samples. 49

Table 4.3: Calorific value of the coal samples (MJ/Kg) 50

Figure 4.4: Comparison of calorific value of Mushithe coal with the Waterberg Coalfield and the Tshikondeni Deposit. 51

Figure 4.5: Maceral types in Mushithe coal. 53

Figure 4.6: Mineral matter free maceral group. 54

Figure 4.7: Micrographs of Coal 1B showing Vitrinite, Inertinite macerals and altered minerals, taken at a magnification of x500, under reflected light using an oil immersion lens. 55

Figure 4.8: Micrographs of Coal 2A showing Vitrinite, Inertinite macerals and alteration minerals, taken at a magnification of x500, under reflected light using an oil immersion lens. 56

Figure 4.9: Micrographs of Coal 3C showing Vitrinite, Inertinite macerals and alteration minerals, taken at a magnification of x500, under reflected light using an oil immersion lens. 57

Figure 4.10: Interpretation of mineral matter in coal. 58

Figure 4.11: Histogram representing vitrinite reflectance data. 59

Figure 4.12: Major element oxides present in coal samples. 61

Figure 4.13: Major oxide enrichment of Mushithe coal relative to UCC. 61

Figure 4.14: Trace element concentration in coal (ppm). 62

Figure 4.15: Enrichment factor of trace elements in coal (ppm) relative to UCC. 63

Figure 4.16: TGI – GI model by Diessel (1986) showing Coal 2A. 67

Figure 4.17: Geological map of Mushithe area. 69

Figure 4.18: Cross section of the geological map of Mushithe area. 70

Figure 4.19: Photomicrograph of red mudstone in thin section showing quartz grains with fine texture. 72

Figure 4.20: Photomicrograph of quartzite in thin section showing with tiny grains and quartz veinlet. 74

Figure 4.21: Photomicrograph of calcrete in thin section carbonates with fine grained calcite. 76

Figure 4.22: Photomicrograph of arkosic sandstone in thin section showing arenaceous texture..... 78

Figure 4.23: Photomicrograph of Shale in thin section showing abundance of biotite. 79

Figure 4.24: Photomicrograph of ironstone in thin section showing iron oxide with quartz grains. 80

Figure 4.25: Photomicrograph of grey mudstone in thin section with fine grain texture. 82

Figure 4.26: Photomicrograph of quartz vein in thin section with skeletal quartz grains. 83

Figure 4.27: Photomicrograph of quartz arenite in thin section showing quartz, plagioclase and biotite..... 84

Figure 4.28: Photomicrograph of dolerite in thin section showing mafic minerals. ... 86

Figure 4.29: Major oxides in rock samples. 90

Figure 4.30: Major oxides enrichment relative to UCC in host rock samples. 90

Figure 4.31: Bar graph showing concentrations of Large-ion Lithophile Elements (ppm)..... 94

Figure 4.32: Bar graph showing concentrations of High Field Strength Elements (ppm)..... 96

Figure 4.33: Bar graph showing concentrations of Transition Trace Elements in (ppm)..... 97

Figure 4.34: Bar graph showing concentrations of Rare Earth Elements (ppm)..... 99

LIST OF PLATES

Plate 4.1: Red mudstone specimen showing clay sized grains and clay minerals. .. 71

Plate 4.2: quartzite specimen showing interlocked grains and quartz veinlet. 73

Plate 4.3: Calcrete specimen containing carbonate minerals with very fine texture. 74

Plate 4.4: Arkosic sandstone specimen with sand sized grains and biotite flakes.... 76

Plate 4.5: Shale specimen showing very fine texture. 77

Plate 4.6: Ironstone specimen showing iron oxide. 79

Plate 4.7: Grey mudstone specimen showing clay sized grains. 80

Plate 4.8 Quartz vein specimen with inclusion of biotite. 81

Plate 4.9: Quartz arenite specimen showing fine sand sized grains. 83

Plate 4.10: Dolerite specimen showing mafic minerals. 84

LIST OF TABLES

Table 4.1: Results of proximate analysis 42

Table 4.2: Results of ultimate coal analysis 46

Table 4.3: Calorific value of the coal samples 48

Table 4.4: Maceral group summary in coal 52

Table 4.5: Depositional environment indices of Mushithe coal 64

Table 4.6: Mineralogical analysis of rocks mapped around Mushithe Coal occurrence 85

Table 4.7: Textural and grain analysis of rocks mapped around Mushithe Coal occurrence 86

LIST OF ABBREVIATIONS AND ACRONYMS

Al	Aluminium
Al_2O_3	Aluminium oxide
As	Arsenic
ASTM	American Society for Testing Materials
Ca	Calcium
CGS	Council of Geosciences
Co	Cobalt
CoAL	Coal of Africa Limited
Cd	Cadmium
Cr	Chromium
CZ	Central Zone
Fe	Iron
Fe_2O_3	Iron oxide
GI	Gelification Index
GPS	Global Positioning System
Ga	Billion years
Hf	Hafnium
HFSE	High Field Strength Elements
ICCP	International Committee for Coal and Organic Petrology
ISO	International Organisation of Standardisation

K	Potassium
K_2O	Potassium oxide
La	Lanthanum
LILE	Large Ion Lithophile Elements
LMB	Limpopo Mobile Belt
Mg	Magnesium
MKB	Main Karoo Basin
Mmf	Mineral matter free
Mn	Manganese
Na	Sodium
NaCl	Sodium Chloride
Nb	Niobium
Ni	Nickel
NMZ	Northern Marginal Zone
P_2O_5	Potassium oxide
Ro	Vitrinite reflectance
RoV	Vitrinite reflectance measurement
SABS	South African Bureau of Standards
SACS	South African Committee of Stratigraphy
Sc	Scandium
Si	Silica

SiO_2	Silica dioxide
SMZ	Southern Marginal Zone
Th	Thorium
Ti	Titanium
TPI	Tissue Preservation Index
TTE	Transition Trace Elements
U	Uranium
UCC	Upper Continental Crust
V	Vanadium
XRF	X-Ray Fluorescence
Y	Yttrium
Zr	Zirconium

CHAPTER 1: INTRODUCTION

1.1 Background

According to World Coal Association (2015), in 2014 South Africa was the 7th largest coal producer; more than 90% of South African electric power generation was from coal. The use of coal as an energy source is on the rise regardless of concerns associated with the impact of its utilization; ESKOM supplied 95% of the electricity used in South Africa and 45% on the African continent (ESKOM, 2018). South African coal is contained within the rocks of the Karoo Supergroup and it is distributed across five provinces, namely; Limpopo, Mpumalanga, Kwazulu-Natal, Eastern Cape, Free State and Gauteng Province (Van der Walt, 2012).

The Soutpansberg coalfield has been described as the “forgotten basin” because it is mostly underdeveloped (Sparrow, 2012). It is known to have relatively less coal when compared to other important South African coalfields. Limited information is available and this is attributed to inadequate exploration data accessible especially within the public domain (Hancox and Gotz, 2014). Dwindling economic coal resources in South Africa’s important coalfields is shifting attention towards the less important coalfields such as the Soutpansberg coalfield.

Hancox and Gotz (2014) attributed the limited exploration to access limitations when compared to other coalfields South African coalfields: Witbank, Highveld and Waterberg coalfields. Accordingly, there is limited information about the Soutpansberg coalfield in the public domain. As a result of impending development of the coalfield due to depleting reserves in the prominent coalfields, it is imperative to study the Soutpansberg coalfield in detail.

The most detailed and available published work done in the Soutpansberg Coalfield is based on limited borehole and outcrop data. Furthermore, most of it was done in the Pafuri sub-basin, thus it may not be wholly representative of the Soutpansberg Coal Basin (McCourt and Brandl, 1980; De Jager, 1986; Sullivan, 1995). Other notable works were done by Thabo and Sullivan (2000) as well as Bordy (2006), however they indicate the same discrepancy and limitations in data about the Soutpansberg coalfield. Limited attention has, conversely, been paid to the geology

and characterisation of coal in the Mushithe coal occurrence since the work done is a generalisation based on the areas preferred by ISCOR, Coal of Africa Limited and Rio Tinto. Furthermore geological mapping covering the area was done at a very small scale of 1:1 000 000 (Hancox and Gotz, 2014; Venmyn Deloitte, 2016).

The study therefore focused on detailed geological mapping of the Mushithe area, covering the coal occurrence so as to ascertain the geological environment of coal formation. Further work involved coal sampling and analysis in order to establish coal quality and its physical and chemical characteristics.

1.2 Study area

1.2.1 Location

The study area is located within the Soutpansberg coalfield at Mushithe Village, Limpopo Province, South Africa. It is situated approximately 90 km north east of Thohoyandou town and approximately 153 km south-east of Musina and 16 km to the west of Tshikondeni Mine (Fig. 1.1). The area lies at latitude 22° 31’ 4” S and longitude 30° 47’ 48” E.

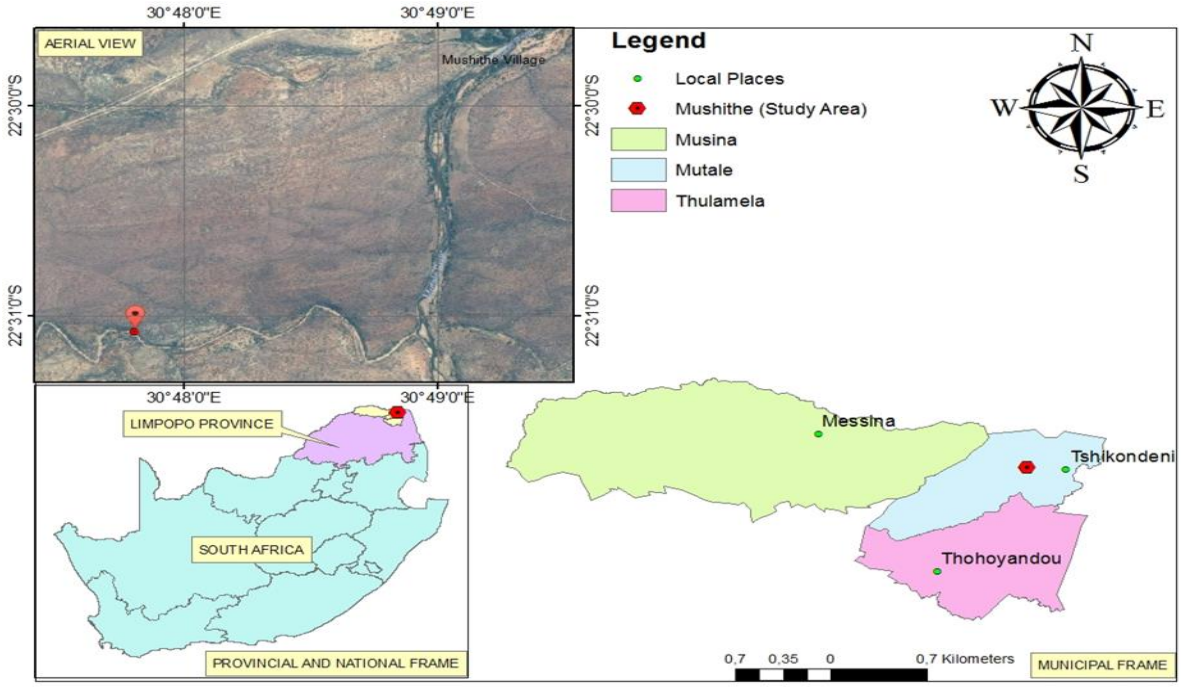

Figure 1.1: Locality map of the study area (ArcGIS, 2018).

1.2.2 Climate

The area is characterized by a warm-wet and a cool-dry season. The warm-wet season occurs between October and March, whilst the cool-dry season is between May and August. April and September are transition months. The area receives most rainfall during the month of January and the least rainfall in August. Rainfall ranges from 300 mm to 500 mm per year. Temperature ranges between 20°C and 30°C in summer from November to February, whereas winter is from May to August with temperature range between 7°C and 28°C (Kabanda, 2004).

1.2.3 Topography and drainage

Topography of the study area is controlled by the underlying geology. Alternating low hills occur in the study area which is characterised by open hills that geographically strike from east–west across the surface. The slope has an inclination of 1:20 in the direction of the mountains to the south, steepening to 1:3 up the mountains.

The area is experiences surface run-off which continues for a short period after rainfall and feeds the Mbodi River. The Mbodi River feeds the perennial Mutale River that feeds the Luvuvhu River, a tributary of the Limpopo River.

1.2.4 Soil and Vegetation

The study area is generally characterised by sandy loam soils as well as shallow or rocky soils that are regarded as wilderness and grazing land. The area is composed of low to medium potential arable land.

The vegetation of the study area is categorised as Tropical Bush and Savannah, with Musina Mopane Bushveld and Soutpansberg Mountain Bushveld as the primary vegetation types. The representative vegetation is dominated by medium to high shrub savannah, with dispersed trees.

1.3 Problem statement

Studies pertaining to the Soutpansberg Coalfield are limited, however, the few studies available in the public domain are generalised and covers the entire coalfield. The only area that had been studied in detail within the Soutpansberg Coalfield is the

Tshikondeni area that hosted coal of economic value. Furthermore, geological maps representing the area had been of small-scale on 1:1 000 000. Areas such as the Mushithe coal occurrence have been overlooked and as a consequence their potential has neither been evaluated nor documented. As a result, no detailed study has been undertaken at the Mushithe coal area to determine its geological setting and nature of coal in the area.

1.4 Justification

Studying the geology of the area will assist in understanding the geological setting, nature and mode of occurrence of the prospect. Furthermore, characterisation of coal will be useful in understanding intrinsic characteristics of coal and coal quality; this can be used in making decisions on whether to undertake detailed exploration in the area.

Hancox and Gotz (2014) indicated that the Soutpansberg coalfield has received limited attention from researchers as a consequence; the physical and chemical characteristics of coal in the area have not been comprehensively studied. This study will serve as a guide to further exploration of the Soutpansberg coalfield.

The proposed study will also contribute knowledge on the geology of the Mushithe coal occurrence and will, thus complement future studies on coal quality and coal mine design in the area.

1.5 Research questions

- What is the nature and character of rocks hosting coal?
- What is the mode of occurrence of the coal and the depositional environment of the coal?
- What is the quality of the coal?

1.6 Objectives

The main objective of the study was to conduct detailed geological mapping of the Mushithe area so as to ascertain the geological environment and petrological characteristics of rocks and coal in the area. Further work involved coal sampling

and analysis in order to establish coal quality and its physical and chemical characteristics.

Specific objectives were to:

- Conduct geological detailed field mapping within the study area;
- Conduct petrographic study, to identify rocks associated with coal and to appraise maceral composition and degree of metamorphism of coal in the area.
- Determine the elemental composition of coal by means of X-ray fluorescence spectrometry;
- Conduct whole rock geochemistry of rocks using X-ray fluorescence spectrometry; and
- Determine the quality of coal using proximate analysis, ultimate analysis, and calorific value analysis;

CHAPTER 2: LITERATURE REVIEW

2.1 Regional geology

This section focuses on the regional setting of the study area, looking at the following: Karoo basin, Soutpansberg Group and Limpopo Mobile Belt.

2.1.1 Karoo Basin

The sedimentary fill of all other basins of the same age contained by the Gondwana subcontinent is referred to as the Karoo; the term ‘‘Karoo’’ was inferred from the Main Karoo Basin of South Africa (Fig. 2.1). Two main allogenic controls, which are tectonism and climate, influenced the sedimentary fill of the Karoo basins. (Catuneanu et *al.,* 2005). The Karoo has the most widespread coal resources as well as the most comprehensive sequence of sedimentary strata (Mphaphuli, 2017). Karoo aged basins were formed during first order cycle of supercontinent consolidation and disintegration. Development of the various basin types in Africa was due to two tectonic systems (Catuneanu *et al*., 2005). Roughly one-third of South Africa is covered by the Late Carboniferous to Middle Jurassic Karoo Basin (Hancox and Gotz, 2014).

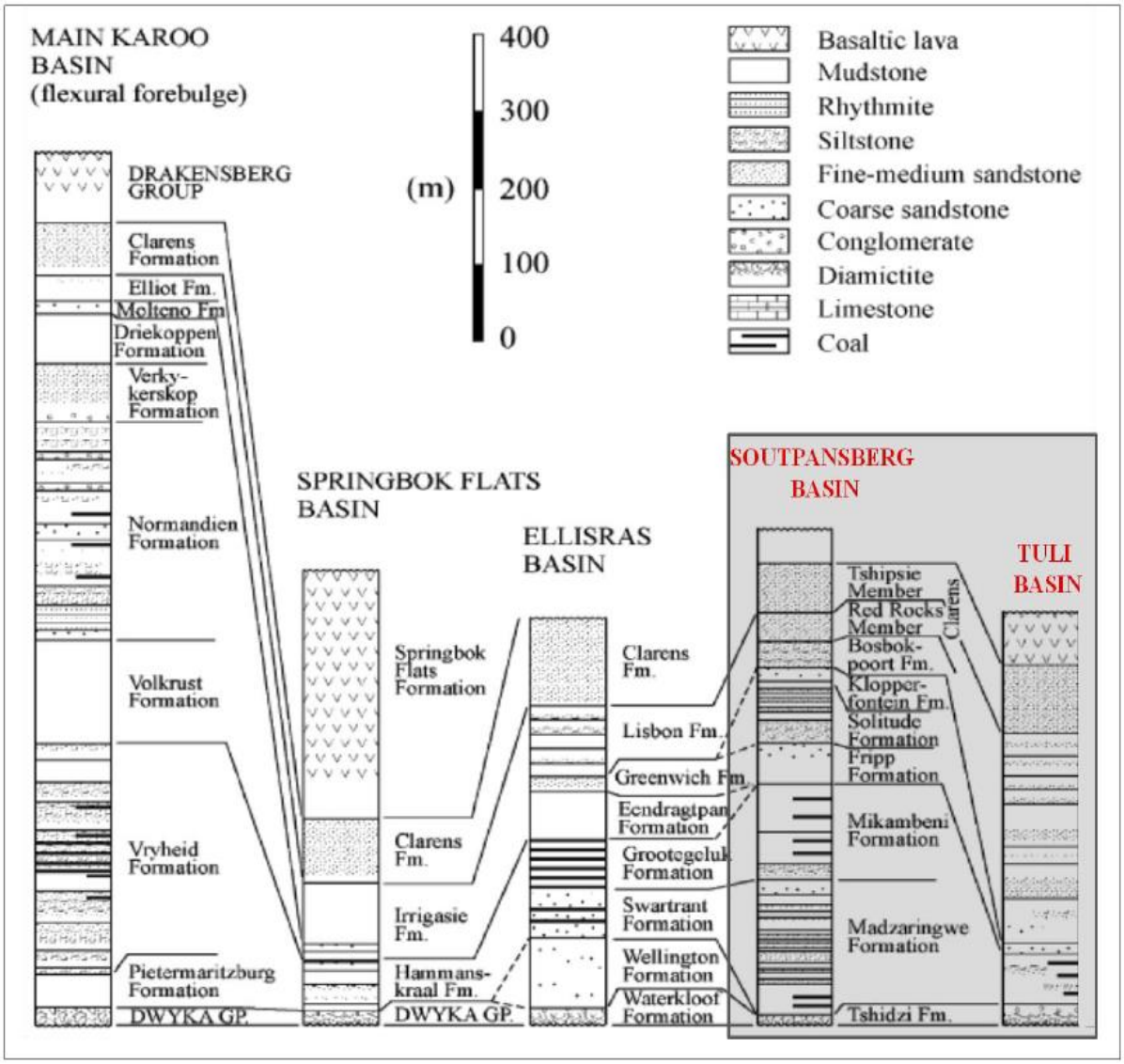

Figure 2.1: Stratigraphic correlation of the Main Karoo Basin and the Northern sub-basins (Malaza, 2013).

The Main Karoo Basin was established by means of the following: subduction, compression, collision and terrane accretion (Hancox and Gotz, 2014). The lithostratigraphic rank of first-order Karoo depositional sequence is Supergroup (Catuneanu *et al*., 2005). The following groups make up the Karoo supergroup: Dwyka, Ecca, Beaufort, Stormberg. In South Africa the Karoo Basins comprise of 19 coalfields (Hancox and Gotz, 2014).

The Soutpansberg Coalfield, which is applicable to this study, is located in the north of the Main Karoo Basin. The dip of the Karoo strata in the Soutpansberg Basin is

usually to the north and fluctuates between 50 and 150 degrees (Brandl, 1986). The full stratigraphy of the Karoo Supergroup is preserved in the Soutpansberg group (Catuneanu et *al.,* 2005). The Tshidzi Formation, is located at the base of the Karoo succession, and is comparable to the Dwyka Group in the Karoo succession. The Tshidzi Formation is overlain by the Madzaringwe Formation, which forms the basal part of the Ecca Group in the coalfield. Mikambeni Formation lies on top of fhe Madzaringwe Formation. McCourt and Brandl (1986) equate the Fripp Formation, which overlies the Mikambeni Formation to the lowermost Beaufort Group.

2.1.2 Soutpansberg Group

The study area falls within the Soutpansberg Group. The Soutpansberg is characterized by mountainous and wedge-shaped terrain that extends from Kruger National Park in the east to Blouberg in the west a distance of 40 km wide (Brandl, 1999).

Formation of the Soutpansberg depositional basin occurred about 1800 million years ago (Brandl, 1999). According to Brandl (2002) this is a volcano-sedimentary sequence. The basin was formed along the Palala shear belt as an east-west trending asymmetrical rift or half-graben. Deposition started with the basalt lavas, which were then followed by sedimentary rocks (syn-rift sequence). A period of erosion occurred subsequently followed by the deposition of pink massive quartzite (Post-rift sequence). The post-rift sequence covered a much larger area than the original rift (Brandl, 1986).

About 150 million years ago, when sedimentation had come to an end, the area became block-faulted and then uniformly tilted to the north. Erosion has been responsible for the landscape as we know it today and this occurred approximately 60 million years ago (Brandl, 1999). The Soutpansberg Group is characterized by a volcano-sedimentary succession which is separated into 7 different formations namely, Tshifhefhe, Sibasa, Fundudzi, Wyllie's Poort, Nzhelele, Stayt, and Mabiligwe (Brandl, 1999).

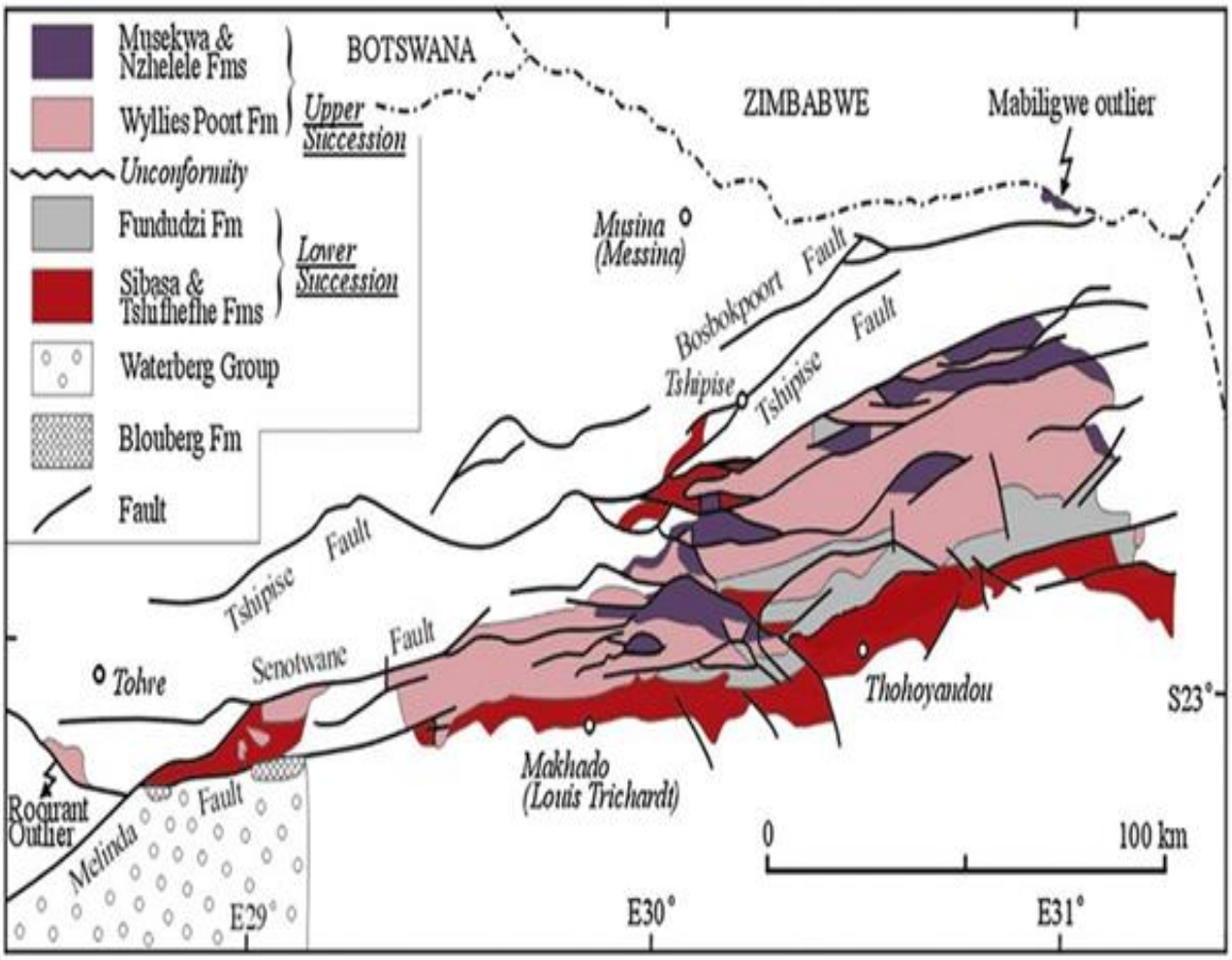

Figure 2.2: Illustrative map showing the distribution of geological formations within the Soutpansberg Group (Geng et al., 2014).

Tshifhefhe Formation

The Tshifhefhe Formation forms the base of the Soutpansberg Group. The formation is only a few meters thick and can be up to 10 m thick in localised areas (Geng *et al.,* 2014). Strongly epidotised and chloritised clastic sediments which include conglomerate, shale, and greywacke made up the composition of the formation (Brandl, 2002). The rocks overlying the Tshifhefhe Formation are strongly believed to have extruded in an almost featureless terrain due to the unit's almost uniform thickness seen across the whole of Soutpansberg (Geng *et al.*, 2014).

Sibasa Basalt Formation

The Sibasa formation succession overlies the Tshifhefhe formation and is composed dominantly of volcanic rocks with minor clastic sediments. The succession is approximately 3 700 m thick in the eastern part of the Soutpansberg and about 100 m thick in the west (Geng *et al.,* 2014). The massive amygdaloidal basalts present in the Sibasa Formation are generally epidotised (Brandl, 2002). Shale, sandstone and infrequent conglomerate are clastic sediments interbedded within the formation and often form persistent marker beds which are up to 50 m in thickness (Geng *et al*., 2014).

Fundudzi Formation

The Fundudzi Formation is a predominantly siliciclastic unit which only developed on the eastern half of the Soutpansberg Group (Brandl,1999). The unit is approximately 1 900 m thick, mainly consisting of argillaceous and arenaceous sediments with a few thin pyroclastic layers (Brandl, 2002). The formation is understood to have formed as a result of fluviatile deposition in a braided, alluvial environment due to the presence of immature sandstone, shale and siltstone indicative of a mixed load deposits (Geng *et al*., 2014).

Wyllie's Poort Formation

Wyllie's Poort Formation is a 1 000 m thick unit which forms the base of the Soutpansberg Group's upper succession where its lower contact is a prominent regional unconformity. The entire unit covers the whole of Soutpansberg depositional basin, and it is made up almost entirely of arenaceous succession with rare volcanic rocks and local interbeds of argillaceous sediments (Geng *et al.,* 2014). The formation is made up of red-pink quartzite with few pebble washes. Due to their high textural and mineralogical maturity, the depositional environment of the quartzites is believed to have formed in a deltaic to shallow marine environment (Geng *et al.,* 2014; Brandl, 1999).

Nzhelele Formation

The Nzhelele Formation is the uppermost unit of the Soutpansberg Group. It comprises of approximately 400 m thick layer of basalt at the base and uppermost argillaceous and arenaceous sedimentary rocks (Brandl, 1999). The unit has a maximum of 2300 m of preserved thickness. Dark red argillaceous sandstones make up the composition of the sediments (Geng *et al.,* 2014). Volcanic rocks comprise of basaltic lava and several thin layers of pyroclastic rocks layers is copper-bearing (Brandl, 2002).

Stayt Formation and Mabiligwe Formation

The Stayt and Mabiligwe Formations outcrop north of the Main Soutpansberg outcrop. These formations have maximum thicknesses of approximately 1 800 m and 50 m respectively. The Stayt Formation comprises basalt at the base, overlain by argillaceous sediments containing thin layers of interbedded pyroclastic. The Mabiligwe Formation is entirely a clastic succession restricted to a small area along Limpopo River (Barker, 1999). The strongly fractured portions of the Stayt Formation are known for copper mineralization (Brandl, 2002).

2.1.3 Limpopo Mobile Belt

The Limpopo Mobile Belt (LMB) is underlain by high-grade Precambrian metamorphic rocks. In addition, the underlying rock is characterised by intense polyphase deformation. The LMB is defined as a linear east –northeast trending zone (Watkeys, 1984).

The Southern Marginal Zone (SMZ), Central Zone (CZ) and Northern Marginal Zone (NMZ) are the three zones that divide the LMB (Fig. 2.3) on the basis of lithology and structure (Horrocks, 1981). Basement gneisses, porphyritic gneisses, granitoid gneisses, gabbroic and anorthositic gneisses, as well as supracrustal paragneisses are the main rock types that constitute the LMB (Horrocks, 1981).

Northern Marginal Zone

The Northern Marginal Zone is a long, narrow zone which is approximately 550 km in length and occurs entirely in Botswana and Zimbabwe. Rocks of the Northern Marginal Zone comprise high-grade metamorphic equivalents of the nearby Archean granite-greenstones of the Zimbabwe Craton (Gore *et al*., 2009). The Northern Marginal Zone is separated from the Zimbabwe Craton by a southward-dipping ductile North Limpopo Thrust Zone (Rigby *et al*., 2011).

Central Zone

The Central Zone is situated between the two marginal zones. The Central Zone has been divided into three metamorphic complexes, namely: the Phikwe Complex, Beit Bridge Complex and the Mahalapye Complex (Watkeys, 1984). The Central Zone is separated from the Northern Marginal Zone and Southern Marginal Zone by the Palala-Sunnyside and Magagohate-Triangle shear zones respectively (Rigby *et al.,* 2011). Sand River Gneiss formed about 3283 Ma is the oldest unit in the Central Zone and it consist of grey migmatitic quartz-diorite gneiss (Watkeys, 1984).

Southern Marginal Zone

The Southern Marginal Zone lies within South Africa and encompasses the high-grade metamorphic equivalents of the nearby Archaean granite-greenstones of the Kaapvaal Craton (Gore *et al.*, 2009). Rocks of the Southern Marginal Zone are divided into two categories, Baviaanskloof Gneiss and Bandelierkop Formation. The Southern Marginal Zone comprise granulite-facies granitoid-greenstone material of the Kaapvaal Craton (Watkeys, 1984). The northwards-dipping Hout River Shear Zone separates the Southern Marginal Zone from the Kaapvaal Craton (Rigby *et al.,* 2011).

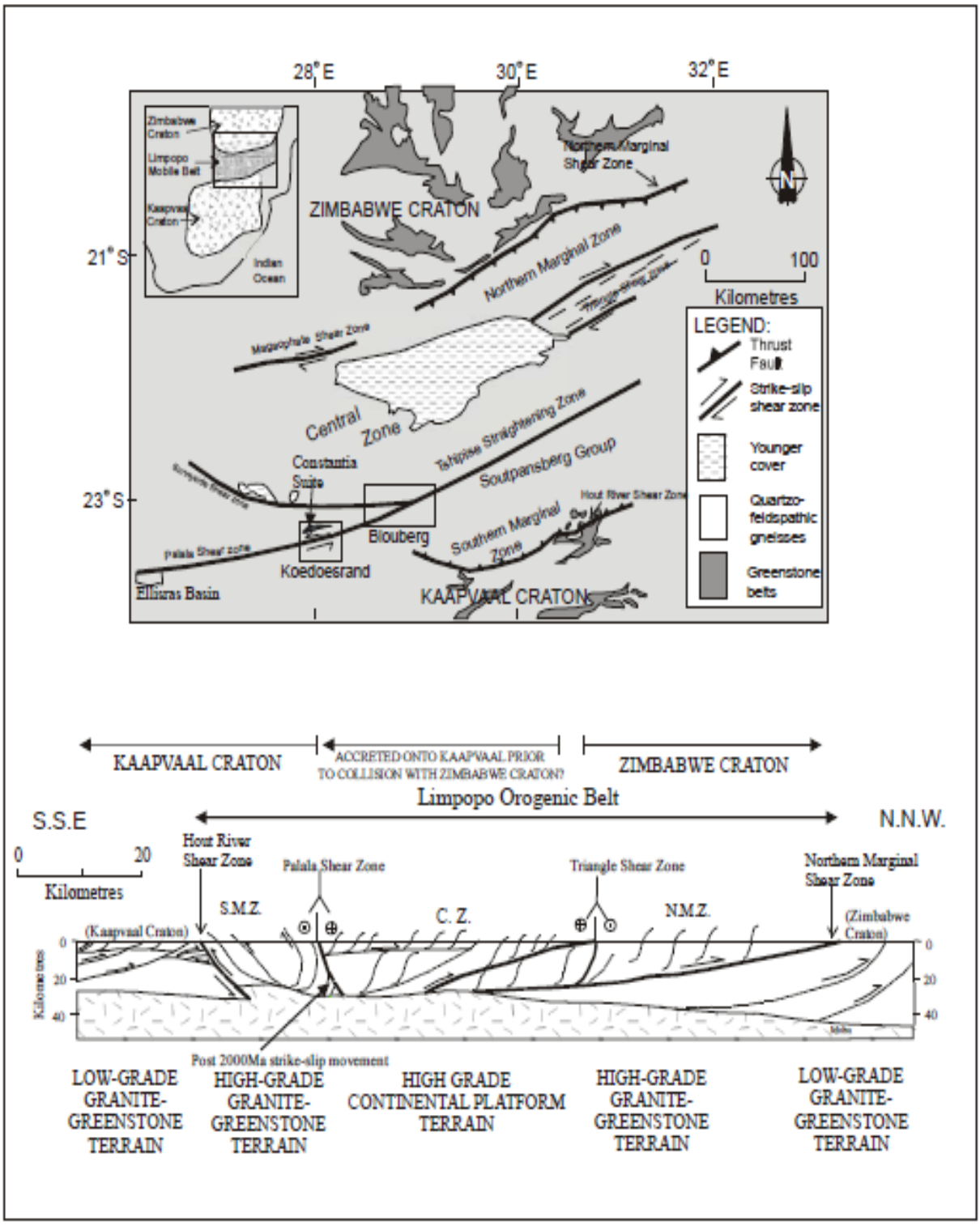

Figure 2.3: Simplified geological map of the Limpopo Mobile Belt (Gore et al., 2009).

2.2 General overview of prominent South African Coalfields

South Africa has Coalfields in five of its provinces (Fig 2.4) and the most prominent are Witbank, Highveld and the Waterberg Coalfield (Hancox and Gotz, 2014). Based on sedimentation, quality, origin, formation and distribution of coal, 19 coalfields are generally recognised in South Africa (Hancox and Gotz, 2014). Based on variations in sedimentation, origin, formation, distribution and quality of the coals most coal in South Africa was formed during the Permian period (Mphaphuli, 2017; Hancox and Gotz, 2014). According to Mphaphuli (2017), the majority of coal in South Africa are bituminous while some anthracite is also present in the KwaZulu-Natal coalfields. Coal in South Africa is used for power generations, synthetic fuel production and for metallurgical purposes (Hancox and Gotz, 2014). Coal in South Africa is preserved within rocks of the Karoo Supergroup. The Karoo Supergroup can be divided into four Groups, Namely; Dwyka, Ecca, Beaufort and Stormberg. The Vryheid Formation of the Ecca Group hosts the most economically extractable coal (Mphaphuli, 2017).

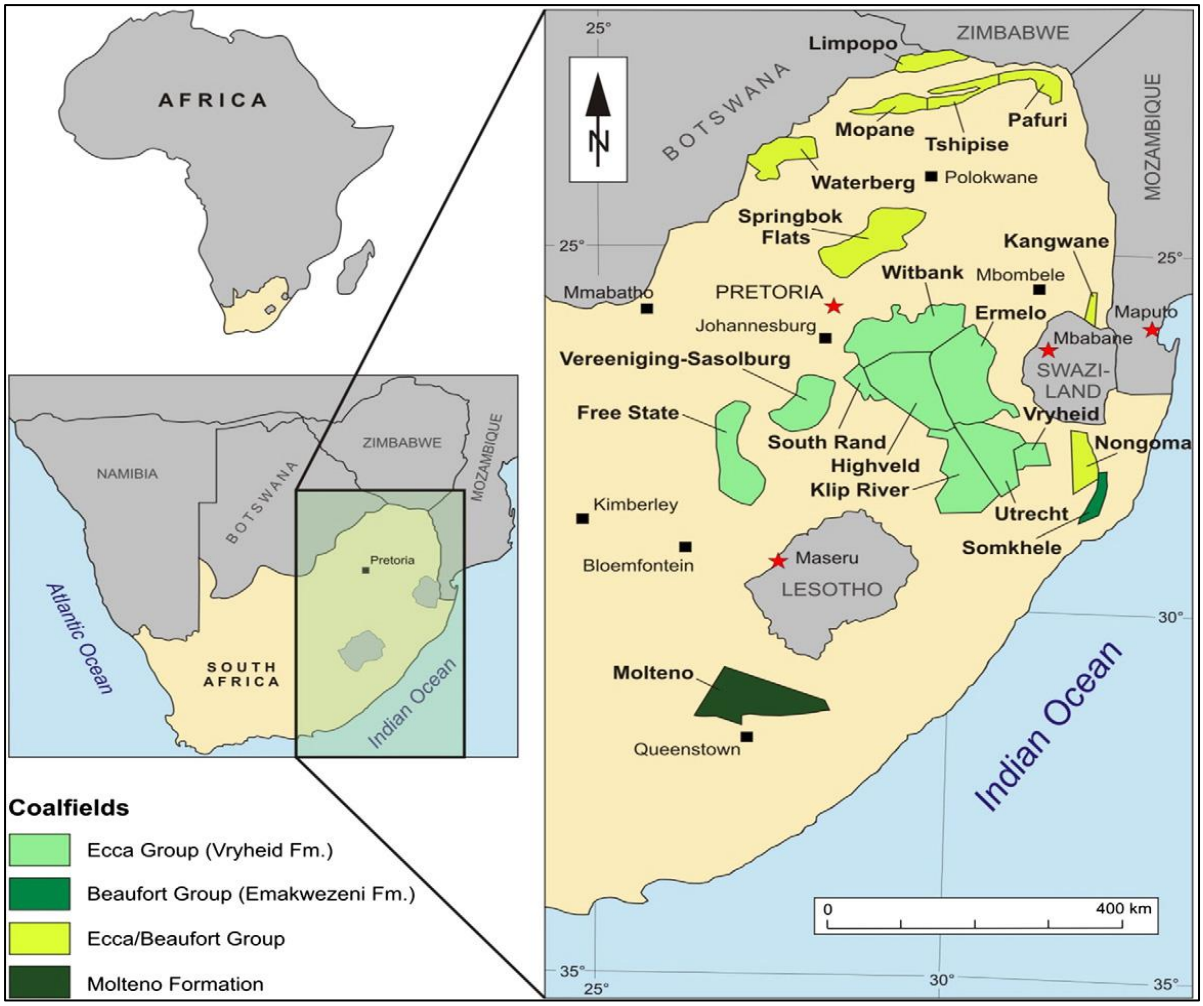

Figure 2.4 Coalfields of South Africa (Hancox and Gotz, 2014).

2.2.1 Witbank Coalfield

The Witbank Coalfield is located from Brakpan to Belfast in a West - East direction (Mahanyele, 2010). The coalfield extends 90 km in the West – East direction and 50 Km the North – South direction covering a distance of approximately 568000 ha (Hancox and Gotz, 2014). The Witbank Coalfield is the largest producing Coalfield in South Africa as well as the most documented (Jeffrey, 2005).

Pre-Karoo basement rocks form the northern boundary of the Witbank Coalfield; however, the Southern boundary is formed by a protruding pre-Karoo felsite known as the Smithfield Ridge (Le Blanc Smith, 1980). The basin is categorised as a multiple seam deposit type with five most important seam horizons which might be defined as composite seams in some portions (Hancox and Gotz, 2014). The

following are economic coal seams of the Coalfield: number 2 seams, number 4 seam, and although limited to a number of places, the number 5 seam (Wheeler, 2015; Jeffrey, 2005). The Ogies dyke is the most distinctive dyke and intrudes vertically with an east-west strike (Msomi, 2014).

Metasedimentary, metavolcanic, and dolomitic rocks comprise the basement from east to west. Unusually thick coals filling karst topography occur where dolomites of the Transvaal supergroup form the basement. The stratigraphic column is reduced to roughly 80 m in some areas close to the north-western basin margin. The top part of the eastern sector succession is the primary economically valuable seam (Le Blanc Smith, 1980). In the western sector, coal is of relatively low quality compared to the central and eastern sector (Msomi, 2014; Hancox and Gotz, 2014).

2.2.2 Waterberg Coalfield

The Waterberg Coalfield which is located in the Limpopo province has been identified as a runner up of the Witbank and Highveld coalfields as South Africa's most prominent coal basin (Wheeler, 2015) The Waterberg Coalfield is located in the Limpopo province, approximately 400km northwest of Johannesburg. The coalfield spans an area of approxiamtely 360 000 ha and extends, east to west, from the Palala shear zone to the Botswana border (Hancox and Gotz, 2014). The Waterberg coalfield has been identified as a replacement of the Witbank and Highveld coalfields as South Africa's most prominent coal basin (Wheeler, 2015). A fault basin with dimensions of approximately 90 km and 40 km surrounds this basin. The preservation and depositional characteristics of coal occurrences in the area are a result of the faulting (Hancox and Gotz, 2014).

Coal Zones are to be found on both the Vryheid Formation and the Grootgeluk formation. Coals from the Vryheid Formation are primarily dull however the coal from the Grootgeluk is bright with organic mudrock intercalations (Wheeler, 2015). Eleven coal zones are identified in the Waterberg coal field (Hancox and Gotz, 2014).

2.2.3 Highveld Coalfield

The Highveld Coalfield is situated adjacent to the Witbank Coalfield in Mpumalanga Province. The coalfield spans an area of roughly 7000 km^2. The coalfield has a width of 95 km E –W stretching from Davel to Nigel, it has a length of 90 km N –S extending from Kriel and Standerton. The Highveld Coalfield is the second biggest Coalfield in South Africa (Hancox and Gotz, 2014).

There are five coal seams contained in the coalfield; these coal seams are hosted within the Ecca group sediments of the Karoo Supergroup, the coal seams comprise the Vryheid Formation (Jeffrey, 2005). The sediments of the Karoo supergroup are attributed to glacial to fluvio-glacial and from shallow marine to fluvio-deltitic depositional environments (Van der Walt, 2012). The No. 4 and No. 2 seams are characterised by a division in particular areas of the coal seams made up of clastic partings. The No. 3 seam is the only coal seam, out of the 5, that lacks mineable thickness with economic potential in the northern region of the coalfield (Jefrey, 2005). The No. 4 seam is the only coal seam with mineable dimensions with economic potential throughout the southern region, however, the mineable dimension with the economic potential of the No. 2 and No. 5 seam are confined to lesser areas (Hancox and Gotz, 2014).

The depth to the coal seams increases from north to south, e.g. the No.4 Seam is mineable by opencast in the northern region, whereas it is positioned at a distance of approximately 200 m in the southern region. In general, the coal seams are horizontal albeit with slightly dipping undulations with a small regional dip to the south (Hancox and Gotz, 2014; Wheeler, 2015).

2.2.4 Soutpansberg coalfield

The Soutpansberg Coal basin is situated north of the Soutpansberg mountain range in the Limpopo Province (Fig. 2.4). The coalfield is divided into three sections or sub-basins namely: Mopani, Tshipise, and Venda-Pafuri (Malaza, 2013). Outcrops in the area are allocated to three chronological units which encompass the Karoo Supergroup in the area, namely: Permian period, Triassic period and Jurassic period. The Permian Period is made up of Tshidzi, Madzaringwe, Mikambeni and

Fripp Formations. The Triassic Period consists of the Solitude, Klopperfontein, Bosbokpoort and Clarens Formations .The Jurassic Period also comprises of the Letaba and Jozini Formations (Malaza, 2013; Hancox and Gotz, 2014).

The coal seams strike in an east-west direction between major faults, the upper (or main fault) and the lower seam are the main coal seams in the Soutpansberg Coal Basin. The two coal seams are divided by a vertical 95 metre trough with an absence of marine sedimentation (Hancox and Gotz, 2014).

Coal in the Venda-Pafuri sub-basin is located in the sandstone-rich Madzaringwe and Mikambeni Formations (McCourt and Brandl, 1980). The Main seam is at most 3.5 m thick and is a amalgamated seam composed of a number of coal bands interbedded with carbonaceous shale. The Tshidzi Formation is located at the base of the sub-basin and its comprised of diamictite interbedded with comparatively coarse-grained sandstones (Malaza, 2013).

The Tshipise Sub-basin is stratigraphically similar to the Pafuri Sub-basin, however the coal-bearing sequence is thinner and the coal seams are relatively more closely interlaminated with the mudrock/shale and siltstone. The middle of the basin contains quartzite outcrops of the Soutpansberg Group as well as metasedimentary, amphibolites and granitoids of the Beit Bridge Complex. Furthermore the coal seams are composite, comprises of interchanging bands of coal and mudstone (Malaza, 2013).

The Mopani sub-basin consists of rocks of the Karoo supergroup that strike east-west and dip towards the north. This deposit is fault bounded and has been fragmented into fault blocks by numerous strike faults. Karoo sediments are absent in the south of the area owing to uplift and erosion, hence exposing the Beit Bridge Complex and Waterberg Group rocks (De Jager, 1986). The arenaceous Madzaringwe Formation is somewhat limited as well as absent in the area either because of non-deposition or pinch-out of this unit, from east to west (Malaza, 2013).

ENE-WSW faults control the shape and location of the coalfield; these faults follow the trend of the Limpopo Belt (Malaza, 2013). Karoo Supergroup rocks, basalts and quaternary sediments dominate the surface geology of the area. Dolerite intrusions

are also very common. Structures in the extensively faulted sequence are pre-, syn- and post-depositional (Hancox and Gotz, 2014). According to Sparrow (2012) Coal rank, yield and coke strength after reaction (CSR) increases from west to east in the Soutpansberg coalfield, whereas phosphorus decreases towards the north (Fig. 2.5).

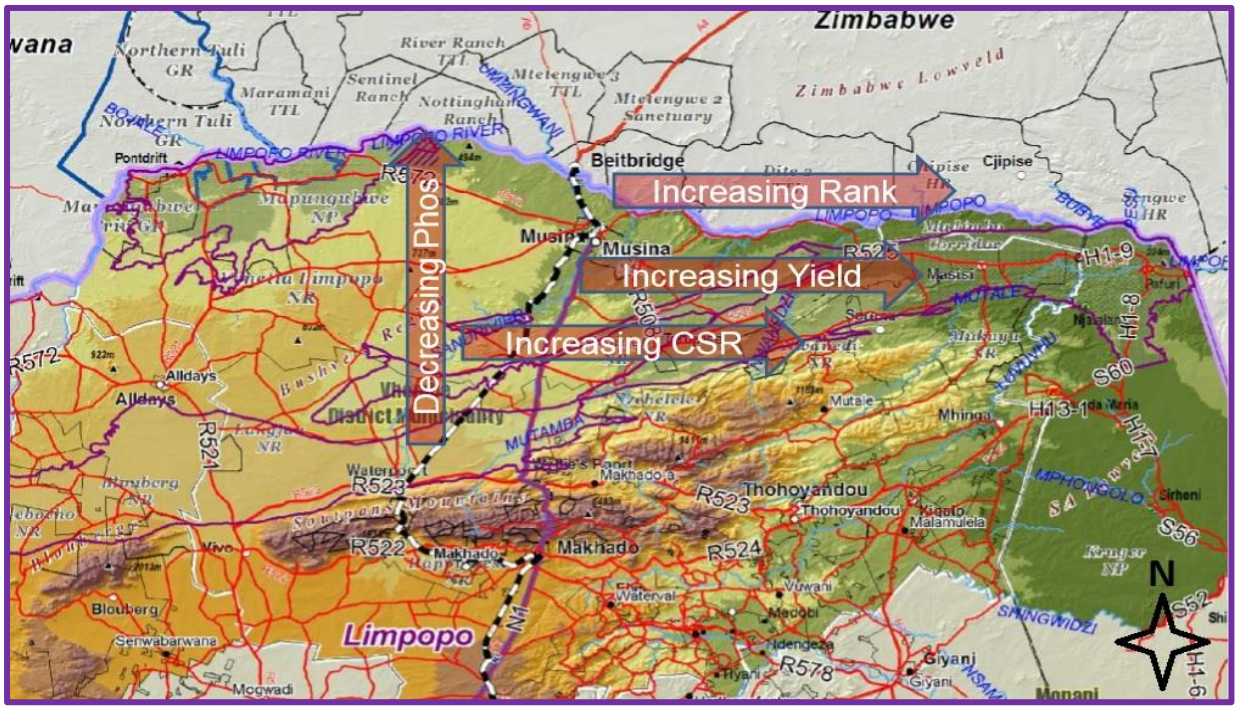

Figure 2.5: Map illustrating metallurgical coal trends of the Soutpansberg coalfield (Sparrow, 2012).

2.3 Coal formation and occurrence

Coal is an organic rock composed of fossilised remains of plant material which have underwent gradual chemical and physical change through time. It consists of the chemical constituents which contains carbon, hydrogen, oxygen, nitrogen and sulphur (Phupheli, 2007). According to the World Coal Association (2018), coal formation began about 360 million to 290 million years ago during the Carboniferous Period (Thomas, 2013). Coal begins as peat which forms in a swampy environment that contains the necessary conditions that allow peat to form and be concentrated into beds which are then gradually converted to coal. After the decomposition of plants, inorganic compounds remain in the peat and combine to form discrete minerals (Schweinfurth, 2009).

Coal is formed through alteration of organic matter under high temperature and pressure through a process called coalification. During coalification, peat is converted to lignite, sub-bituminous coal, bituminous coal, anthracite and then meta-anthracite (Stach *et al*, 1982). Coalification occurs in three stages namely: aerobic decay, anaerobic decay and metamorphism/bituminisation succeeding the accumulation of plant debris in swamps (Williams *et al*., 2000).

Aerobic decay occurs in the early stages of coalification due to aerobic bacteria which in due course die owing to oxygen deficiency in the swamp (Falcon and Snyman, 1986). The decay process also produces acid which is also controlled by anaerobic bacteria until the pH is in the region of 4.0, where the bacteria eventually dies leaving the peat that has been changed into a black, gel-like material called gytta. It is this material that is a precursor of coal (Stach *et al*, 1982).

Once the peat is formed in the biochemical stage, the thermal processes arise for the concluding phases of coalification. The peat is then concealed by debris which preserves the natural heat that escalates to the earth's surface (Falcon and Snyman, 1986). The bituminisation process activates after the temperature reaches 100 °C this is however a very slow process (Schobert, 1995).

Temperature and pressure carries on rising, and chemical reactions that drive off moisture, oxygen and hydrogen occur as a consequence increasing the carbon content (Williams *et al*., 2000). As the bituminization process develops, the volatile matter and moisture contents continue to decrease, the distinct plant remains are lost and the shiny black macerals are produced by the geochemical gellification of the humic substances and thus culminates into subbituminous coal (Stach *et al*, 1982).

Additional decrease in moisture content results in high-volatile bituminous coal. The aromatization of humic complexes results in a decrease in volatile matter and thus an increase in rank to bituminous coal (Schobert, 1995). Rapid decreases in the hydrogen content and atomic H/C ratio as well as a strong increase in reflectivity and optical anisotropy characterize the anthracite stage (Stach *et al*, 1982).

Coal occurs in deposits called seams where by most coal seams originate from peat deposited in mires (Taylor *et al*, 1998). Mire is the environment that is swampy with required setting to allow the formation of peat (Schweinfurth, 2009).

From the Carboniferous Period to the Quaternary Period, coal deposits have been formed throughout the geological column (Walker, 2000). There are three major episodes of coal accumulation. The first took place during the Late Carboniferous to Early Permian periods. The second episode occurred during the Jurassic–Cretaceous period. The third major episode occurred during the Paleogene–Neogene Periods. Coals formed during this period range from lignite to anthracite.

The Permian Period is made up of: Tshidzi, Madzaringwe, Mikambeni and Fripp Formations whereas the Triassic Period consists of the Solitude, Klopperfontein, Bosbokpoort and Clarens Formation, moreover Jurassic Period consists of the Letaba and Jozini Formations (Malaza, 2015). Permian Geology is a host of the coalfields in the northern part of the South Africa which includes Soutpansberg Coalfield (Malaza, 2015). This means that coal in the Soutpansberg coalfield formed during the Permian period.

Humification is the process whereby plants and animals residues are altered into intricate heterogenous amalgamations of humic substances through abiotic and biochemical pathways (Zaccone *et al*., 2018). These remains accumulate in a waterlogged and somewhat decayed vegetations settle at the bottom of the bog or swamp and transform in to peat if appropriate circumstances inhibit complete decay. Oxidative browning reactions of biomolecules such as polyphenols, sugars, proteins, and amino acids result in the dark colouration of humic substances (Hardie *et al*., 2009). Subsequently the peat is buried, and undergoes a series of physical and chemical alterations known as coalification (Schweinfurth, 2009).

Coalification is a continuous process wherein coal increases in rank is brought about by increase in both pressure and temperature resulting from burial in the earth (Schweinfurth, 2009). High temperatures are the most vital controlling factor affecting coalification; high temperature may be produced by an igneous intrusion or linked to depth of burial heat which is related to earth's crust geothermal heat (Schweinfurth, 2009; Mphaphuli, 2017). Organic matter and mineral matter in coal are affected by

coalification. Organic matter constituents which are rich in water, hydrogen, and oxygen are progressively expelled from the coal and the coal comes to be reasonably enriched in fixed carbon as coalification proceeds (Schweinfurth, 2009). The level that a coal has accomplished in a coalification stage is identified as its rank (Thomas, 2013). Major coal ranks from highest to lowest are anthracite, bituminous coal, sub-bituminous coal and lignite (Schweinfurth, 2009).

2.4 Constituents of coal

Coal is a type of sedimentary rock composed of organic carbonaceous matter, macerals, minerals, and fluids which occur in the pores between solid constituents (Pierce and Dennen, 2009). The organic component originates from the plants, and animals, that existed in the environment of formation. The inorganic component was introduced by either sediment that was brought into the area; however, they are also inherited from living organisms that were present in the environment of deposition (Xie, 2015).

2.4.1 Coal mineralogy

According to Scheetz and Earle (1998), the geology of the immediate environment of the coal deposits controls the mineralogy of coal constituents. It is necessary to study the composition and spatial distribution of coal inorganic constituents to optimise coal use. Due to environmental concerns associated with trace elements from coal in the course of mining, combustion, and waste disposal, there is renewed attention in the modes of occurrence of potential environmental sensitive elements.

Ward (2016) defined mineral matter within coal as comprising the following: dissolved salts, discrete inorganic particles, crystalline particles, inorganic elements dissolved in pore water, and inorganic elements associated with organic matrix in coals.

Coal is composed of siliceous and non-siliceous minerals. Siliceous minerals generally consist of aluminium silicates such as mica and kaolin. Non-siliceous minerals include the following (Akinyemi, 2011): carbonates, chlorides, pyrites as well as related trace sulfates. Kaolinite, illite, gypsum, pyrite, marcasite, quartz,

microcline, albite-anorthite and calcite are the major mineral phases in coal (Silva *et al*., 2010).

The greatest ratio of the total mineral matter is composed of discrete minerals in coals notably those above the bituminous rank; lower ranking coals have a substantial fraction that is composed of non-crystalline components, dissolved salts or exchangeable cations (Xie, 2015).

2.4.2 Major and trace elements of coal

Around 76 of the 90 naturally occurring elements of the periodic table are present in coal. A majority of these elements are present as trace elements, that is, in the order of parts per million, with roughly eight existing in concentrations adequate for consideration as major elements (Pierce and Dennen, 2009).

The following elements are the main constituents of coal and make the maceral matter or organic structure of coal: C, H, N, O, and S (Pierce and Dennen, 2009).

The following trace elements are of environmental concern and thus have received substantial attention (Ward, 2016; Pierce and Dennen, 2009): antimony, arsenic, beryllium, cadmium, chromium, cobalt, lead, manganese, mercury, nickel, uranium, and selenium. Owing to their differences and modes of formation each trace element needs to be individually considered.

2.4.3 Maceral composition

Coal is composed of biological components known as macerals (Meyers and Attar, 1982). They have various chemical and physical properties that control their overall behaviour (Scott, 2002). The classification of macerals consists of three main groups, Vitrinite, Inertinite, and Liptinite (Maphala, 2012). The individual coal fractions become increasingly similar in many properties due to the following processes: Peatification, lithification, and coalification. Coal is composed of biological components, with various chemical and physical properties, known as macerals that control its overall behaviour (Scott, 2002). Macerals are classified based on their reflectance, origin, and morphology (Jones, 2010). Spackman (1958) defined the term maceral in the following manner: “macerals are organic substance, or optically

homogeneous aggregates of organic substances, possessing distinctive physical and chemical properties, and occurring naturally in the sedimentary, metamorphic, and igneous materials of the earth."

The original plant, and sometimes animal matter, is already immensely diverse morphologically and chemically prior to consolidation into peat. The concentration of S and N in coal is dependent on maceral composition (Jones, 2010).

Macerals of the vitrinite group are collinite and tellinite. The macerals are mostly found in Bituminous coals and they originate from plant matter of plants that accumulated and were found in anaerobic ancient swamps that are not flowing. The inertinite group macerals are fusinite, semi-fusinite, sclerotinite and micrinite. Fusinite is formed by alteration and rapid oxidation of vitrinite which takes place before or immediately after metamorphism into sediment (Jones, 2010). Semi-fusinite is the intermediate phase in the middle of vitrinite and fusinite which is characterised by fairly limited alteration. Sclerotinite originates from the fungal material. Micrinite originates from physical degradation and metamorphism of cell wall material (Shibaoka, 1978). Exinite group macerals originate from spores, cuticles, resins, waxes and oils contained in the original plant material. Exinite group macerals include exudatinite, bituminite, sporinite, cutinite, resinite, and alginate (Jones, 2010).

Vitrinite

Vitrinite is the most common coal maceral, resulting from coalification of structureless decayed plant materials. Vitrinite is sometimes referred to as "pure coal" due to its tendency to become denser, tougher and glassy when subjected to high heat levels as a result of depth in the earth or heat from igneous intrusion (Schweinfurth, 2009). Level of heat or maturity to which coal has been subjected is determined by an index of vitrinite reflectance (Studer, 2008). Vitrinite is difficult to differentiate from other macerals in high rank coal (Mphaphuli, 2017). Humic-acid portion of humic substances from which vitrinite originates contains carbon, hydrogen and nitrogen (Studer, 2008).

Liptinite

Liptinite maceral group is also referred to as exinite. It develops from relatively hydrogen-rich plant parts such as such as algae, spores and resin (Studer, 2008). Based on the original plant parts, exinite maceral group is further grouped into alganite, sporinite and resinite (Schweinfurth, 2009). When heated, exinite group yields much more volatile matter compared to other maceral groups. Its reflectance increases with the increase of coal rank (Mphaphuli, 2017). Compared to other maceral groups, exinite macerals are more enriched in hydrogen resulting in exinite-rich coal to produce large amount and high-grade liquid fuel when they are subjected to destructive distillation (Schweinfurth, 2009).

Inertinite

Plant materials that are highly altered and degraded during peat stage formation of coal form the inertinite maceral group. The group is formed from the same type of plant material as the vitrinite group, but they are exposed to an erratic degree of partial burning and oxidation (Mphaphuli, 2017). Inertinite macerals shows very little change in its chemical and physical properties with increasing coal rank (Phupheli, 2007). Inertinite group is subdivided into: fusinite, semifusinite, funginite, macrinite, secretinite, inertodetrinite and micrinite. Fusinite is the most prominent maceral group of Inertinite and it is believed to have formed from combusted fossilised wood resulting from ancient forest fires (Studer, 2008; Mphaphuli, 2017).

2.5 Physical properties of coal

Characterizing and understanding the physical properties of coal is essential to comprehending the behaviour of coal (Osborne, 2013). The bulk properties of coal, particularly the mechanical and thermal properties, have a substantial effect on coal and coal use (Speight, 2005). Furthermore, the microstructure and porosity of coal contribute to the complex heterogeneous reactivity of coal (Xie, 2015).

The mechanical strength of coal is associated with characteristics including the following (Xie, 2015): the degree of coalification, lithotype, mineral content, and weathering. High ranking and low-rank coals have greater mechanical strengths

compared to medium rank fat coals and coking coals (Osborne, 2013). The relative ease with which a coal could be pulverised assessed alongside coals selected as standards are determined using an index known as grindability. There is a general relationship between coal grindability and rank (Xie, 2015).

Density indicates the nature and structure of a material (Xie, 2015). The density is influenced by the closeness of the molecular structure and the molecular arrangement (Osborne, 2013). In addition, density and degree of coalification are associated. The bulk density of coal refers to the ratio of the total mass of coal grains filling a vessel using the free-stacking method to the vessel volume (Xie, 2015). The minerals have considerably greater densities than those of organic matter, therefore the content and composition of the minerals in coal has an important impact on the coal density (Xie, 2015).

Optical properties of coal are important in determining the following information on its structure: coalification, anisotropy, sizes and arrangement of aromatic layers (Speight, 2005). They can also be beneficial in determining the shape, orientation, and accumulation of the internal constituent of the coal (Osborne, 2013). Reflectivity and refractive index are significant optical properties that can be identified in coal (Speight, 2005).

Reflectivity is defined as the capability of a polished coal surface to reflect vertically incident light (Xie, 2015). The reflectivity of vitrinite in bituminous coal is related to the following coal classification indicators: volatile matter content and calorific value (Osborne, 2013).

The moisture content of coal originates from a number of sources (Xie, 2015). Moisture may possibly originate from vegetation responsible for coal formation or water present at the time of coal formation; as such moisture content at different stages of coalification is different. Moisture varies between 3 and 6% in anthracite, between 2 and 15% in bituminous coals and almost 45% in lignite (Speight, 2005).

Volatile matter is the percentage of volatile product, not including moisture vapour, discharged in the course of the heating of coal or coke under a strictly controlled setting (Osborne, 2013). Volatile matter is important in coal classification as well as

appraising the fitness of coal for combustion and carbonisation (Xie, 2015). Volatile matter varies between 2 and 12% in anthracite, between 14 and 45% in bituminous coals and between 24 and 32% in lignite (Speight, 2005).

The heat given off by the combustion of a unit quantity of coal in a bomb calorimeter with oxygen and exposed to particular environment is known as the calorific value (Xie, 2015). Hence the calorific value directly indicates the heat content or energy value of coal. Furthermore, it is a representation of the collective heats of combustion of the following: carbon, hydrogen, nitrogen, and sulfur in the organic matter and of the sulfur in pyrite (Osborne, 2013).

The residue left over after the combustion of coal under specified conditions is known as ash, and it is predominantly comprised of oxides and sulphates (Xie, 2015). Ash can be equivalent, less than or more than mineral matter; this is subject to the nature of mineral and chemical variations that take place for the period of ashing (Speight, 2005). The following variations (Osborne, 2013) take place in the course of ashing: loss of water from silicate minerals, loss of carbon dioxide from carbonate minerals, oxidation of iron pyrite to iron oxide and fixation of oxides of sulfur by bases such as calcium and magnesium (Xie, 2015).

CHAPTER 3: MATERIALS AND METHODS

This chapter comprises the methods and procedures that were used for the study as given in Fig. 3.1.

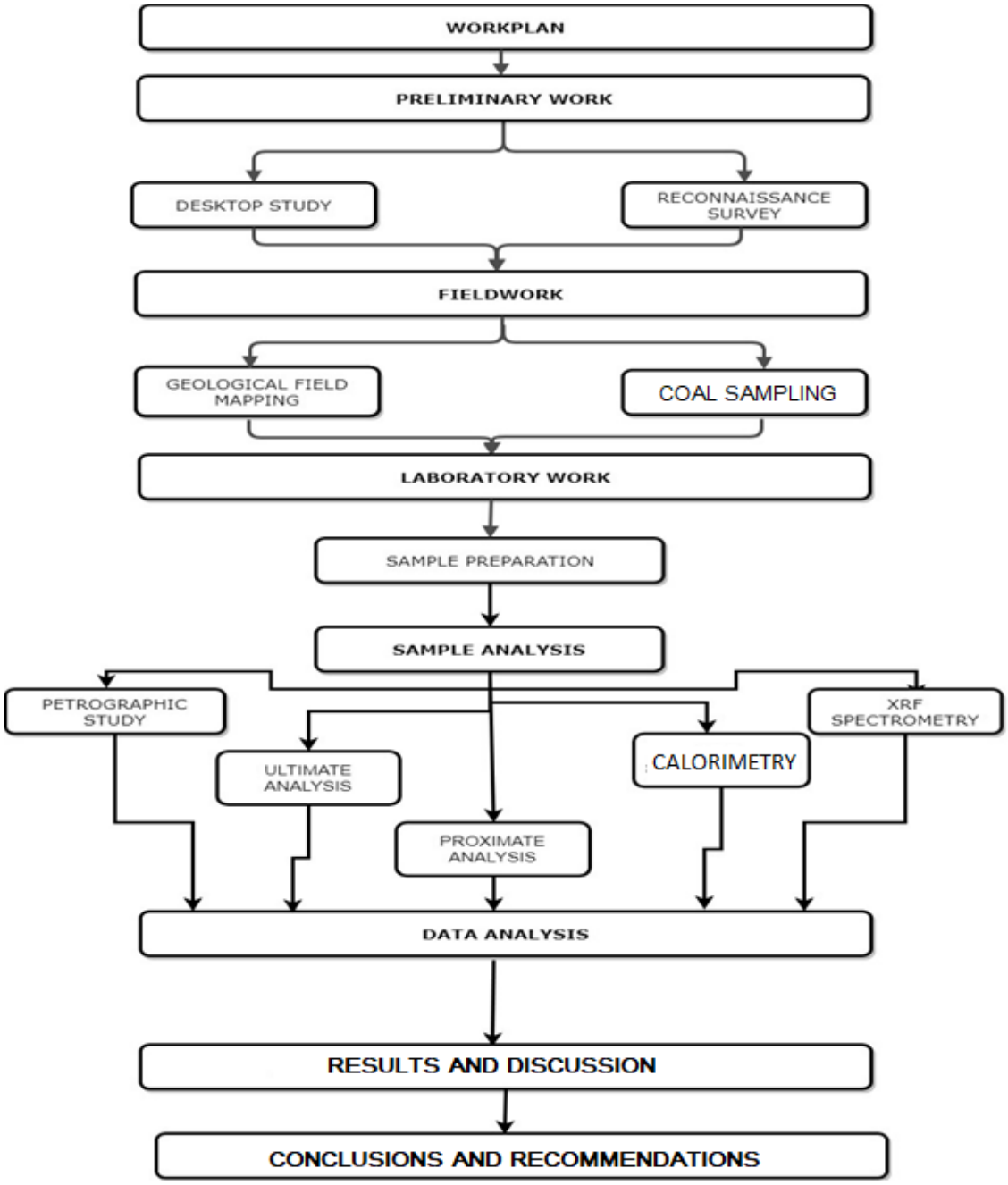

Figure 3.1: Flowchart illustrating methods and procedures applied in the study.

3.1 Preliminary work

Preliminary work is the procedure of preparation for undertaking actual fieldwork. The common idea of the procedure was to outline methods and materials compulsory to embark on the study before actual fieldwork was carried out. The preliminary work provided knowledge about the study area and the possible constraints that may have an impact on accomplishing the set objectives.

3.1.1 Desktop study

The desktop study comprised acquiring information about the study area from published and unpublished literature that may be beneficial in conducting the study. The literature used includes but was not limited to books, journals, photographs, online resources, theses, maps and unpublished sources. The data and information attained are associated with the planned project and aids in providing knowledge about the work that will be carried out in the study area. The desktop study also prepared the researcher psychologically and contributed towards the selection of equipment necessary for undertaking the study.

3.1.2 Reconnaissance survey

A reconnaissance survey was undertaken by travelling to the field with the objective of familiarizing the researcher with the immediate surroundings of the study area. This provided the researcher with assistance in the identification of areas of significant interest to the study and to be aware of the surroundings. During this stage, the geological setting, topography, drainage, soil type and general rock characteristics were identified

3.2 Fieldwork

Fieldwork consisted of the collection of information within the study area. The information acquired includes the following: identification of rock bodies, their attitudes and their structural features. Geological field mapping and in-situ coal sampling were carried out to collect field data. The primary objective of carrying out fieldwork was to provide a description of outcrops in the area; in addition, sampling was accomplished to collect samples for laboratory analysis.

Tools that were used during fieldwork included the following: spade, pickaxe, tape measure, geological hammers, hand lens, sample bags, clino-ruler, GPS, topographic map, dilute hydrochloric acid, notebook and marking pens.

3.2.1 Geological field mapping of Mushithe area

Geological field mapping was carried out to produce a geological map of the study area. Field data was compiled by studying outcrops as well as their immediate environment. The survey area (Fig 3.2) was divided into five traverses of 500 m wide each that cut across the general strike of lithologies in the area. The study area had a total area of 7 km^2 with dimensions 2.5 km by 2.8 km. Field data was collected by mapping each individual outcrop in a zigzag motion as well as following the Mbodi stream from downstream to upstream and paths and roads that cut across the strike in the survey area.

Brunton compass and GPS was used to locate ourselves in the field. However, the compass was also used to measure attitudes of lithologies while the GPS was used to record the location of outcrops and altitude of the outcrop.

Notes were recorded throughout mapping and the following information was recorded, characteristics of the outcrop environment as well as those of the outcrop, this data includes amongst others: description of rock units, contacts and structures.

A total of 92 rock specimens were collected during geological field mapping using geological hammer by chip sampling method. These samples were collected for further laboratory analysis using petrographic study and whole rock geochemistry.

Data collected from the geological mapping was used to compile a geological map of the area as well as a cross-section.

Figure 3.2: Map indicating the traverses that were mapped in the study area (Google Earth, 2018).

3.2.2 Coal sampling

The coal outcrop located along the Mbodi stream (Fig, 3.3) was sampled in-situ using a channel sampling procedure akin to the one indicated by Thomas (2013). The outcrop was cleaned and cut back to expose as fresh a section as possible using spade and pickaxe. Exposed area was sectioned based on lithological changes and sampled accordingly using a geological hammer, collected samples were placed in bags which were sealed and labelled. The samples were collected perpendicular to the bedding.

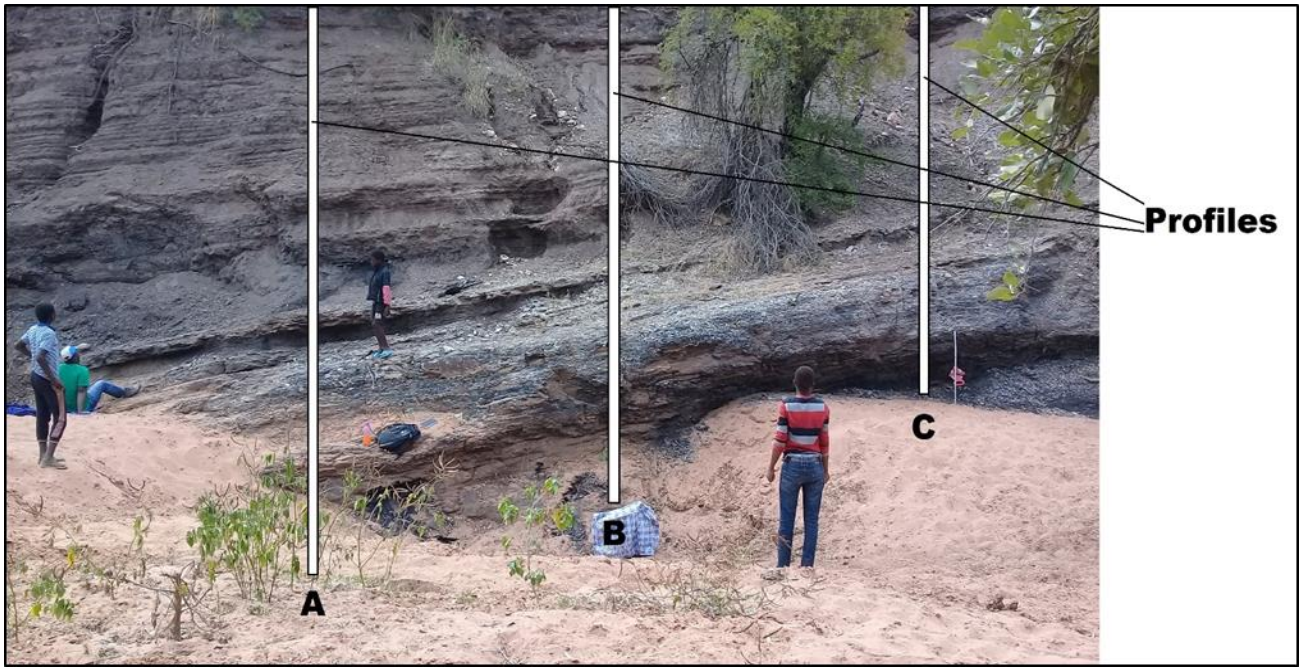

Figure 3.3: Coalbed image showing three profiles (A-C) delineated for channel sampling.

The exposed outcrop measured 18 metres horizontally and three distinct seams were identified thus sampling was done at intervals of 6 metres from west to east. Three profiles were marked A, B, C. This was done to allow vertical and horizontal evaluation of the outcrop. The following information was recorded during sampling: lithological description, thickness of each layer in the coal bed outcrop, attitudes of the outcrop, extent of weathering and frustration as well as the contact between different layers.

A total of 21 samples were collected, 9 of those were identified as coal while the remainder were identified as shale samples. The samples weighed at least 2 kg each.

3.3 Laboratory work

Laboratory tests were conducted to gain information on the physical and chemical characteristics of coal and rock samples collected from the study area. To fulfil the objectives of the study, samples were subjected to laboratory analysis.

3.3.1 Sample preparation

This section details how the samples were prepared for laboratory analysis and study.

Preparation of thin sections

Samples for petrographic study were prepared according to the procedure outlined by Malaza (2013). From the total of 92 samples collected, ten representative rock samples collected around the Mushithe Coal occurrence were selected and prepared for thin sections. Several steps were followed for preparation of thin sections, which include; cutting, trimming and bonding samples, cutting of bonded samples, grinding and polishing.

Cutting: The large rock samples were cut using a diamond saw (Figure 3.4A) to cut the rocks to smaller sizes. Samples were cut into rectangular blocks of approximately 50 x 80 mm size using the diamond saw.

Trimming: The rectangular blocks were trimmed to 30 x 40 mm sizes using Streuers Accutum-50 machine (Figure 3.4C) and they were polished using silicon carbide grit in sequence of 120, 220 and 1000 grit sizes until they were smooth for bonding process. The polished samples were cleaned by using deionized water and dried in a Vacutec drying oven (Figure 3.4A). They were cooled to room temperature after being dried for 15 minutes at a temperature of 85 °C before bonding.

Bonding: An epoxy bonding solution was prepared by mixing hardener and resin using ratio of 2:15 translating to 2 parts hardener and 15 parts resin. Samples were bonded on frosted glass slides using epoxy. The samples were placed on a bonding jig (Figure 3.4B) for a period of 24 hours for effective bonding.

Grinding**:** The bonded samples were first cut to reduce the thickness from 40 mm to 10 mm using Streuers Accutum-50 cutting machine (Figure 3.4C). Cutting process took approximately 8 to 20 minutes. The samples were then ground to 50 micrometers for approximately 30 minutes. The instrument was programmed to grind and stop the process automatically.

Polishing**:** Ground samples were placed onto a Streuers RotoPol-35 polishing machine (Figure 3.4D) and polished using the polishing disk for approximately two hours. The sample thickness was checked using a micrometer gangue to confirm the required thickness of approximately 35 µm or less for petrographic studies.

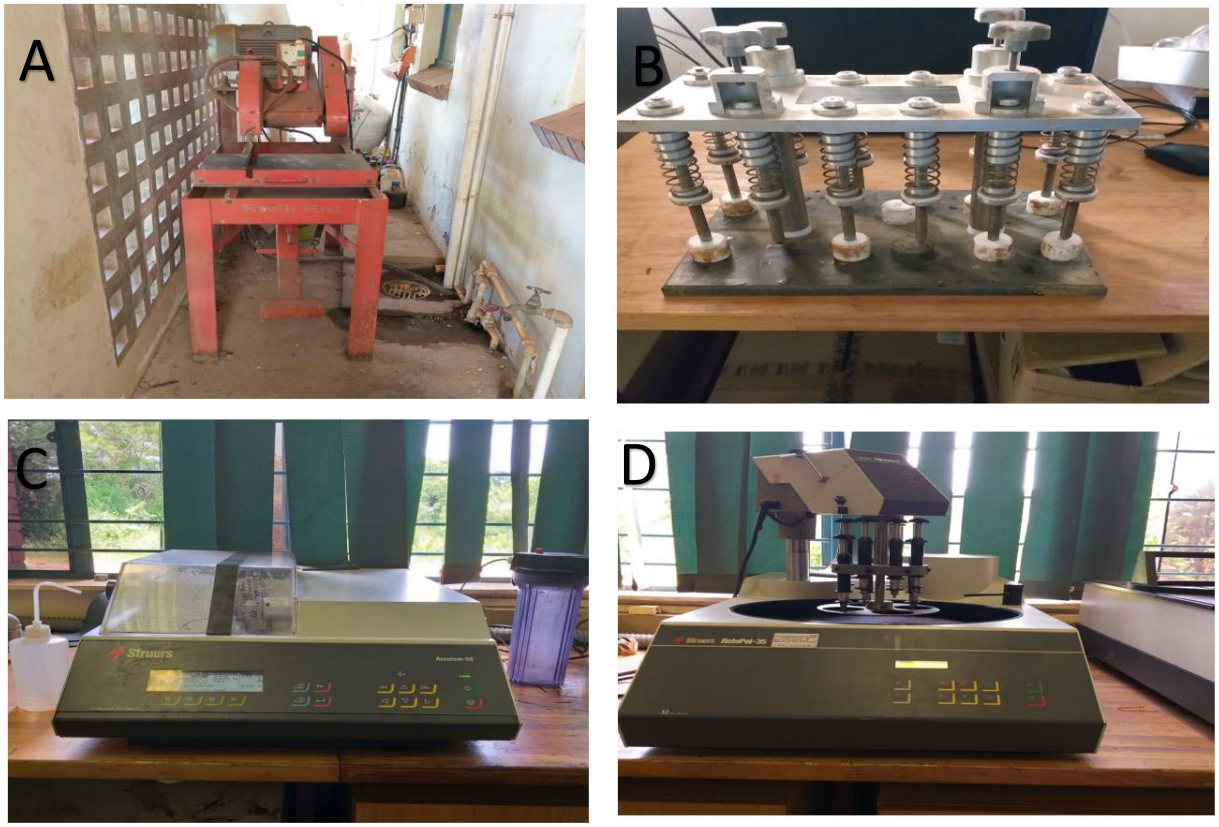

Figure 3.4: Thin section preparation equipment;A) Diamond saw; B) Bonding jig; C) Streuers Accutum-50 cutting machine; and D) Streuers RotoPol-35 polishing machines.

Preparation of polished coal samples

Three representative samples were selected for preparation, these samples were selected according to carbon content from ultimate analysis as well as calorific value, and a sample was selected from each of the three identified seams based on the above criteria. Thereafter each coal sample was crushed and sieved to obtain coal samples of -1000 µm. Each of this was sent to the University of Johannesburg where the samples were prepared into blocks by mixing coal samples with IMP Cold Mounting raising and then left for 24 hours to set. The blocks were polished in a

series of steps on the Stuers TegraForce-1 polishing machine to a 0.05 µm finish, as per South African Bureau of Standards ISO standard 7404-2 similar to the analysis done by Mphaphuli (2017).

Preparation of samples for geochemical analysis

Coal samples were prepared according to Speight (2012). The samples were first oven-dried at 110^{o}C overnight in the laboratory using a Vacutec 970 oven (Fig. 3.5A). Afterward the samples were milled in Retsch RS 200 milling machine (Fig. 3.5B) for 8 minutes until pulverised to about 75 micons. The milling dishes were cleaned using quartz to prevent contamination before analysis, the pot were also cleaned with the sample to be milled to ensure quartz did not affect the SiO_2 content during analysis. The milled samples were put in a separate sample bag and labeled.

Ten representative rock samples from rock outcrops and the 21 coal bed samples were palletized for XRF spectrometry. The samples were palletized by adding the sample into a pallet cup using boric acid as a binding agent and acetone to prevent cross contamination of samples. Milled powder weighing 15±5 g was pressed with 3±1 g of boric acid as a binding agent .The pellet cup was then centrally placed in an automatic hydraulic operated press and was pressed at 30 tons load for 30 seconds hold time using a hand operated pressing machine. Once the pellet was ready it was removed from the die-set and placed in a container which was also labelled. This procedure was repeated for all the samples to be analysed.

Coal analysis was carried out at labs in Witbank and Witwatersrand University

Figure 3.5: Laboratory equipment: A) Vacutec drying oven; and B) Restsch RS 200 milling machine used to prepare coal samples.

3.3.2 Sample analysis

Samples were analysed by petrographic study, X-Ray Fluorescence and coal analysis.

3.3.3 Petrographic study

Petrographic analysis of coal was undertaken by Prof. Wagner at the University of Johannesburg using a Leica DM 4500P reflected light microscope with oil immersion lens at a magnification of 500X.

The three samples were analysed for maceral group and mineral matter identification in addition to vitrinite reflectance. Maceral group analysis which also included mineral matter was conducted following South African Bureau of Standards ISO standard 7404-part 4 (Mphaphuli, 2017). The main maceral groups were identified as well as recording petrographically observable mineral phases.

This analyses was point count based, recording 500 particles per sample. Petroglite software and an automated stage were used for point counting. Photomicrographs of each sample were taken on a Zeiss Universal petrographic microscope with Axiovision software.

3.3.4 Coal analysis

The following techniques were utilized for coal analysis: Proximate analysis, ultimate analysis and calorimetry. The process discussed in Speight (2012) was used for these analyses.

3.3.4.1 Proximate analysis

The proximate analysis involved determining the percentage of four main constituents of coal, namely: Moisture, ash, volatile matter and fixed carbons. Proximate analysis was undertaken at Witlab laboratories in Witbank.

Moisture

The total moisture in coal is the moisture, not including water of crystallization of the mineral matter, which resides within the coal matrix (Speight, 2005). Determination of moisture was done in accordance with ISO 11722 (Speight, 2005). 0.9 - 1.5g of pulverised coal in a ceramic crucible was combusted in a Nitrogen rich atmosphere, with a flow rate of 15× per hour. The temperature was raised gradually from 25°C to 110°C and sustained until the sample reached a constant mass. The moisture content was calculated from the loss in mass.

Ash

Ash is the residue left over after the combustion of coal under specified conditions and comprises predominantly oxides and sulfates (Speight, 2005). A coal sample

was put in a porcelain dish for 4 hours in an adequately ventilated furnace at a temperature of 700±50 °C. This was done so that there was total removal of the organic matter from the sample through incineration. The burnt coal was then weighed to get its total mass. This was done in accordance with ISO 1171(Speight, 2005).

Volatile matter

Volatile matter is the fraction of volatile products, apart from moisture vapour, discharged during the heating of coal or coke under severely meticulous conditions (Speight, 2005). To determine the volatile matter, 1 g of coal was weighed and placed in a pre-weighed platinum crucible with a tight-fitting cover. The crucible was then suspended at a stated height in the furnace chamber. The temperature of the region in the furnace where the crucible is suspended was kept at 950 ± 20°C. After the more rapid discharge of volatile matter, as showed by the loss of the luminous flame, the cover of the crucible was tapped to make sure that the lid is still appropriately held to guard against the entrance of air. After heating for precisely 7 minutes, the crucible was removed from the furnace and cooled. The crucible was weighed immediately when it was cold. The percentage loss of weight minus the percentage moisture is equivalent to the volatile matter. This was done in accordance with ISO 562 (Speight, 2005).

Fixed carbons

Fixed carbon is useful in the determination of the proficiency of coal-burning equipment. It is a measure of the solid combustible material left over after the volatile matter in coal has been removed. Fixed carbon is determined using a calculation involving the moisture content, volatile matter and ash content. The following equation (Speight, 2005) will be used to determine fixed carbons (FC):

$$\mathrm{FC} = 100 - (\%\text{Moisture content} + \%\text{Volatile matter} + \%\text{Ash content})$$

3.3.4.2 Ultimate analysis

The ultimate analysis of coal involves the determination of the weight percentage of carbon, hydrogen, nitrogen, sulphur, as well as oxygen (Speight, 2005). This was

done at Witwatersrand University Department of Analytical Chemistry using a Leco CHNS analyser.

A sample 0.25 g of pulverised coal was weighed and sealed in a tin foil cup and placed into a combustion chamber where furnace temperature and flow of oxygen result in combustion. The process converted elemental C, H, N and S into CO_2, H_2O, N_2 and NO_x which was condensed to N2 as well as SO_2. The analyser infers C, H, N and S from CO_2,H_2O,N_2 and NO_x

Oxygen was determined by calculation as follows (Speight, 2005):

$$\text{Oxygen} = 100 - \%(\text{Moisture} + \text{Ash} + \text{Carbon} + \text{Hydrogen} + \text{Nitrogen} + \text{Sulphur})$$

3.3.4.3 Calorific value

The calorific value is the heat released by the combustion of a unit quantity of coal in a bomb calorimeter with oxygen and under indicated conditions; this test was performed at the Witlab laboratories on all 9 collected coal samples. Calorific value provides information relating to the heat energy of coal. In this study, procedures for calorific value were carried out in pure oxygen at 2500 kPa. This was performed by using a bomb calorimeter connected to a Supercal software. The system was used after the stabilisation temperature of about 36.3°. Before analysis of the actual samples, a benzoic standard of calorific value 26.428 MJ/kg was used for verification and calibration. Following this, pulverised coal was weighed to 0.4 g in a crucible, with a cotton thread dipped in the coal and placed in a bomb for analysis. The bomb was filled with oxygen and then placed in a calorimeter where the analysis started automatically after closing the lid (Speight, 2005)

3.3.5 Whole rock geochemistry

The method used for analysis was described in Malaza (2013) and Speight (2005) XRF analysis is non-destructive elemental analysis which can qualitatively and quantitatively measure periodic table elements which are found in the sample. Samples are comprehensively mixed to ensure its homogeneity. An XRF spectrometer was used to analyse the palletized samples. The pressed pellet was

loaded in the sample port of the X-Ray Fluorescence analyzer which was connected to a computer system and the assembly left for about six to twelve minutes after which the values of elements concentration were displayed on the monitor. This was saved directly on the system and then printed out as the result of the analysis.

Prior to each cycle of analysis the spectrometer was calibrated using a copper disk. A sample was designated as a check sample to ensure precision of the analysis, this sample was analysed after a cycle of analysis. The standardised control sample SARM 42 (South African Reference Materials) from Mintek was also used to ensure accuracy of the instrument.

CHAPTER 4: RESULTS AND DISCUSSION

The results of the analyses done are presented, analysed and discussed in this section. The main sections are coal characterisation and geological map.

4.1 Coal characterisation

This section includes the analysis of samples collected at the coalbed. The following analyses were undertaken: petrographic study, calorimetry, proximate and ultimate analysis. These were done to give an insight on the coalbed stratigraphy, coal quality and depositional environment of coal.

4.1.1 Profile description

Three seams were identified in the study area with alternating partings between coal and shale (Fig. 4.1). The different beds were distinguished in the field through profiling along A, B and C. Shale samples were characterised by fissility whereas coal on the other hand was not fissile. Colour and luster were equally used to identify the coal and shale beds. Shale was greyish in colour and having a dull appearance while coal was black and exhibiting a shiny luster.

The collected coal samples were generally jointed and fractured with cleats running perpendicular to the bedding and had signs of weathering and oxidation. Likewise shale partings exhibited weathering and were fissile and fine. In sections, coal was dull and mixed with minute shale partings (Coal 2B and Coal 2C). According to Thomas (2013) coal at Mushithe can all be termed vitrain or bright coal, albeit for Coal 2B and Coal 2C which can be termed as clarain.

According to Thomas (2013) the zones of thinning may point toward the attenuation of the seams, or that the seam is splitting, bringing about a thinner upper leaf which can be attributed to organic accumulation disturbance and replacement by clastic deposition for a brief period or due to variation in water level. Furthermore, Coal 2B and 2C were mixed with tiny shale partings of less than a centimetre. The coal seam had a dip angle of 15° with a dip direction in the north-eastern direction and striking from north-west to south-east.

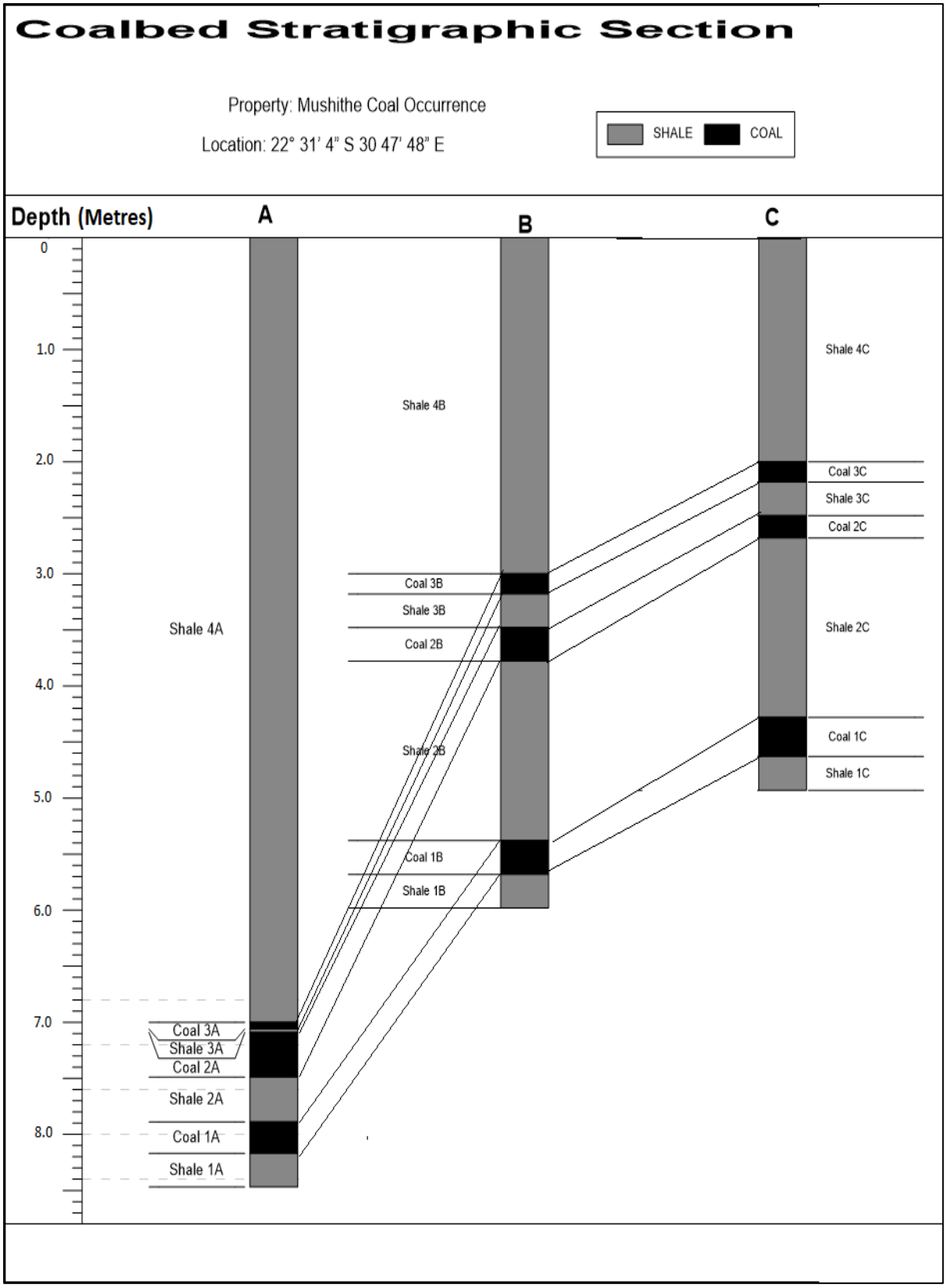

Figure 4.1: Stratigraphic section representing Mushithe coal seams.

4.1.2 Proximate and ultimate analysis

In this section proximate data in Table 4.1 and Figure 4.2 and the ultimate data presented in Table 4.2 and Figure 4.3 are discussed.

4.1.2.1 Proximate analysis

Coal samples were analysed for inherent moisture, ash content, volatile matter and fixed carbon represented in Table 4.1 and the results were graphically presented in Figure 4.2.

The inherent moisture content of the analysed coal samples ranged between 5.60% and 13.60% with an average of 10.47% and a median of 11.60% (Table 4.1). Coal 1C had the highest moisture content of 13.60% whereas the lowest moisture content of 5.60% was in Coal 2C (Fig. 4.2). Furthermore inherent moisture in coal seam 1 had an average of 12.23% whereas coal seam 2 and coal seam 3 had an average of 8.37% and 10.80% respectively (Table 4.1). Moisture content does not correspond with any of the studies done in the Soutpansberg Coalfield and this may be attributed to the fact that these studies are based on core samples and run of mine samples (Thomas, 2013) which are less exposed to water and air. Mphaphuli (2017) and Malaza (2013) reported moisture content of 0.88% and 0.48% in the Soutpansberg Coalfield respectively.

The ash content of the analysed coal ranged between 9.10% and 66.40% with an average of 27.90 % and a median of 18.80% (Table 4.1). Coal 2C had the highest ash content of 66.40 % whereas Coal 2A had the lowest ash content of 9.10% (Fig. 4.2). Furthermore, ash content in coal seam 1 had an average of 22.13%, whereas coal seam 2 and coal seam 3 had average of 41.70% and 19.87% respectively (Table 4.1). The average ash content of seam 1 and seam 3 can be compared with the 21.53% average reported by Malaza (2013) for the Tshipise – Pafuri Sub-basin however coal seam 2 had almost twice this value. Coal 2C with such high ash content can be considered to be carbonaceous shale. Wood *et al.* (1983) designated the following classes to coal according to ash content: low-ash (below 8%), medium-ash (between 8% and 15%) and high-ash coal (above 15%). On average coal at

Mushithe with average 27.90% is classified as high-ash coal. However sample Coal 2A with 9.10% ash can be classified as medium ash coal.

Table 4.1: Results of proximate analysis (Wt. %)

		Inherent Moisture	Ash content	Volatile Matter	Fixed Carbon
Coal Seam 1	**Coal 1A**	11.10	29.30	27.60	32.00
	Coal 1B	12.00	18.30	27.30	42.40
	Coal 1C	13.60	18.80	26.20	41.40
	Average	12.23	22.13	27.03	38.60
Coal Seam 2	**Coal 2A**	11.60	9.10	26.60	57.70
	Coal 2B	7.90	49.60	25.50	17.00
	Coal 2C	5.60	66.40	19.40	8.60
	Average	8.37	41.70	23.83	27.77
Coal seam 3	**Coal 3A**	13.10	13.90	28.50	44.50
	Coal 3B	12.80	27.40	31.20	28.60
	Coal 3C	6.50	18.30	27.10	48.10
	Average	10.80	19.87	28.93	40.40
Median		11.60	18.80	27.10	41.40
Average		10.47	27.90	26.60	35.59

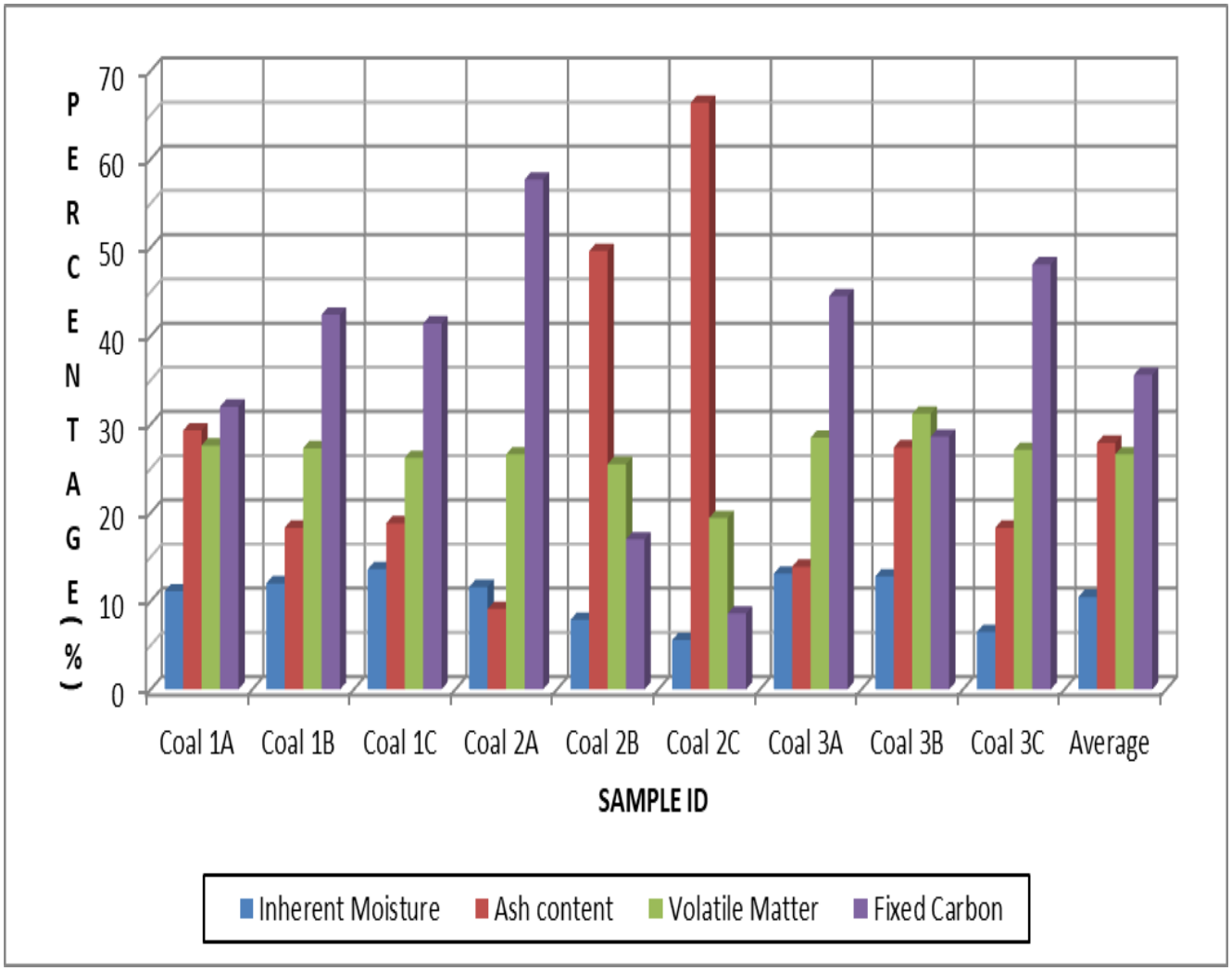

Figure 4.2: Interpretation of proximate analysis for all samples.

The volatile matter of the analysed coal samples ranged between 19.40% and 31.20% with an average of 26.60 % and a median of 27.10% (Table 4.1). Coal 3B has the highest volatile matter with 31.20% whereas Coal 2C has the lowest volatile matter with 31.20 (Fig. 4.2). Furthermore volatile matter in Coal seam 1 had an average of 27.03%, whereas coal seam 2 and coal seam 3 had averages of 23.83% and 28.93% respectively. The volatile matter yields are also slightly comparable to those noted by Mphaphuli (2017) for Tshikondeni Mine (23.55%).

Fixed carbon ranged between 8.60% and 57.70% with an average of 35.59 % and a median of 41.40% (Table 4.1). Coal 2A had the highest fixed carbon of 57.70 whereas Coal 2C had the lowest fixed carbon with 8.60%. Furthermore, fixed carbon in coal seam 1 had an average of 38.60% whereas coal seam 2 and coal seam 3

have average of 27.77% and 40.40% respectively (Table 4.1). The average fixed carbon yield is lower than the 60.72% fixed carbon at Tshikondeni noted by Mphaphuli (2017). However, Coal 2A (57.70%) is slightly lower than Tshikondeni by less than 5%. The low fixed carbon may be attributed to high ash content of Mushithe coal as well as devolitisation of coal by dolerite dyke (Thomas, 2013).

4.1.2.2 Ultimate analysis

Coal samples were analysed for Carbon, Hydrogen, Nitrogen, Oxygen and Sulphur represented in Table 4.2 and these results were graphically represented in Figure 4.3.

The carbon content of the analysed coal samples ranged between 14.21% and 57.19% with an average of 41.02% and a median of 47.77% (Table 4.2). Coal 2A had the highest carbon with 57.19% whereas Coal 2C had the lowest carbon content with 14.21% (Fig.4.2). Furthermore carbon content in Coal seam 1 had an average of 44.77% whereas; Coal seam 2 and Coal seam 3 had average of 31.48% and 46.80% respectively (Table 4.2). The average carbon content of coal at Mushithe is significantly lower than the average carbon content found by White (2015) of 89.7% at Tshikondeni Coal Deposit and this can be attributed to metamorphism of coal by the dolerite dyke which appears to intersect the coal seam.

The hydrogen content of the analysed coal samples ranged between 1.94% and 3.41% with an average of 3.0% and a median of 3.21% (Table 4.2). Coal 1B had the highest hydrogen with 3.41% whereas; Coal 2C had the lowest hydrogen content with 3.0% (Fig. 4.3). Furthermore hydrogen content of samples in coal seam 1 had an average 3.28% whereas coal seam 2 and coal seam 3 have average of 2.54% and 3.18% respectively. The average hydrogen content of coal at Mushithe is significantly lower than the average hydrogen content found by White (2015) of 5.1% at Tshikondeni Coal Deposit

The nitrogen content of the analysed coal samples ranged between 0.41% and 1.47% with an average of 1.13 % and a median of 1.37% (Table 4.2). Coal 3A had the highest nitrogen with 1.47% whereas Coal 2C had the lowest nitrogen content with 0.41% (Fig. 4.3). Furthermore nitrogen content of samples in coal seam 1 had

an average of 1.24% whereas coal seam 2 and coal seam 3 have average of 0.83% and 1.32% respectively (Table 4.2). The average nitrogen content of coal at Mushithe is significantly lower than the average nitrogen content found by White (2015) of 2.1% at Tshikondeni Coal Deposit

The sulphur content of the analysed coal samples ranged between 0.11% and 0.32% with an average of 0.29% and a median of 0.30% (Table 4.2). Coal 2A and Coal 3C had the highest with 0.32% whereas; lowest sulphur content was in Coal 2C with 0.11% (Fig. 4.3). Furthermore sulphur content in coal seam 1 had an average of 0.27% whereas coal seam 2 and coal seam 3 have average of 0.18% and 0.29% respectively (Table 4.2). The average sulphur content of coal at Mushithe is significantly lower than the average sulphur content found by White (2015) of 0.8% at Tshikondeni Coal Deposit. Sulphur content was below 1% and according to Chou (2012) this indicates low sulphur content.

The oxygen content of the analysed coal samples ranged between 16.94% and 32.67% with an average of 26.70% and a median of 28.39% (Table 4.2). Coal 3B had the highest with 32.67% whereas Coal 2C had the lowest oxygen content with 16.94% (Fig. 4.3). Furthermore oxygen content of samples in Coal seam 1 had an average of 28.30% whereas Coal seam 2 and Coal seam 3 had average of 32.67% and 26.70% respectively. The high oxygen content can be attributed to the low carbon as well as moisture in coal. These values are not comparable to White (2015) who reported very low oxygen values of average 2.3%.

Table 4.2: Results of ultimate coal analysis (Wt. %)

		Carbon	Hydrogen	Nitrogen	Sulphur	Oxygen
Coal Seam 1	Coal 1A	37.97	3.05	1.00	0.22	28.47
	Coal 1B	48.58	3.41	1.37	0.30	28.04
	Coal 1C	47.77	3.37	1.37	0.30	28.39
	Average	44.77	3.28	1.24	0.27	28.30
Coal Seam 2	Coal 2A	57.19	3.30	1.47	0.32	28.62
	Coal 2B	23.04	2.39	0.62	0.12	24.24
	Coal 2C	14.21	1.94	0.41	0.11	16.94
	Average	31.48	2.54	0.83	0.18	23.27
Coal Seam 3	Coal 3A	50.57	3.21	1.39	0.31	30.62
	Coal 3B	35.40	3.13	1.17	0.24	32.67
	Coal 3C	54.44	3.21	1.39	0.32	22.34
	Average	46.80	3.18	1.32	0.29	28.54
Median		47.77	3.21	1.37	0.30	28.39
Average		41.02	3.00	1.13	0.25	26.70

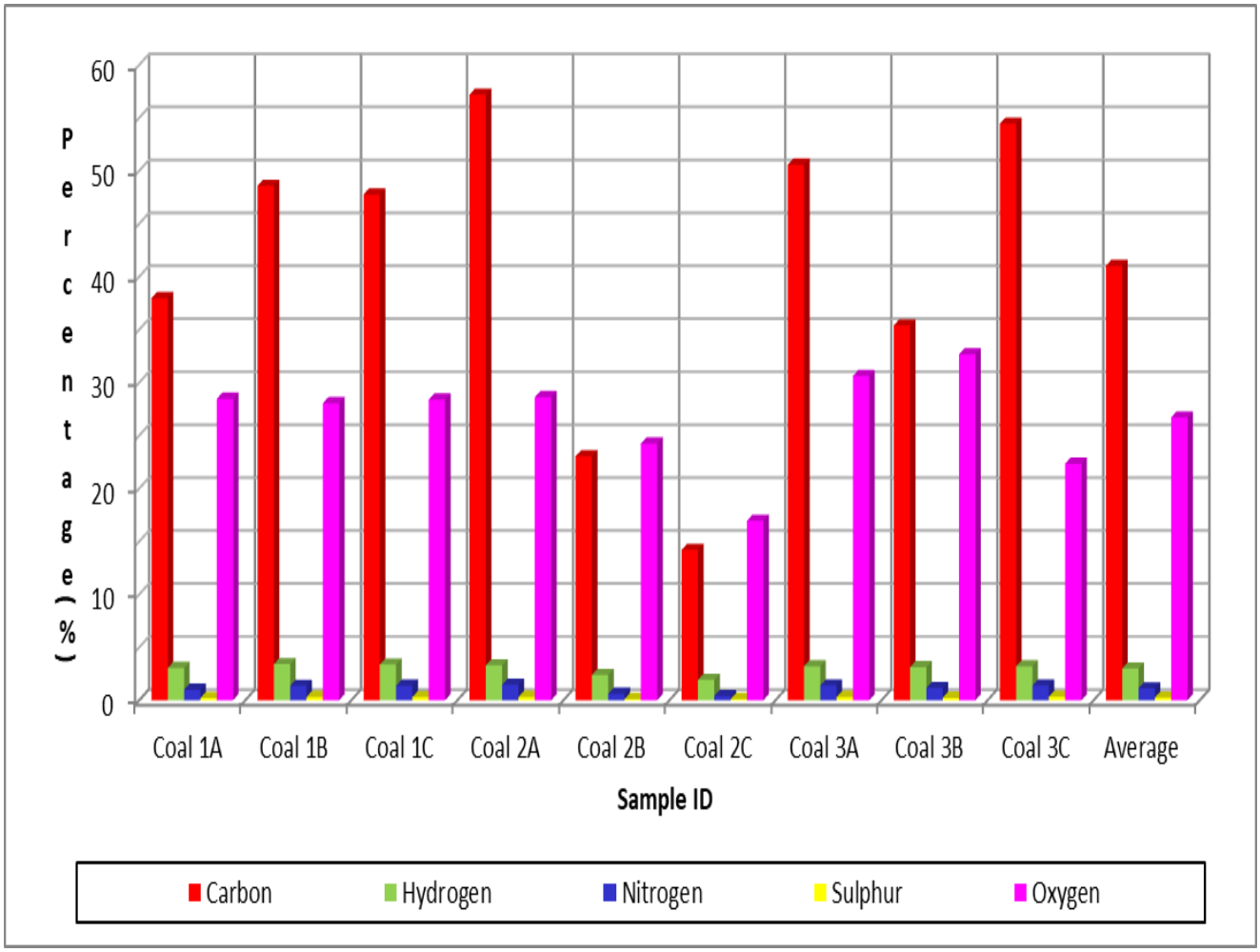

Figure 4.3: Interpretation of ultimate analysis for all coal samples.

4.1.3 Calorific value

Coal samples were analysed for calorific value data presented in Table 4.3 and the results are graphically presented in Figure 4.4. Data from Mphaphuli (2017) for Tshikondeni Deposit and Waterberg Coalfield are included for comparison.

The calorific value of the analysed coal ranged between 4.66 MJ/Kg and 20.99 MJ/Kg with an average of 14.26 MJ/Kg and a median of 16.68 MJ/Kg (Table 4.3). Coal 2A had the highest calorific value with 20.99 MJ/Kg whereas Coal 2C had the lowest with 4.66 MJ/Kg (Fig.4.4). Furthermore, calorific value in Coal Seam 1 had an average of 15.65 MJ/Kg whereas coal seam 2 and coal seam 3 had average values of 10.96 MJ/Kg and 16.18 MJ/Kg respectively. The calorific value of coal in the Mushithe corresponds with the findings of Mphaphuli (2017) (Fig. 4.4). Coal at

Mushithe had average calorific value (14.26 MJ/Kg) higher than that of the Waterberg Coalfield (12.99 MJ/Kg) in the west, but lower than that of Tshikondeni Deposit (28.24 MJ/Kg) in the east. This corresponds with the increase in coal rank from east to west noted by Sparrow (2012).

Table 4.3: Calorific value of the coal samples (MJ/Kg)

	Sample ID	**Calorific Value (MJ/Kg)**
Coal Seam 1	Coal 1A	12.88
	Coal 1B	17.40
	Coal 1C	16.68
	Average	15.65
Coal Seam 2	Coal 2A	20.99
	Coal 2B	7.22
	Coal 2C	4.66
	Average	10.96
Coal Seam 3	Coal 3A	17.63
	Coal 3B	11.20
	Coal 3C	19.72
	Average	16.18
Median		16.68
Average		14.26

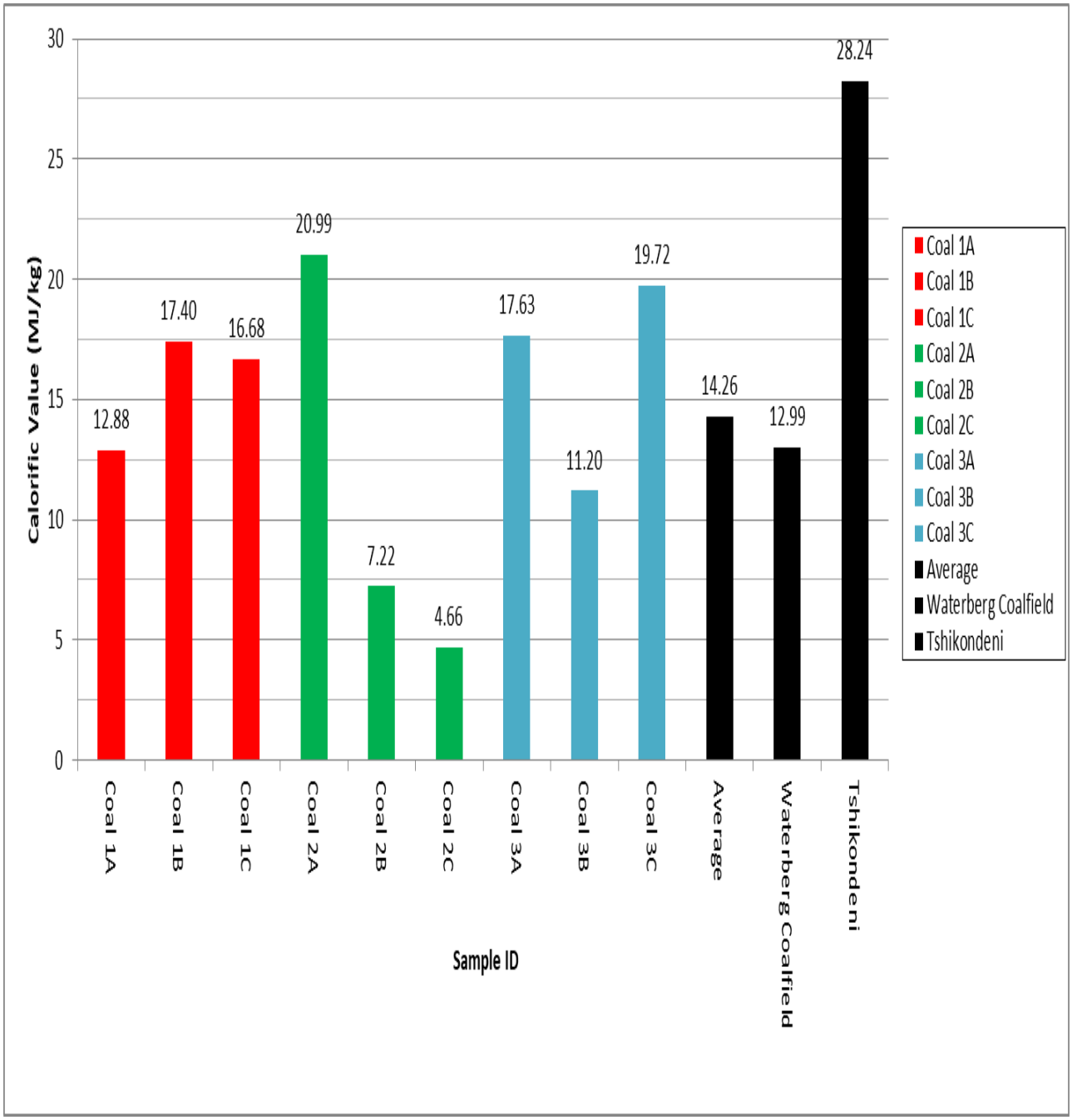

Figure 4.4: Comparison of calorific value of Mushithe coal with the Waterberg Coalfield and the Tshikondeni Deposit.

4.1.4 Petrographic description of coal

The full maceral analysis dataset is contained in appendix A. The Maceral group summary is presented as a histogram (Fig. 4.5) from Table 4.5. The macerals were present as mineral matter free. The dataset was equally used to graphically represent maceral types (Fig. 4.6) as well as mineral matter (Fig. 4.10). Images representing; Coal 1B (Fig. 4.7), Coal 2A (Fig. 4.8) and Coal 3C (Fig. 4.9) were also acquired and used as a graphic aid.

Vitrinite content in coal ranged between 70.16 vol% and 81.96 vol% with average 77.75 vol% (Table 4.5). Coal 3C had the highest vitrinite content with 81.96 vol% whereas Coal 2A had lowest vitrinite content with 70.16 vol% (Fig. 4.5). Collotelinite is the most dominant vitrinite group maceral with an average of 45.9 vol% followed by collodetrinite (22.03 Vol%) and telinite (9.83 vol%). Corpogelinite, gelinite, pseudovitrinite and vitrodetrinite macerals were not found in the Mushithe coal (Fig. 4.6). The absence of pseudovitrinite maceral points towards the good coking properties of the coal samples at Mushithe. Collotelinite is the most dominant vitrinite group macerals; these findings are comparable with Kruszewska (2003) who found that collotelinite dominates collodetrinite in Soutpansberg coals.

Inertinite ranged between 18.04 vol% and 29.84 vol% with average 22.25 vol%. Coal 2A had the highest inertinite content with 29.84 whereas Coal 1B had the lowest Inertinite with 18.04 vol%. Mushithe coal had fusinite with average 11.02 vol% and inert semi-fusinite with average (9.88 vol%) these are the most prevalent inertinite group macerals in Mushithe coal. The following Inertinite macerals were present in values below 1 vol%: micrinite, secretinite, funginite and inertodetrinite with average values (vol %) of 0.15, 070, 0.07 and 0.44 respectively. Reactive semifusinite, macrinite and inertodetrinite were not found in Mushithe coal (Fig. 4.6).

Liptinite group macerals were absent in Mushithe coal (Fig 4.5). Due to the absence of liptinite and reactive fusinite, vitrinite was the only reactive maceral observed in coal. Coetzee (2015) also observed the absence of liptinite in the Soutpansberg Coalfield .

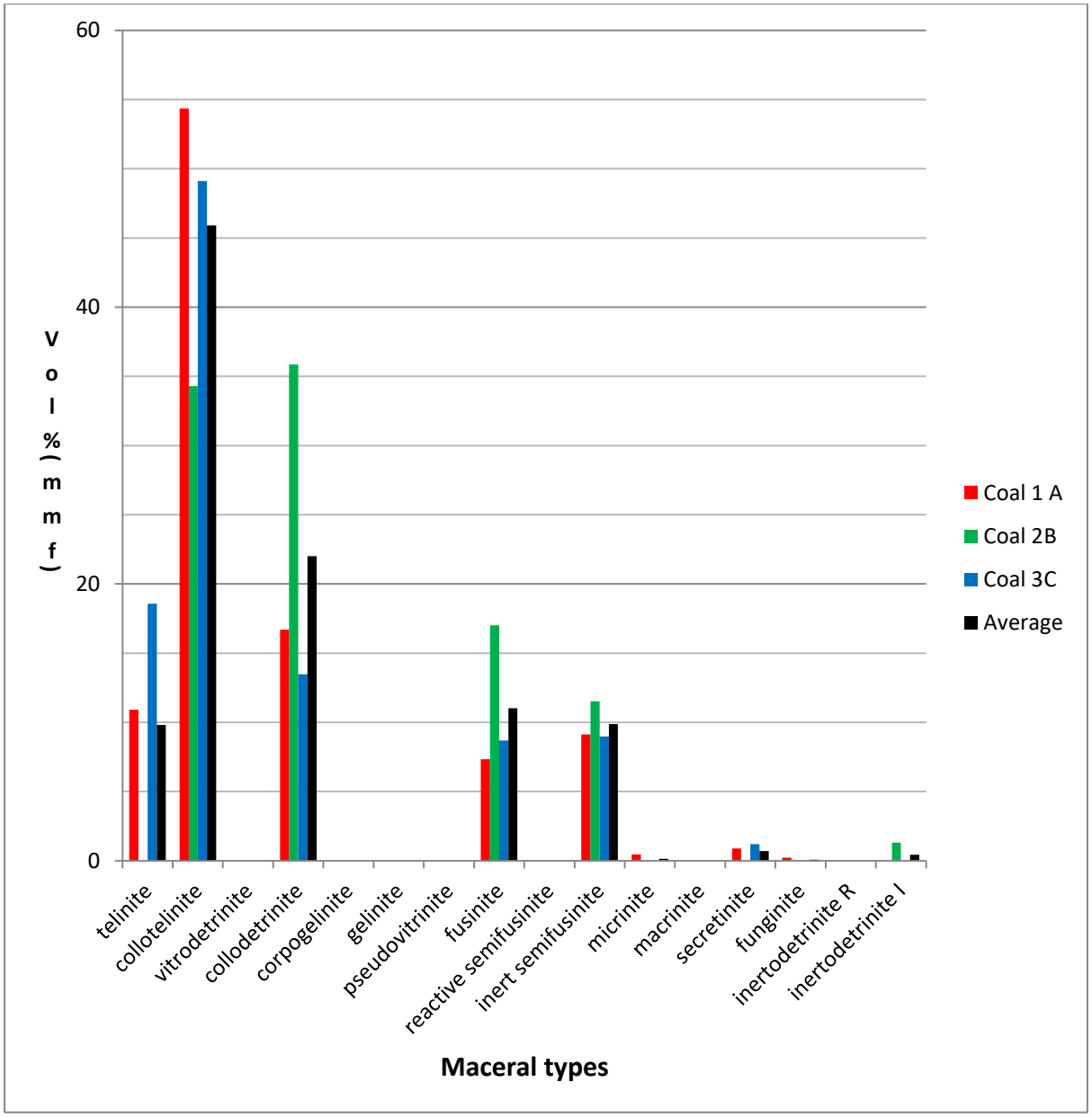

Figure 4.5: Maceral types in Mushithe coal.

The coal samples observed to be rich in vitrinite and low in inertinite, while liptinite group macerals were absent (Fig. 4.5). The samples were observed to be weathered with cracks being evident in all analysed samples as shown in Coal 1B (Fig. 4.7), Coal 2A (Fig. 4.8) and Coal 3C (Fig. 4.9). The mineral content appears low and alteration minerals were also observed.

Table 4.4: Maceral group summary in coal (% by Volume)

	Vitrinite	Inertinite	Liptinite	Total reactive macerals
Coal 1B	81.96	18.04	0.00	81.96
Coal 2A	70.16	29.84	0.00	70.16
Coal 3C	81.14	18.86	0.00	81.14
Average	77.75	22.25	0.00	77.75

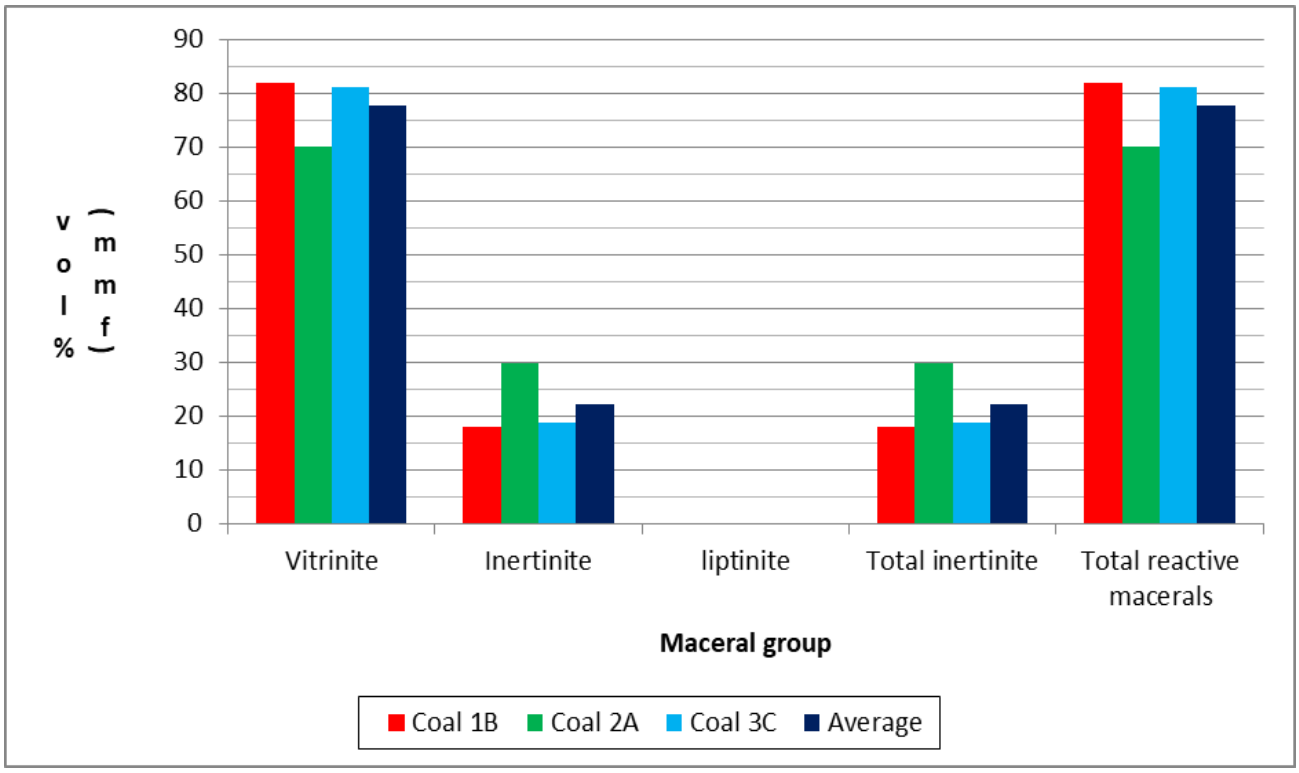

Figure 4.6: Mineral matter free maceral group.

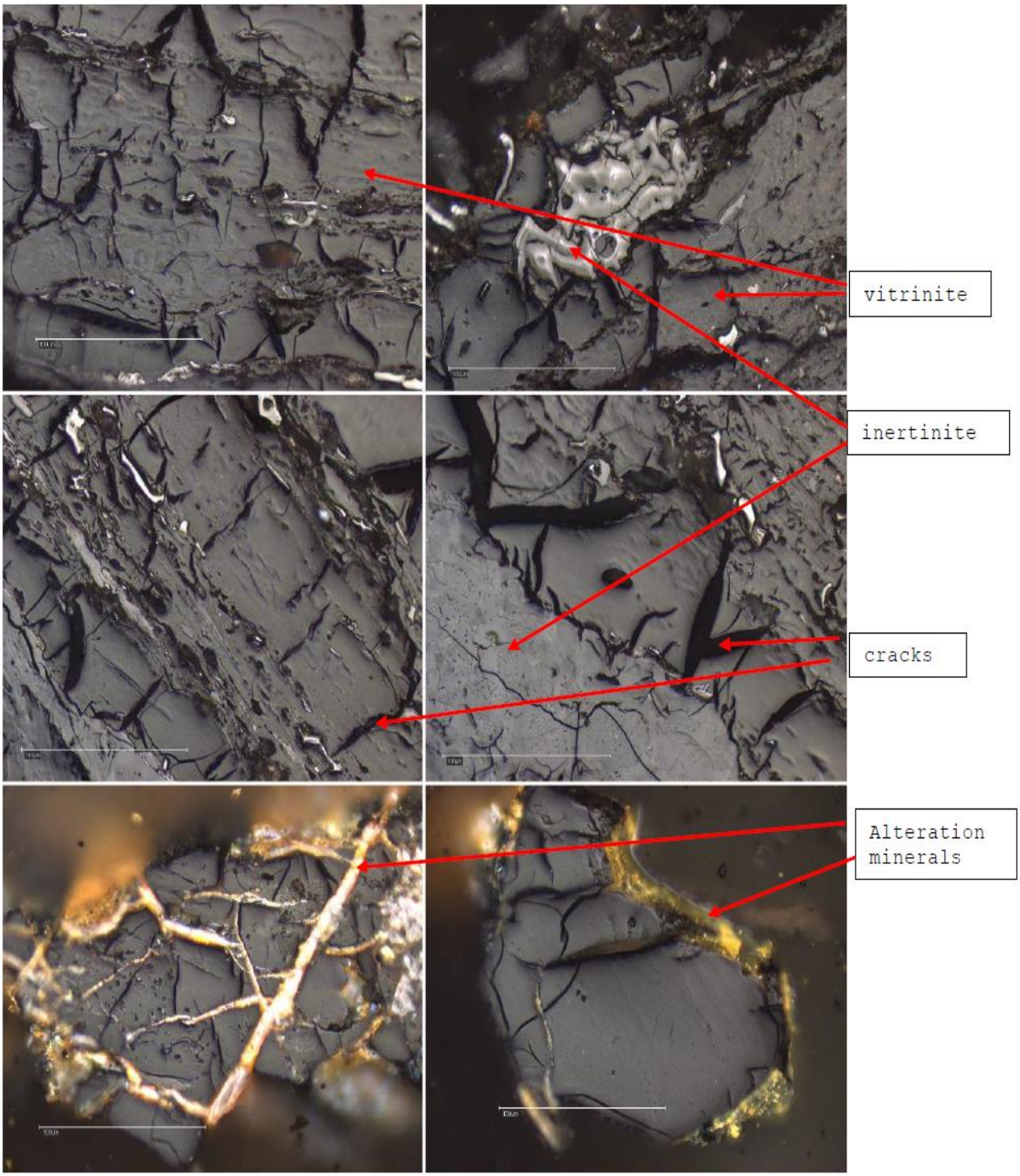

Figure 4.7: micrographs of Coal 1B showing Vitrinite, Inertinite macerals and altered minerals, taken at a magnification of x500, under reflected light using an oil immersion lens.

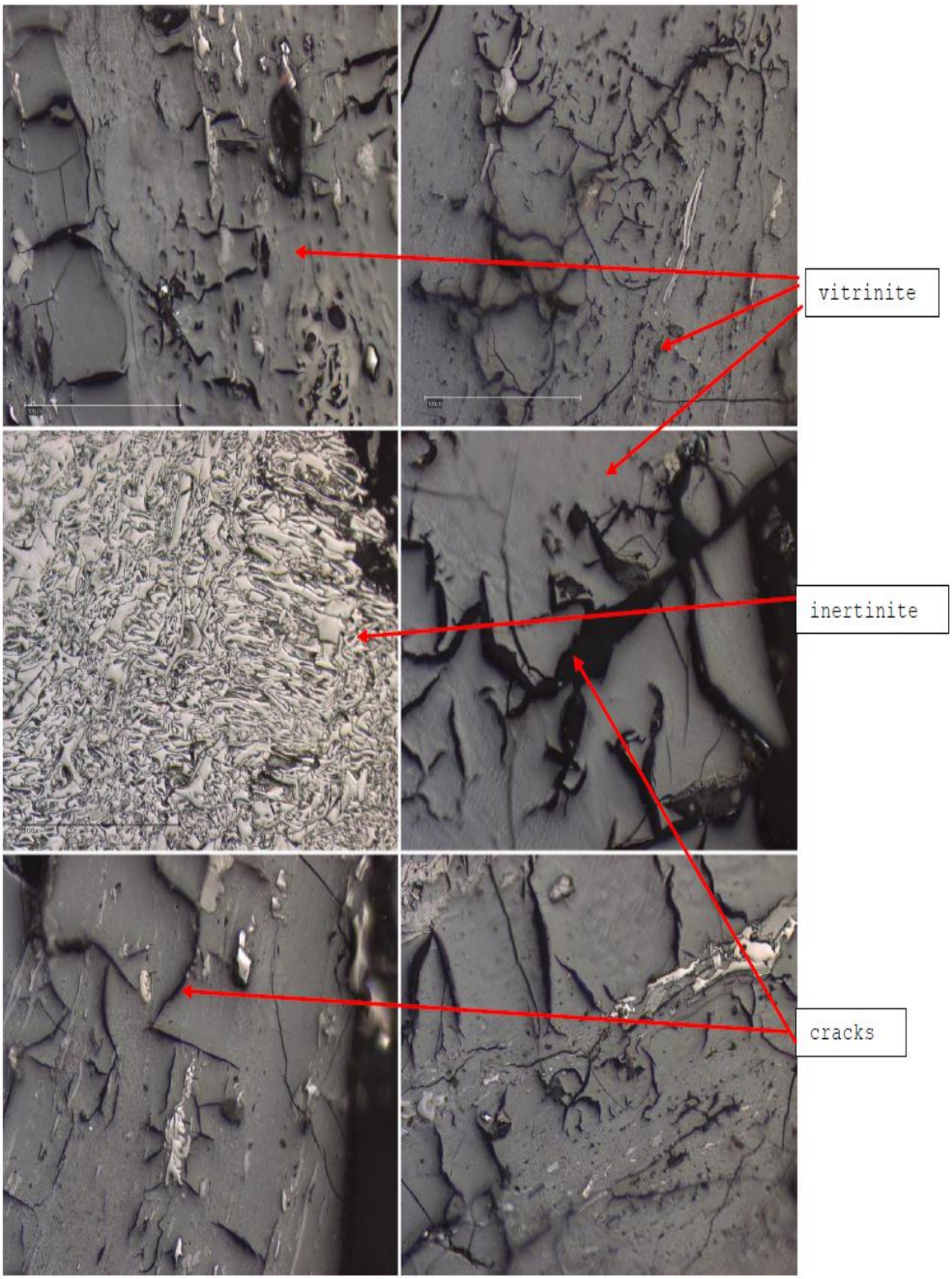

Figure 4.8: Micrographs of Coal 2A showing Vitrinite, Inertinite macerals and alteration minerals, taken at a magnification of x500, under reflected light using an oil immersion lens.

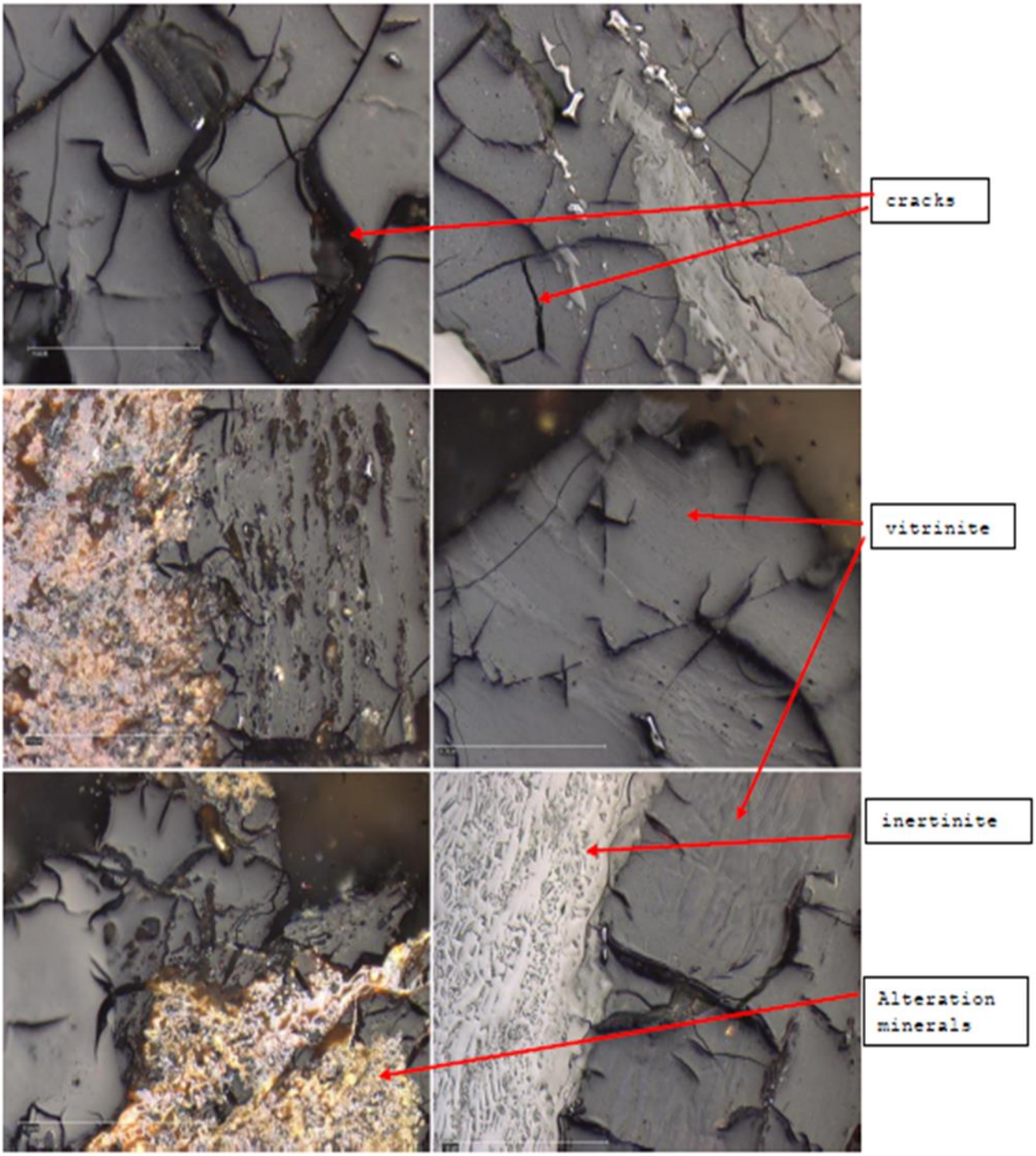

Figure 4.9: micrographs of Coal 3C showing Vitrinite, Inertinite macerals and alteration minerals, taken at a magnification of x500, under reflected light using an oil immersion lens.

The following minerals were identified petrographically in the coal samples (Fig. 4.9): silicates, sulphides and carbonates. The silicates identified were clay minerals and quartz with average value of 8.23 vol% and 0.33 vol% respectively. The sulphide mineral identified was pyrite with 1.57 vol%. Carbonates and other minerals had 0.07 vol% and 0.02 vol% respectively. Clay minerals and pyrite were the most dominant minerals and this is consistent with the prevailing enrichment of TiO_2 and Fe_2O_3 in coal. Coal 3C had clay with 14 vol% whereas; Coal 2A had the least clay at 3.8 vol%. Quartz was most dominant in Coal 3C with a value of 0.5 vol% whereas the least quartz was in coal 1B with 0.2 vol%. Pyrite ranged between 0.5 vol% and 2.2 vol% with the highest abundance in Coal 3C. The presence of cracks and mineral infilling can be attributed to faulting in the area as well as the brittleness of vitrinite.

The mineral matter was identified as infilling cracks as well as located in vitrinite material as cell or pore structure infilling. The cracks in vitrinite are due to its brittleness and the presence of mineral matter in the structure is indicative of formation during peat formation.

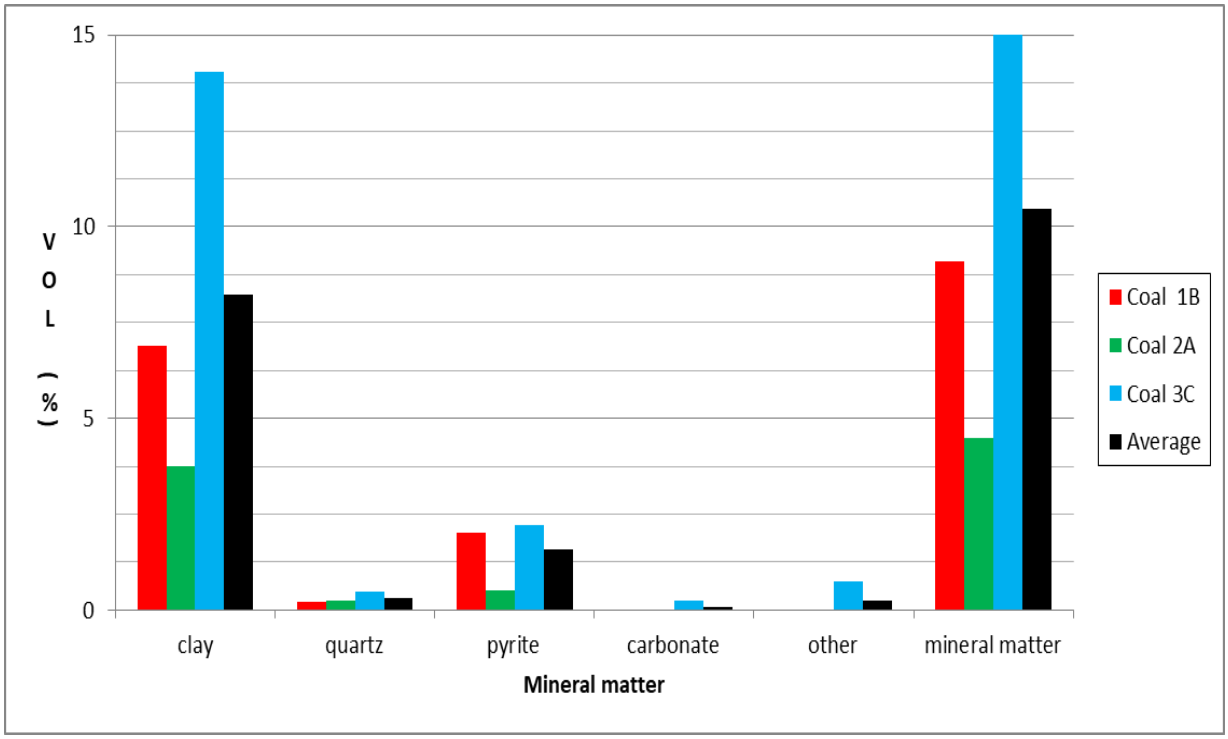

Figure 4.10: Interpretation of mineral matter in coal.

Mushithe coal samples coal occurrence had vitrinite reflectance ranging between 0.738% ROV and 1.172% ROV (Fig. 4.10). Coal 1B had average vitrinite reflectance of 0.94%, Coal 2A had vitrinite reflectance 1% furthermore Coal 3C had 0.95%. According to Thomas (2013) high vitrinite reflectance indicates higher coal rank. The disparity in vitrinite reflectance indicates that Coal 2A is more mature than the other two analysed samples. A comparison of vitrinite reflectance from Tshikondeni coal mine (Mphaphuli, 2017) with the analysed coal from Mushithe indicates that Tshikondeni coal with mean reflectance of 1.23% is greater than the mean reflectance of 0.96% for Mushithe coal. This is consistent with Sparrow (2012) and Hancox and Gotz (2014) who noted that coal rank decreases from east to west across the Soutpansberg coalfield.

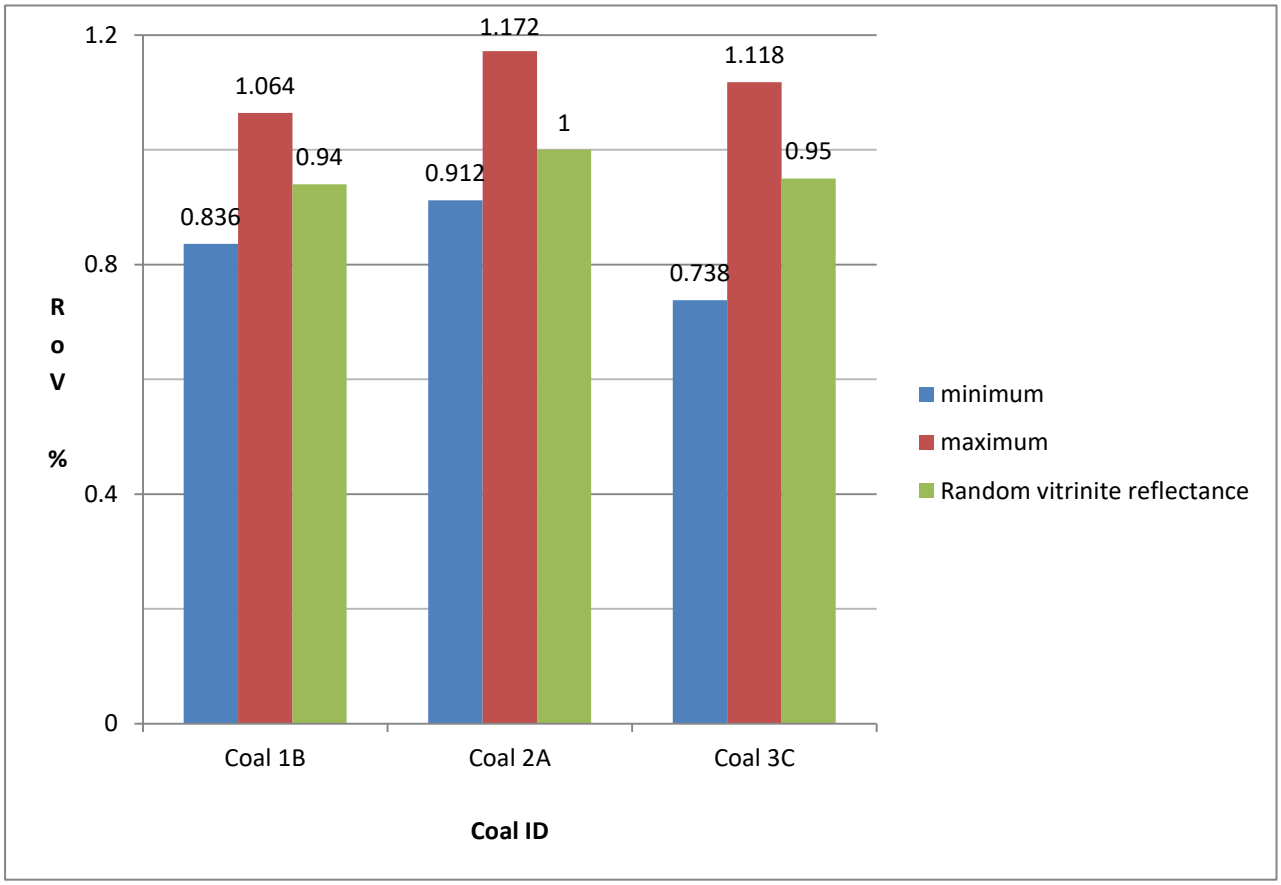

Figure 4.11: Histogram representing vitrinite reflectance data.

4.1.5 Geochemical composition analysis of coal

The geochemical dataset for coal is presented in Appendix B.1. The average data from Upper Continental Crust (UCC) was used to determine enrichment and using the following formula (Taylor and McLennan, 1985):

$$Enrichment = \frac{Value\ from\ study}{value\ from\ UCC}$$

Enrichment value greater than 1 indicated enrichment whereas values below 1 indicated depletion.

Major Oxides

Geochemical data from appendix B.1 was used to graphically represent major oxides (Fig 4.12) as well as enrichment compared to UCC (Fig 4.13)

The bulk chemical composition of coal samples revealed the occurrence of the following major oxides :SiO_2, Al_2O_3, Fe_2O_3, MgO, CaO and Na_2O as well as minor oxides of TiO_2, MnO, K_2O and P_2O_5 (Fig. 4.11).The Mushithe coal was dominated by the presence of SiO_2, Al_2O_3 and Fe_2O_3 with average of 24.16%, 7.69% and 4.58% respectively.

TiO_2, Fe_2O_3 and P_2O_5 were the most abundant oxides at Mushithe relative to UCC values (Fig. 4.13) and this enrichment can be corroborated by the prevalence of clay minerals and pyrite in the coal noted in petrographic study of coal.

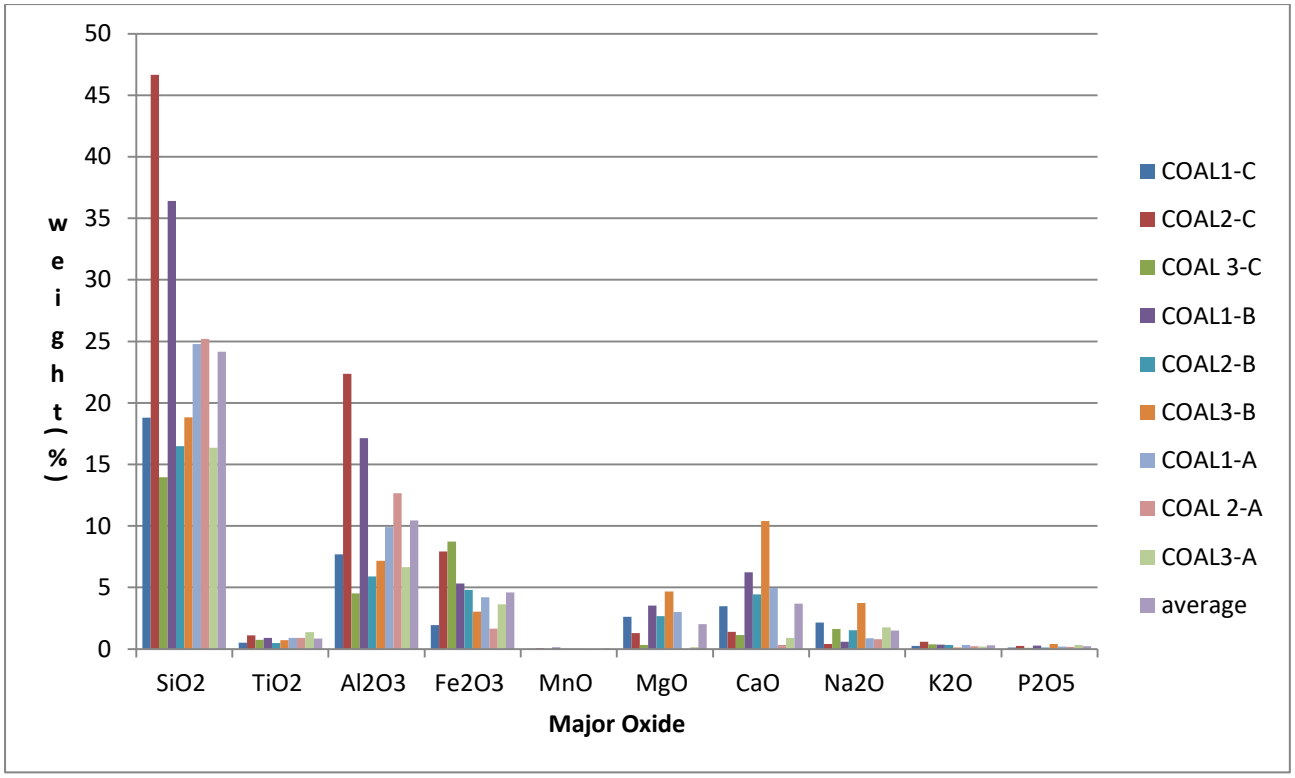

Figure 4.12: Major element oxides present in coal samples.

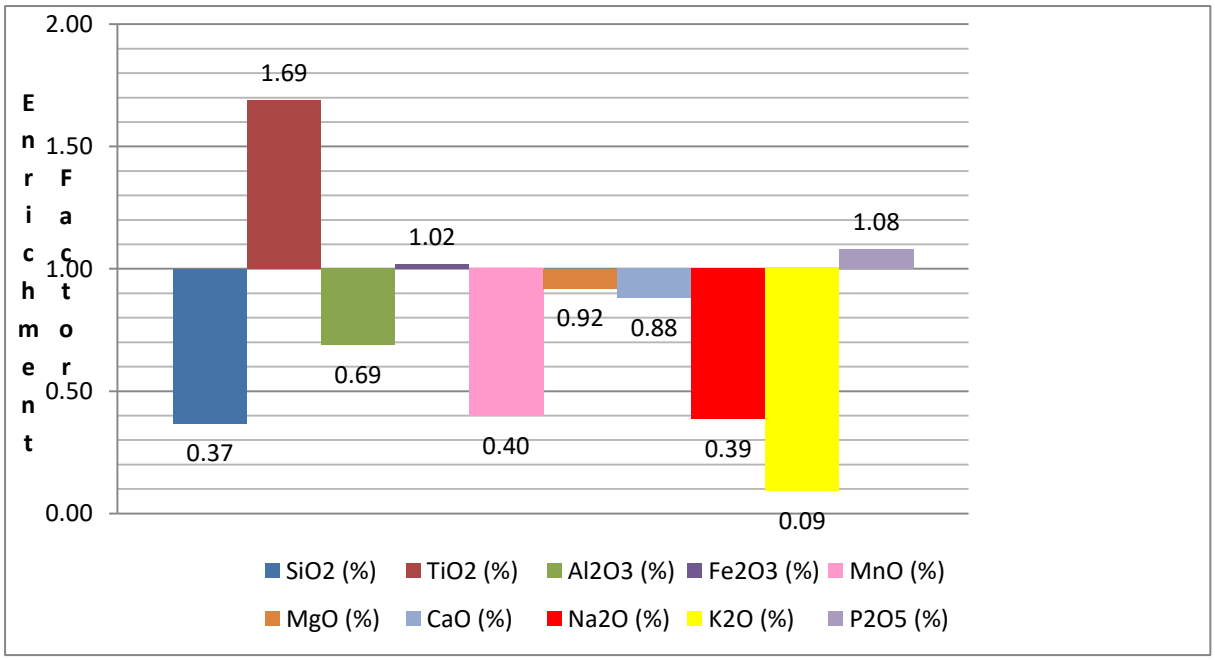

Figure 4.13: Major oxide enrichment of Mushithe coal relative to UCC.

Trace elements

Trace elements were sub-divided into the following groups to allow for more efficient analysis: transition metals, high-field strength elements, alkali and alkaline-earth elements and rare earth elements (Taylor and McLennan, 1985).

Geochemical data from appendix B.1 was used to graphically represent major oxides (Fig 4.14) as well as enrichment compared to UCC (Fig 4.15)

Elements with concentration of below 100 ppm are classified as trace elements whereas those with concentration of above 100 ppm are classified as minor elements (Swaine, 1990).

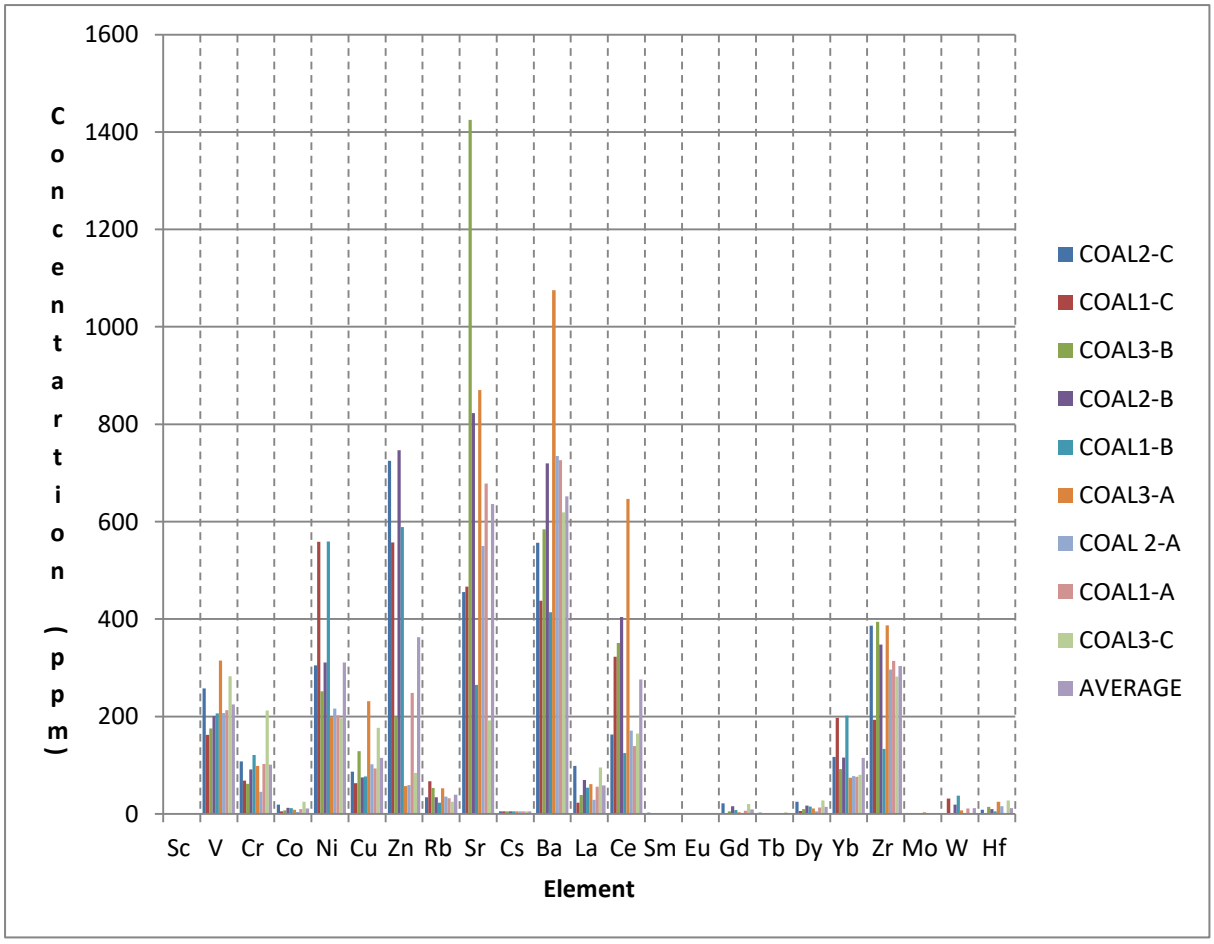

Figure 4.14: Trace element concentration in coal (ppm).

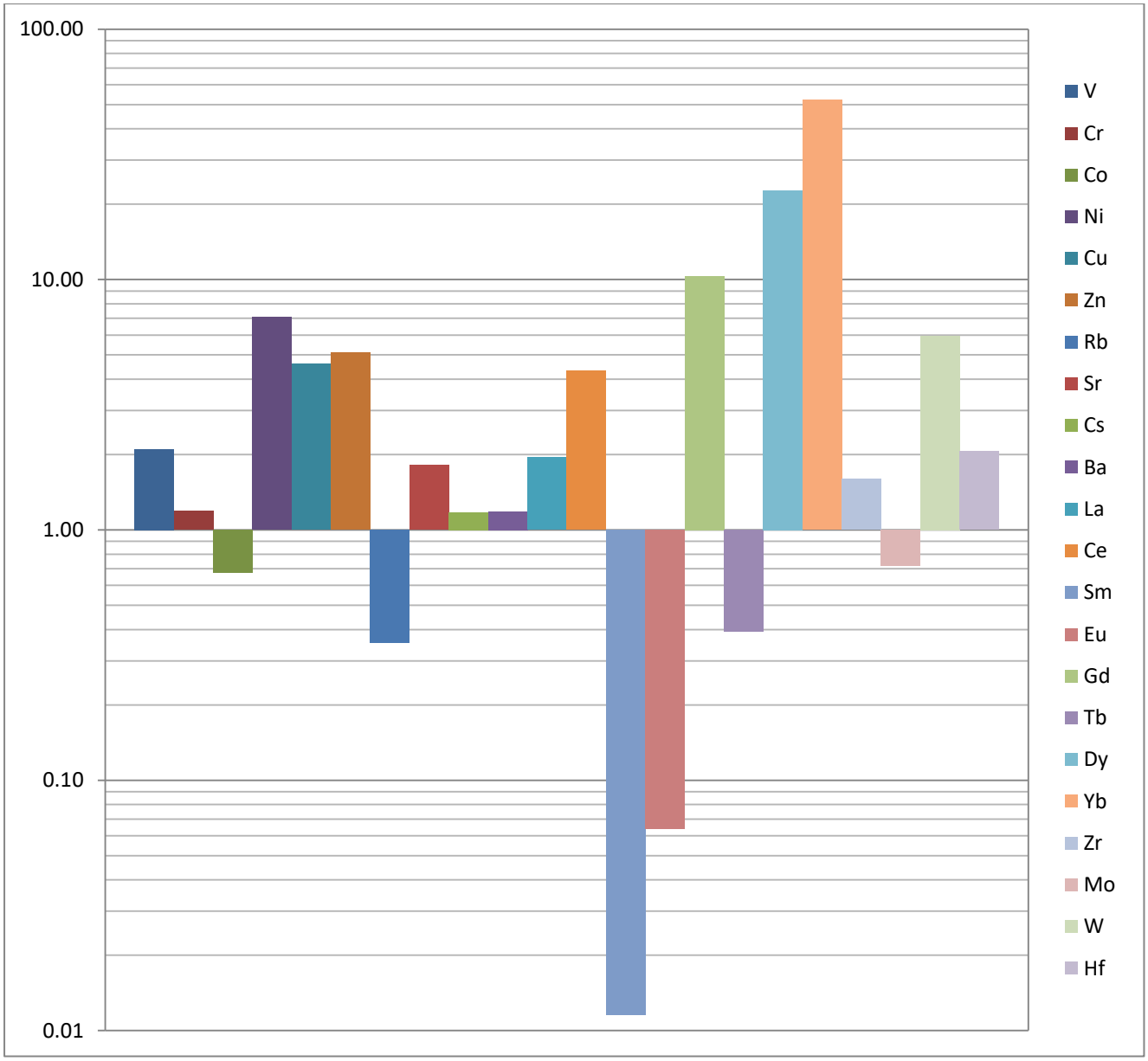

Figure 4.15: Enrichment factor of trace elements in coal (ppm) relative to UCC.

a) Transition metals

The following elements are classified as transition elements: V, Cr, Co, Ni, Cu and Zn.

V, Cr, Ni, Cu and Zn are present in minor concentrations within coal conversely; Co and Sc are present in trace concentrations. The transition elements are present in the following trend within coal: Zn > Ni > V > Cu > Cr > Co > Sc ranging between 363 ppm and 0.33 ppm(Fig 4.14). All the above transition elements are enriched in

coal with the exception of Co which is only enriched in sample Coal 2C and Coal 3C (Fig. 4.15). Ni is the most enriched element in the coal samples relative to UCC with an enrichment factor of 7.07(Fig 4.15). The abundance of Ni can be attributed to the presence of sulphide mineralisation particularly pyrite as well as the presence of detrital silicates, in particular clay minerals (Swaine, 1990). The enrichment of Co within Coal 2C and Coal 3C can be associated with the greater clay content due to the presence of shale partings on the samples.

b) High-field strength elements

The following elements are classified as High field strength elements: Zr, Mo, W, Hf

All the high-field strength elements are present as trace elements albeit for Zr. These elements follow the following trend in coal Zr > Mo > W > Hf (Fig. 4.14). Only Mo is depleted whereas W is the most enriched with an enrichment factor of 5.94. However the enrichment of High-field strength elements in coal is erratic (Fig. 4.15). And this may be affected by leaching as W is soluble in alkaline water. The abundance of Zr can be associated with the presence of detrital silicates as well as its adsorption by organic matter (Swaine, 1990).

c) Alkali and alkaline-earth elements

The following elements are classified as alkali and alkali-earth elements: Rb, Sr, Cs and Ba.

Sr and Ba are present in minor concentrations within coal; conversely Rb and Cs are present in trace concentrations. The alkali and alkali-earth elements are present in the following trend within coal: Ba > Sr > Rb > Cs ranging between 651.96 ppm and 5.40 ppm (Fig. 4.14). All the alkali and alkaline-earth elements are enriched in coal with the exception of Rb. Sr is the most enriched element in the coal samples relative to UCC with an enrichment factor of 1.81 (Fig 4.15). The enrichment of Sr can be attributed to its affinity for organic matter as well clay minerals. Furthermore Sr can be associated with the presence of carbonates in coal (Swaine, 1990).

d) Rare earth elements

The following elements are classified as rare earth elements: La, Ce, Sm, Eu, Gd, Tb and Yb.

Ce and Yb are the only REEs present in minor concentrations within coal, while the rest are present in trace concentrations. REE abundance is present in the following trend within coal: Ce > Yb > La > Dy > Gd > Tb > Sm>Eu ranging between 276.32 ppm and 0.29 ppm (Fig 4.14). Sm, Eu, and Tb are depleted in the coal samples whereas Ce, Dy, and Yb are the only enriched REEs. Yb is the most enriched REE with an enrichment factor of 52 (Fig 4.15). Yb is however an excessive REE and its abundance is indicative of felsic origin of the sediments (Swaine, 1990). Of the studied REEs the only critical element that is enriched is Dy with and enrichment factor of 14.56.

4.1.6 Coal classification

The coal from the Mushithe was ranked bituminous rank C-B according to the UNECE (1988) main coal classification which is based on the vitrinite reflectance as well as calorific value of coal samples. Coal 2B was ranked medium B bituminous, whereas Coal 1A and Coal 3C were ranked medium C bituminous. The coals ranked lower than the Tshikondeni coal that was ranked bituminous rank C – A. (Mphaphuli, 2017).

According to the domestic coal specifications (Steyn and Minnitt, 2010) Mushithe coal was classified as below grade D since it had calorific below 24.5 MJ/kg. Coal 2A had the highest calorific value of 20.99 MJ/kg. However, Coal 3C had ash content characteristic of coals graded D and Coal 2A had very low ash content which is characteristic of grade A. The sulphur content of Mushithe coal was below 1% typical of grade A coals.

This is consistent with the findings of Mphaphuli (2017) who noted that coal ranged between bituminous medium rank C to medium rank A. Malaza (2013) classified coals in the Tshipise-Pafuri area as bituminous in rank. Furthermore, Mphaphuli (2017) classified the coal in the Soutpansberg Coalfield as below grade D.

4.1.7 Depositional environment of coal

Petrographic indices were utilised to infer the depositional environment of coal from the Mushithe coal occurrence (Table 4.5). These indices were calculated using maceral data in appendix A. Tissue preservation index (TPI) and gelification index (GI) were used to reconstruct the depositional environment of coal, using Diessel (1986) facies model. The Vitrinite to Inertinite ratio (V/I) as well as oxidising ratio (O/I) were also used to reconstruct the deposition environment.

The indices were calculated using the following formualas (Stach *et al,* 1982) :

$$\text{TPI} = \frac{(\text{tellinite}+\text{collotelinte})+\text{fusinite}+\text{semifusinite}}{\text{collodetrinite}+\text{micrinite}+\text{inertodetrinite}}$$

$$\text{GI} = \frac{\text{vitrinite}+\text{macrinite}}{\text{fusinite}+\text{semifusinite}+\text{inertodetrinite}}$$

$$\text{V/I} = \frac{\text{vitrinite}}{\text{inertinite}}$$

$$\text{O/I} = \frac{\text{inertinite}}{\text{vitrinite}+\text{liptinite}}$$

Table 4.5: Depositional environment indices of Mushithe coal

	Coal 1 B	Coal 2A	Coal 3C
V/I	4.54	2.35	4.30
O/I	0.22	0.43	0.23
TPI	4.77	1.69	6.33
GI	4.97	2.35	4.59

Mushithe coal had V/I value ranging between 2.35 and 4.54, Coal 1B had the highest V/I with 4.54 whereas Coal 2A had the lowest V/I with 2.35. The oxidisation ratio of Mushithe coal ranged between 0.22 and 0.43, Coal 2A had the highest O/I whereas Coal 1B had the lowest O/I (Table 4.5). According to Xu and Feng (2005) V/I values greater than 4 indicate deep overlying water whereas V/I values between 1 and 4 indicate overlying water environments. Furthermore, O/I of less than 0.5 indicate overlying water environment. O/I values for all samples are less than 0.5 indicating

overlying water environments. Albeit for coal 2A all the other coal samples have V/I values greater than 4 indicating deep overlying water.

TPI ranged between 1.69 and 6.33 in Mushithe coal. Coal 3C had the highest TPI index with 6.33 whereas Coal 2A had the lowest TPI index with 1.69. Furthermore, GI index ranged between 2.35 and 4.97. The highest GI was observed in Coal 1B whereas the lowest was observed in Coal 2A. Only sample COAL 2A was utilised to determine coal formation conditions since the other 2 samples plotted outside the TPI range of the TPI-GI model (Fig. 4.14). Based on the model TPI-GI indicates that coal formed in a wet swamp on land. These findings are consistent with the findings of Falcon (2013) who associated vitrinite rich coals with wet or waterlogged conditions. Furthermore these findings are corroborated by Mphaphuli (2017) who found that the coal at the Soutpansberg Coalfield is formed in a wet forest. Malaza (2013) also indicated that the coal in Soutpansberg coalfield was deposited in a fluvial environment.

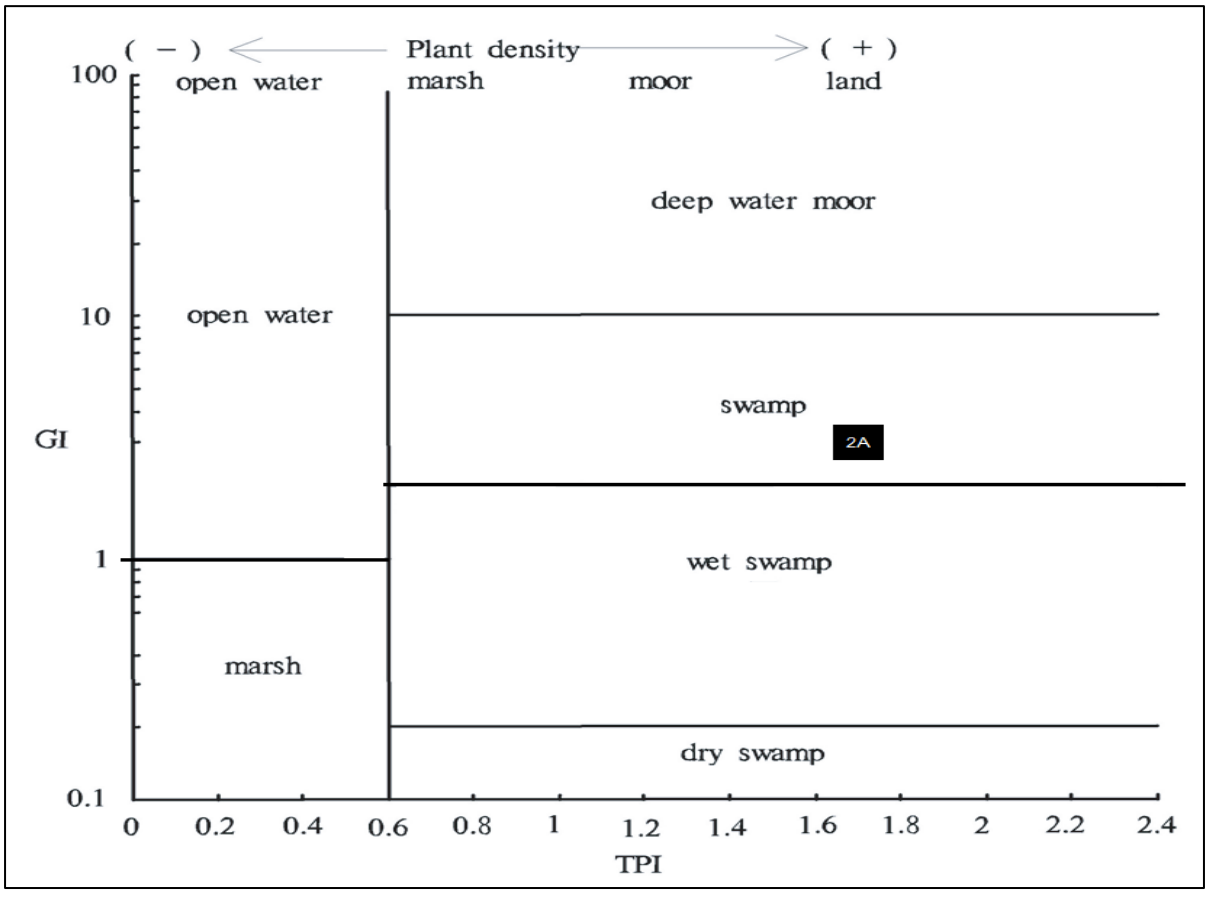

Figure 4.16: TGI – GI model by Diessel (1986) showing Coal 2A.

4.2 Geological map

The following lithological units were encountered at Mushithe coal occurrence (Fig 4.17): sandstone, mudstone, ironstone, shale, calcrete, dolerite, quartzite and quartz vein. Mudstone and sandstone were the most widely distributed lithological units and were encountered as interbedding. Mudstone was in contact with all encountered lithologies albeit for ironstone. The general strike direction of the lithological units was NE direction.

Sandstone was prominent throughout the study area. It had a gradual contact with quartzite and with shale, ironstone and calcrete as well as interbedded with mudstone. The sandstone in the north was coarser than those in the south. Both the sandstone and mudrock had no visible signs of weathering.

Quartzite was found adjacent to sandstone and dolerite and this can attributed to contact metamorphism of sandstone by dolerite to form quartzite. All quartzite outcrops were striking in the NE direction. The outcrops of quartzite were very competent with quartz veins in them; these veins can be attributed to metasomatism during metamorphism.

Shale was encountered further SW of the study area with visible signs of weathering. It was very fissile and most encounters were along streams. The Mushithe coal bed was interbedded with shale. The shale also had interbedding with sandstone as well gradual contact with quartzite, localised ironstone was found with the shale.

Dolerite outcrops were localized outcrops as well as weathered with cracks and iron oxide. Quartzite and mudrock were in contact with dolerite whenever it was encountered. The occurrence of dolerite along the quartzite is indicative of contact metamorphism of sandstone, the localised nature of the dolerite outcrops indicate a dyke.

Calcrete was encountered once towards south in the area. It was in gradual contact with shale and mudstone. The outcrop was eroded and highly weathered. Ironstone was also encountered towards the SW direction. Both outcrops were very incompetent and highly weathered.

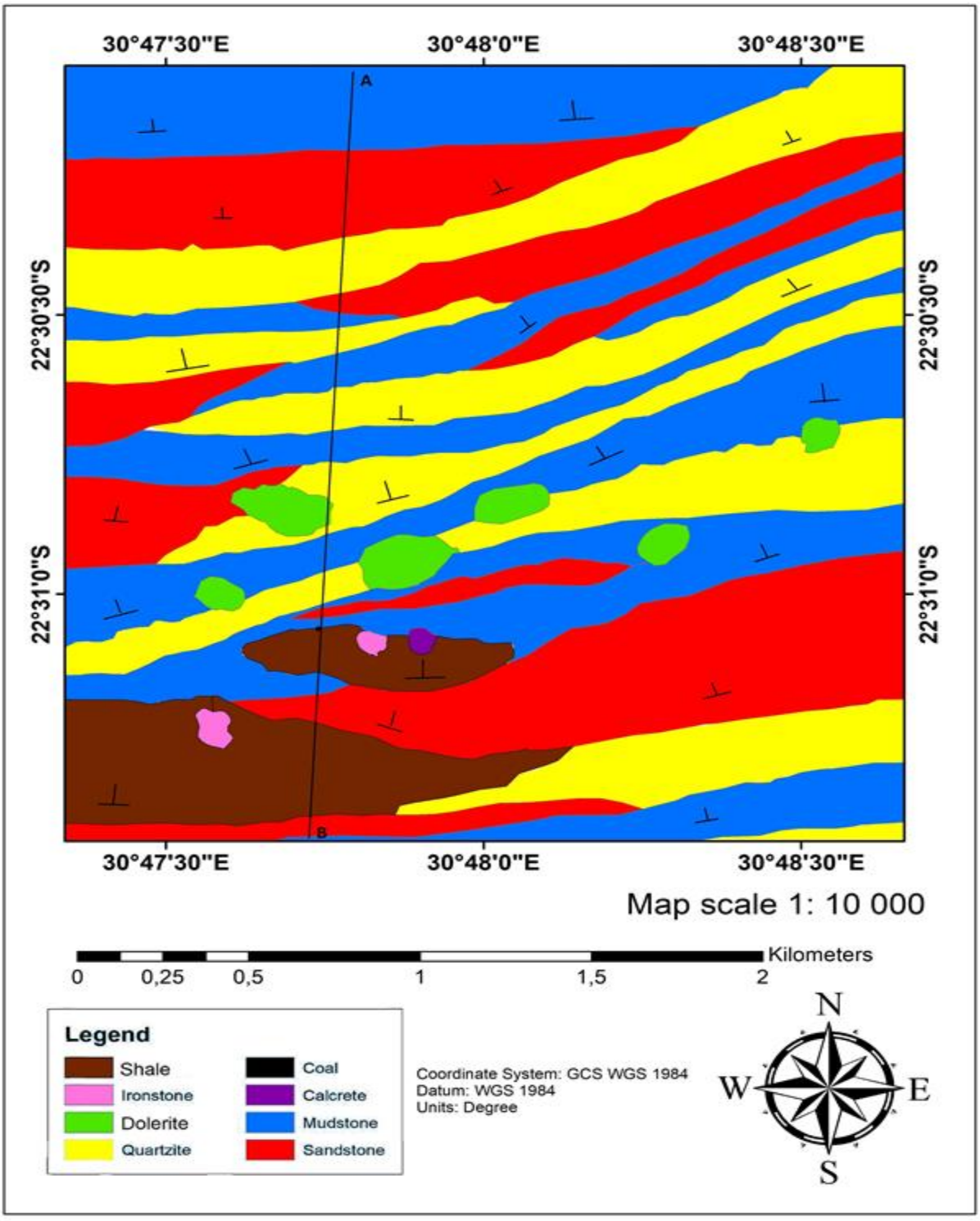

Figure 4.17: Geological map of Mushithe area.

The cross section (Fig 4.18) of the Mushithe coal occurrence geological map was done from point A to point B in the geological map (Fig. 4.17), this was done to allow

representation of all lithologies. Lithological units were plotted on the cross section using their dip angles and dip directions as well their altitudes. This helped to give a representation of how lithologies are below the surface.

From the cross section the interbedding of sandstone with mudstone is evident as well as the interbedding of shale with coal. The dolerite dyke intersects with the coal occurrence which resulted in devolatilization as indicated by low carbon and high fixed carbon associated with contact and/or proximity to dolerite dykes , the samples already have signs of heat and this is also evident in the low carbon content of the coal which may indicate devolatilization of coal.

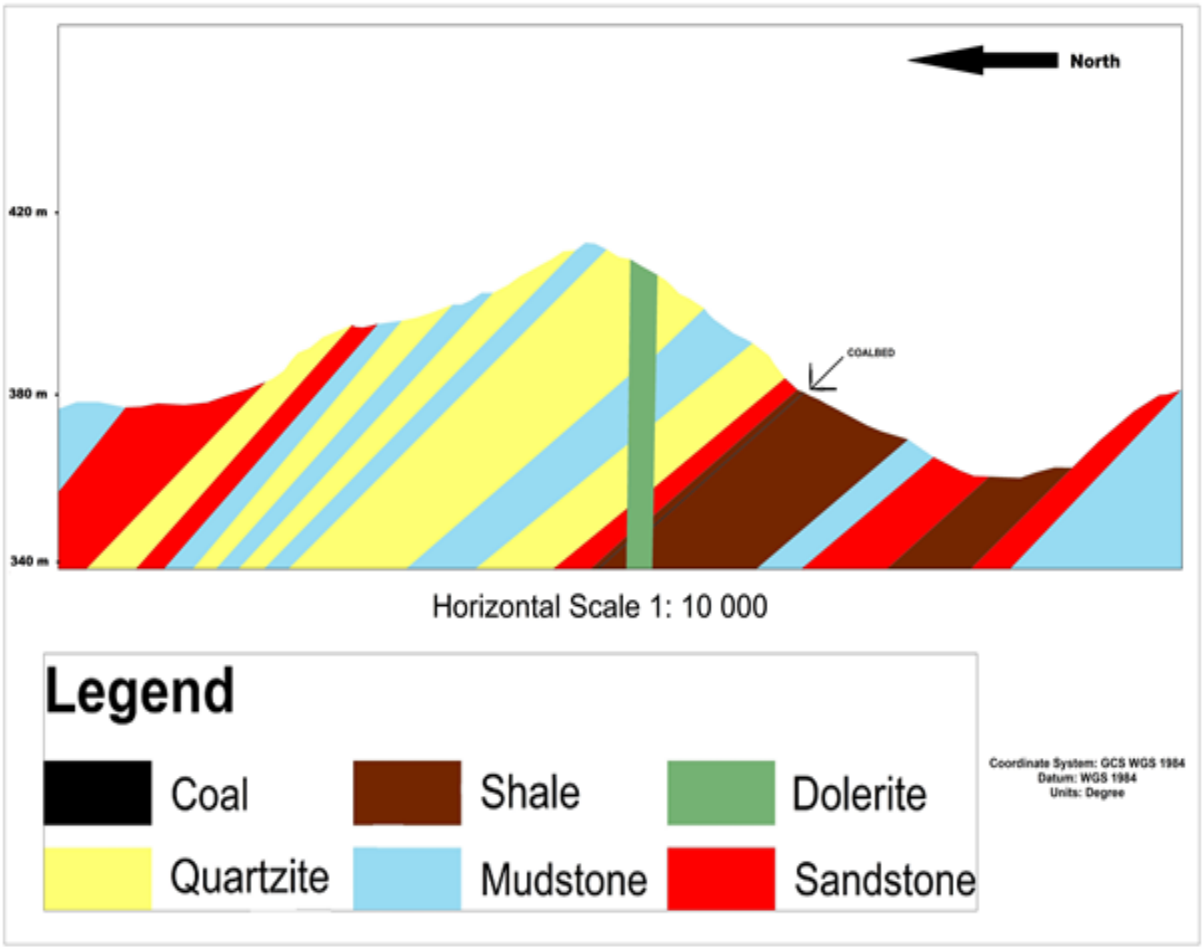

Figure 4.18: Cross section of the geological map of Mushithe area.

4.3 Description of rocks

The rocks were described both macroscopically and microscopically. Macroscopic analysis was done using a hand lens through observation and insight. Attention was paid to colour, mineralogy, texture, grain size and structures. Microscopic analysis was done using Olympus BX51 petrographic microscope to identify optical properties in the rocks. Detailed description of the rocks that were identified in the study area is presented below.

Red mudstone

The rock sample was observed to be reddish to brown in colour and it had clay sized grains which felt very smooth by merely rubbing with a finger and individual grains couldn't be distinguished using the naked eye. It was highly competent and it was difficult to acquire the sample. It was composed of clay minerals and some carbonaceous material. The red colour can be attributed to the presence of iron oxide as a colouring as a cementing agent (Plate 4.1).

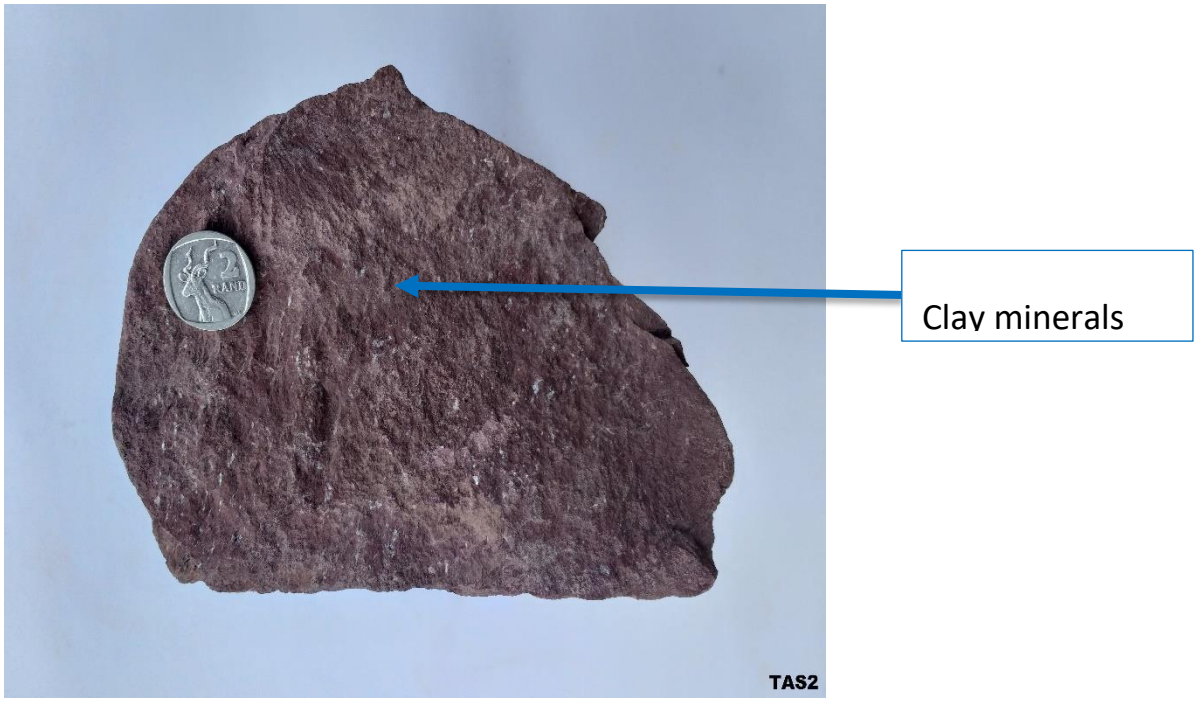

Plate 4.1: Red mudstone specimen showing clay sized grains and clay minerals.

In thin section, the rock sample exhibited a very fine texture with grain sizes of clay minerals less than 75 µm. Serpentine grains showed colour range from colourless to pale green and low pleochroism. Some clay minerals and the iron oxides were not clearly visible and distinguished since most of the clay minerals are opaque in thin section (Fig. 4.19).

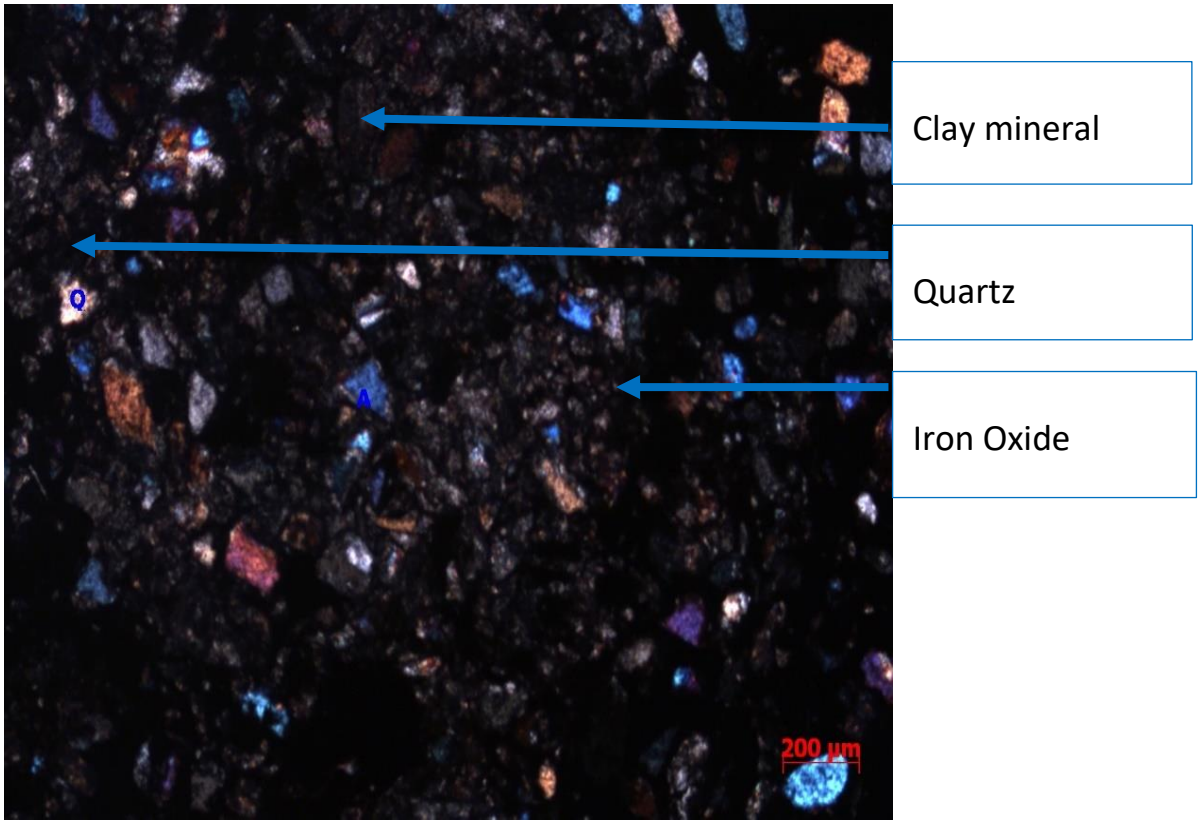

Figure 4.19: Photomicrograph of red mudstone in thin section showing quartz grains with fine texture.

Quartzite

The sample was light brown in colour with quartz veinlets. It was dominated by quartz grains although some shiny flaky minerals could be viewed using a hand lens. The rock was highly competent making collecting the sample from the outcrop a tough exercise. No form of layering visible indicating no foliation. The texture was equigranular and the rock was most probably metamorphosed from sandstone of high mineralogical maturity that was well sorted giving rise to the equigranular texture (Plate 4.2).

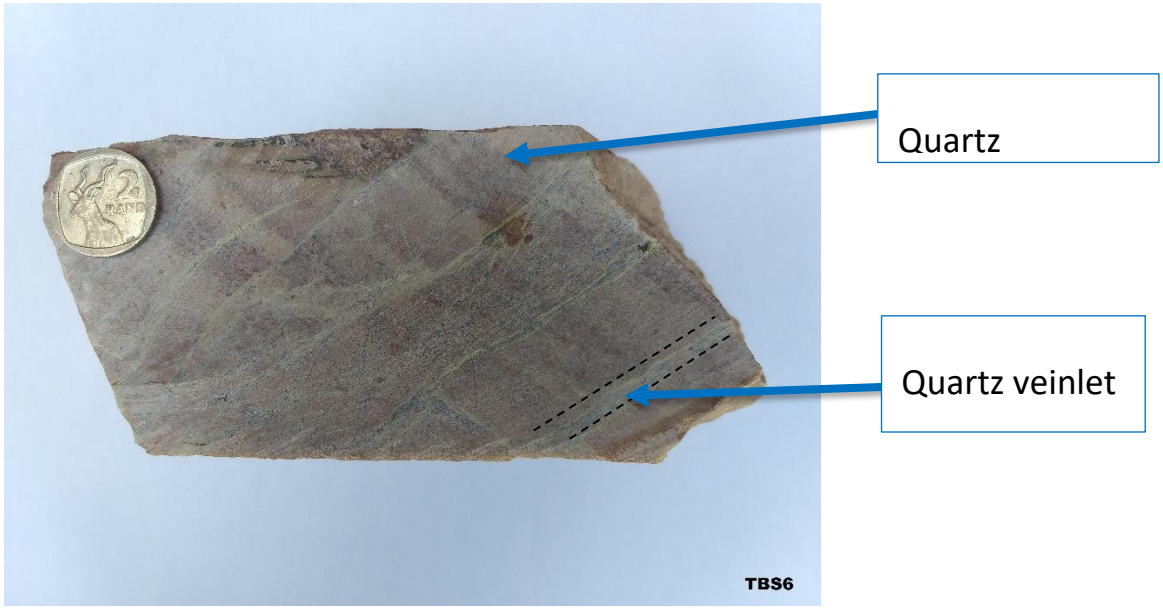

Plate 4.2: quartzite specimen showing interlocked grains and quartz veinlet.

In thin section, the rock was observed to consist of anhedral quartz grains. Quartz veinlets were noticeably visible with thickness of about 100 µm to 200 µm. It showed low relief and birefringence colours. Grain sizes of quartz were ranging between 256.22 µm and 1000 µm. Biotite was observed as brown in colour showing little evidence of alteration with grain sizes ranging between 188.20 µm and 462.80 µm (Fig. 4.20).

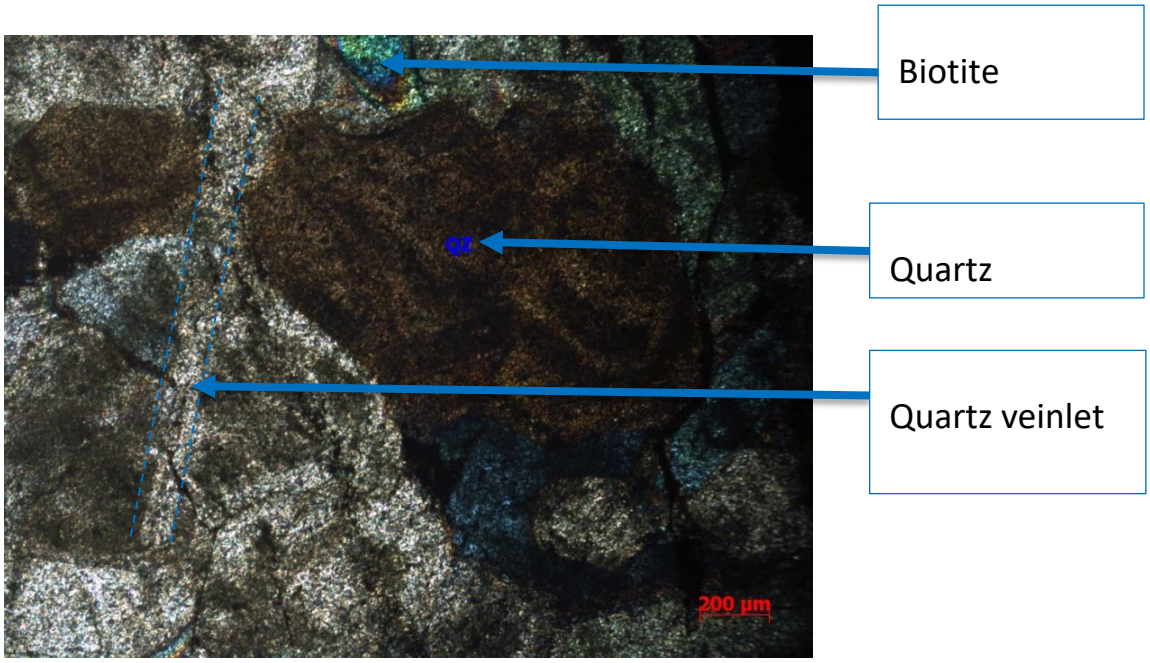

Figure 4.20: Photomicrograph of quartzite in thin section showing with tiny grains and quartz veinlet.

Calcrete

The rock sample was observed to whitish to be light grey in colour and very dull with very fine texture which felt very smooth by merely rubbing with a finger. Individual grains were not apparent. The outcrop was competent and highly weathered with small lateral extent. It was dominated by carbonate minerals as evidenced by the white colour and erosion by water (Plate 4.3).

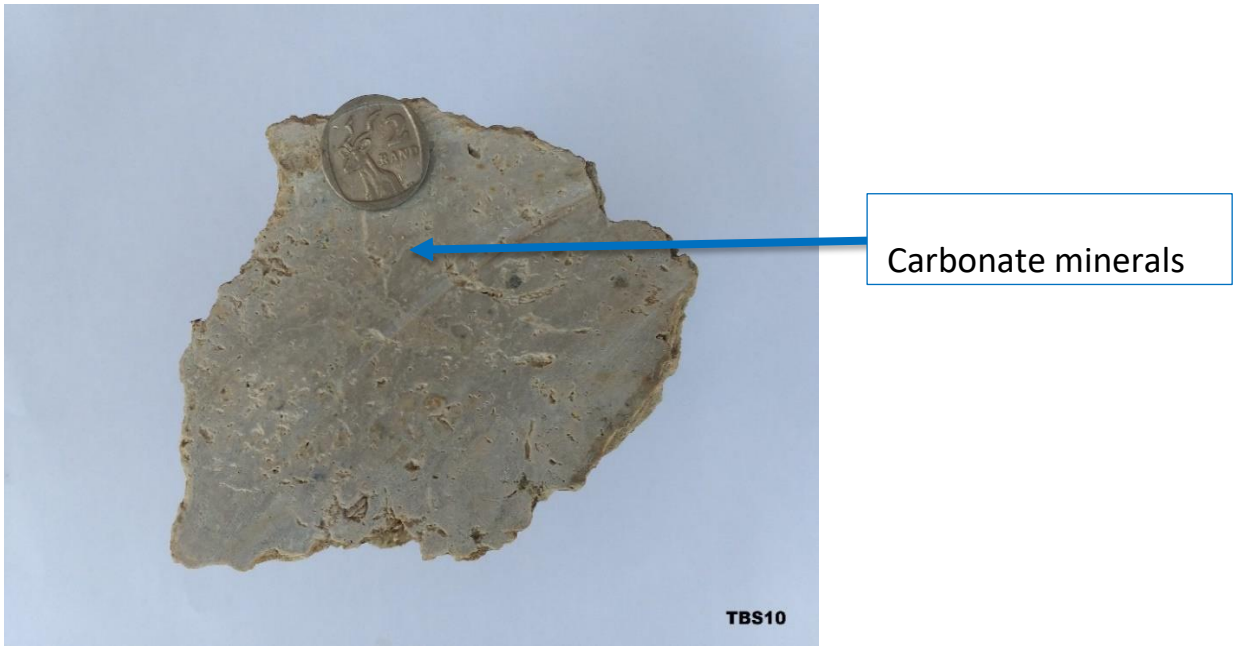

Plate 4.3: Calcrete specimen containing carbonate minerals with very fine texture.

In thin section, the rock sample was observed to contain calcite which was colourless as well as carbonate groundmass. Some grains of these calcite showed lamellar twins. Calcite was also recognized by cleavage, extreme high birefringence and change of relief with the stage being turned. The rock sample showed very fine texture with grain sizes less than 75 µm (Fig. 4.21).

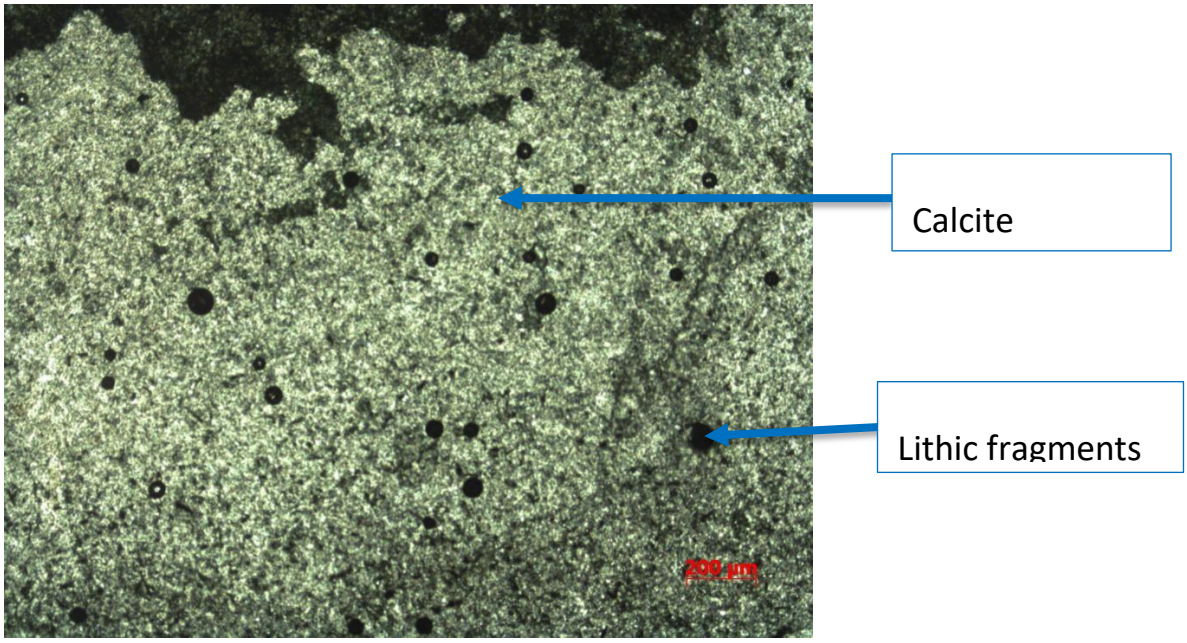

Figure 4.21: Photomicrograph of calcrete in thin section carbonates with fine grained calcite.

Arkosic Sandstone

The sample was observed to be brownish in colour and coarse grained. Some dark minerals were observable on the fresh part of the sample which was identifiable as feldspar and quartz grains together with some shiny flaky minerals identified as micas (Muscovite and Biotite). The grains were almost of the same size and for this reason they were said to well sorted. Mineral grains were angular in shape and they were sand sized. Due to the grains being angular in shape the rock was describe as being texturally immature although it was well sorted (Plate 4.4).

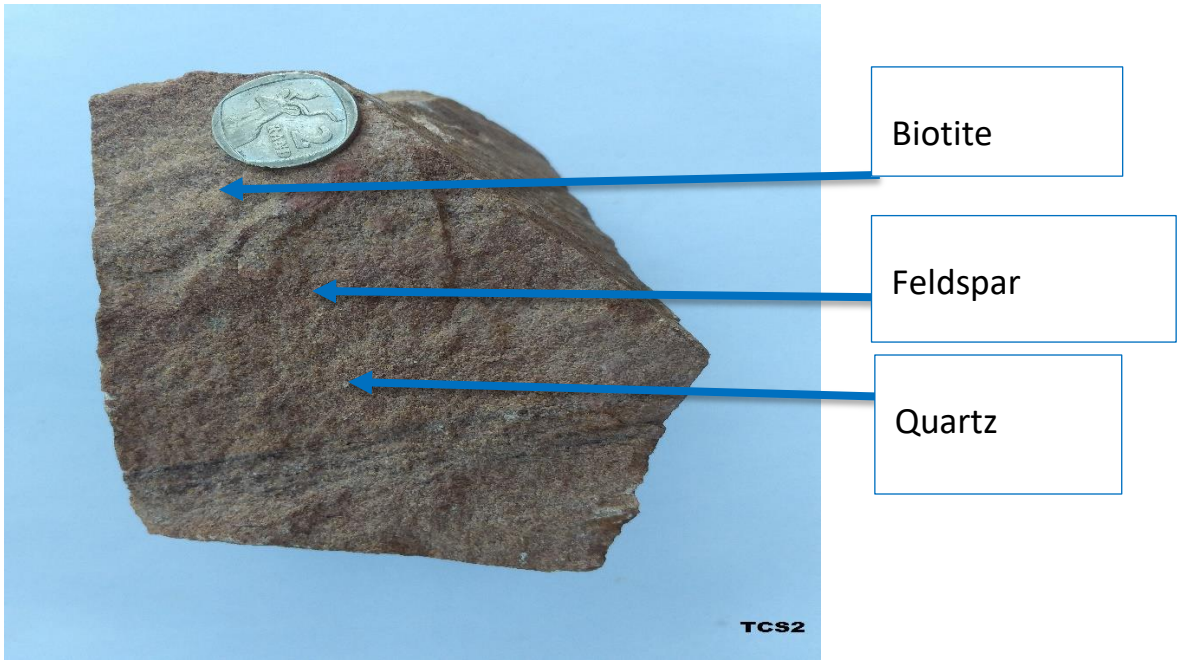

Plate 4.4: Arkosic sandstone specimen with sand sized grains and biotite flakes.

In thin section, the rock sample showed quartz with angular grains and grain sizes ranging from 153.30 µm to 744,64 µm. Plagioclase feldspar showed an albite twinning with an inclusion of biotite within its grains. The rock sample exhibited a medium to coarse texture with about 166.30 µm to 378.60 µm grain sizes of biotite while plagioclase grain sizes were ranging from 212,30 µm to 432.10 µm (Fig. 4.22).

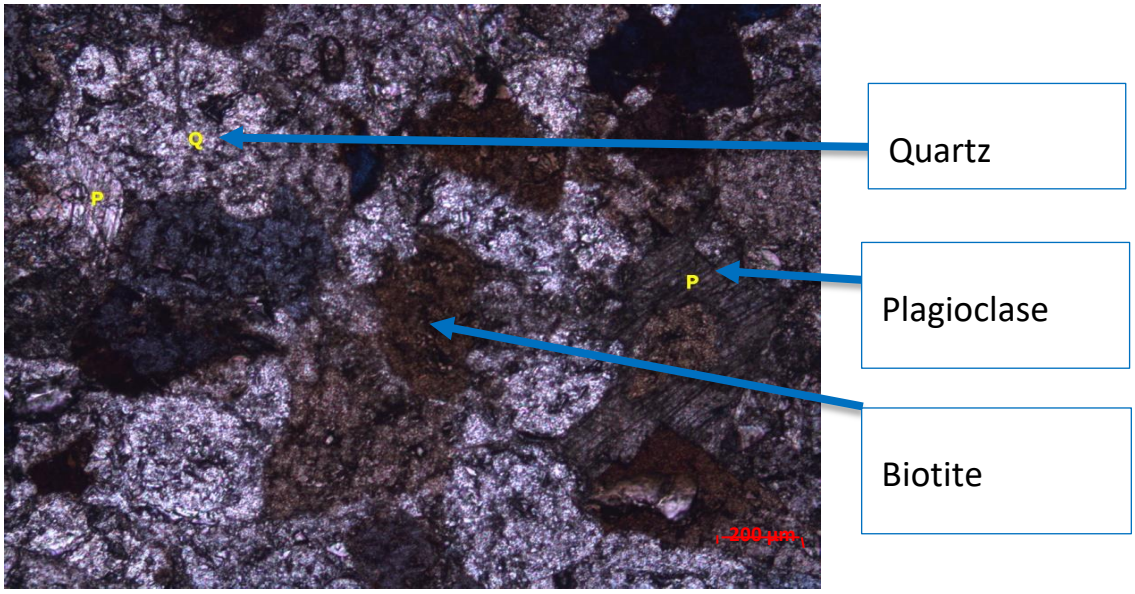

Figure 4.22: Photomicrograph of arkosic sandstone in thin section showing arenaceous texture**.**

Shale

The sample was grey in colour and it was fine grained such that the grains were not visible with the naked eye. It was composed of various amount of clay minerals and Feldspars. It was fissile, i.e. breaking along closely spaced bedding planes. Black colour was also the indication of organic materials (Plate 4.5).

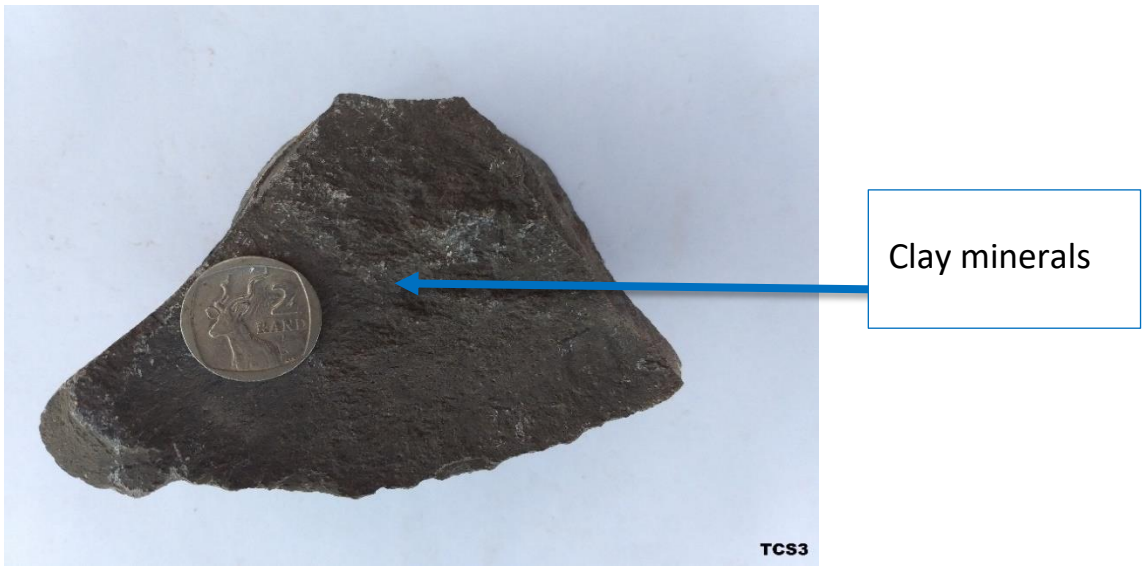

Plate 4.5: Shale specimen showing very fine texture.

In thin section, the rock sample showed different minerals that includes clay minerals, feldspar, quartz and biotite mica. Clay minerals dominated the rock sample with very fine grains. Feldspars were present with light green colour showing no twinning. Quartz mineral showed low relief and low birefringence with no cleavage. Biotite was in brownish colour showing pleochroism and no cleavage (Fig 4.23).

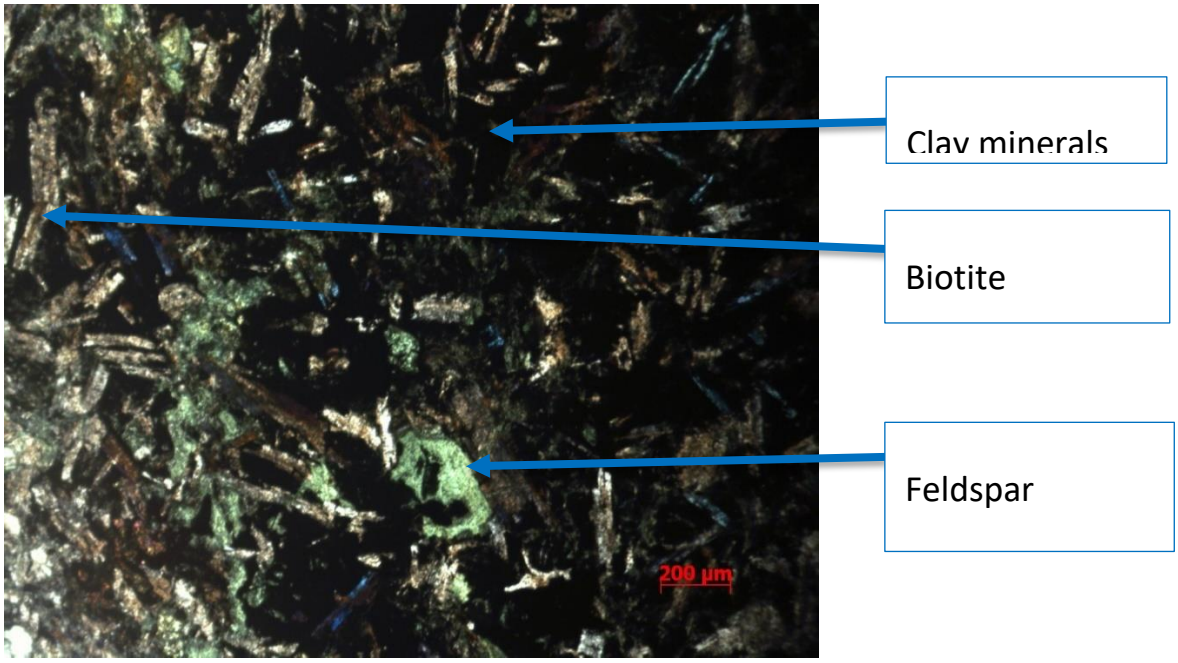

Figure 4.23: Photomicrograph of Shale in thin section showing abundance of biotite.

Ironstone

The rock sample was reddish in colour. The red colour may be due to the presence of iron oxide. It was highly competent and dense. The outcrop was highly weathered with very large lateral extent. These Iron Oxide was, either magnetite (Fe_3O_4) or hematite (Fe_2O_3) (Plate 4.6).

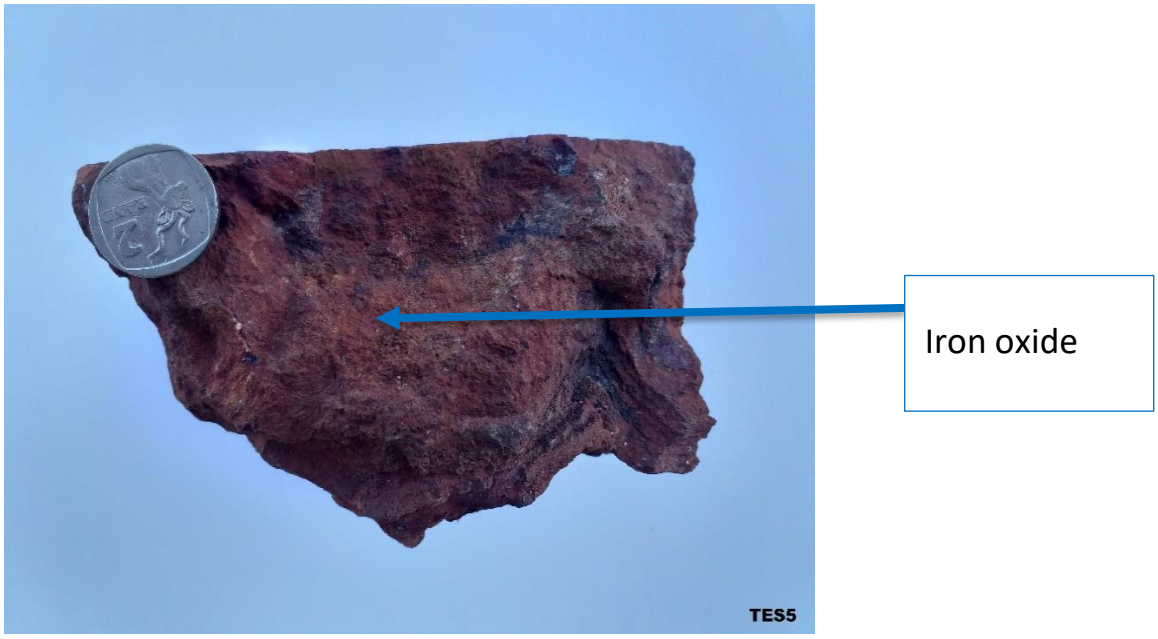

Plate 4.6: Ironstone specimen showing iron oxide.

In thin section, the rock sample displayed a very fine texture with only Quartz grains clearly visible. Quartz was whitish in colour with subhedral shape and extinction as the stage was rotated under polarized light. Iron oxide minerals were not clearly visible because most of them are opaque in thin section (Fig. 4.24).

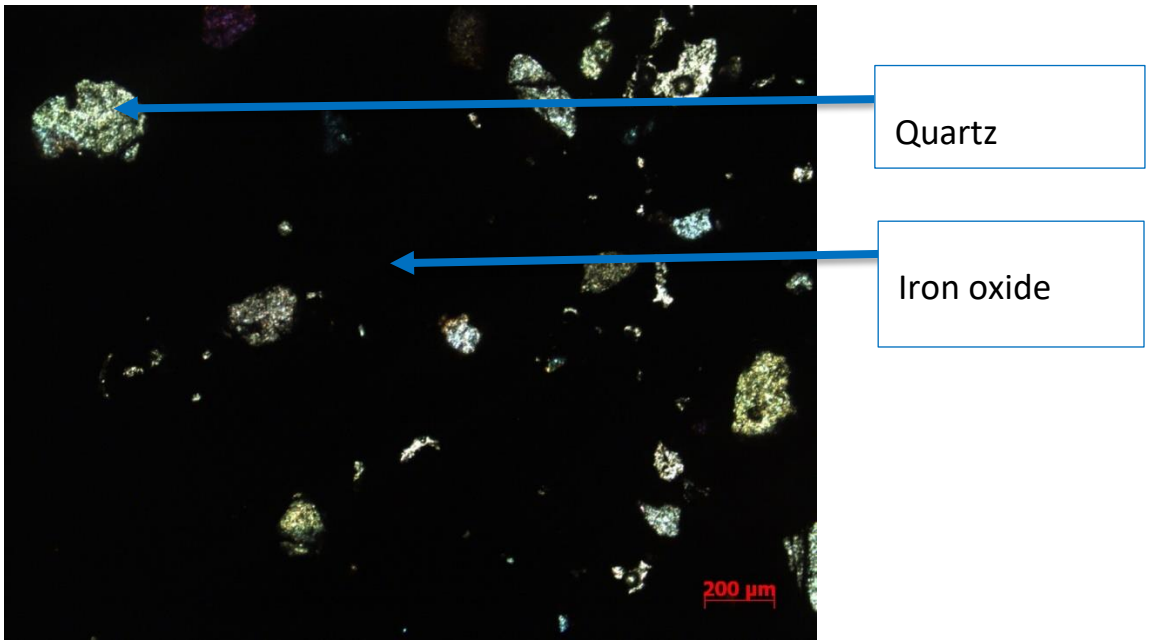

Figure 4.24: Photomicrograph ofIronstone in thin section showing iron oxide with quartz grains.

Grey mudstone

The rock sample was grey in colour and it was very fine grained. It was composed of clay minerals and some Feldspars. The outcrop was very competent, and it covered large area. The sample was non-fissile i.e. it did not exhibit any form of layering. Black colouring may be due to the carbonaceous content or pyrite (Plate 4.7).

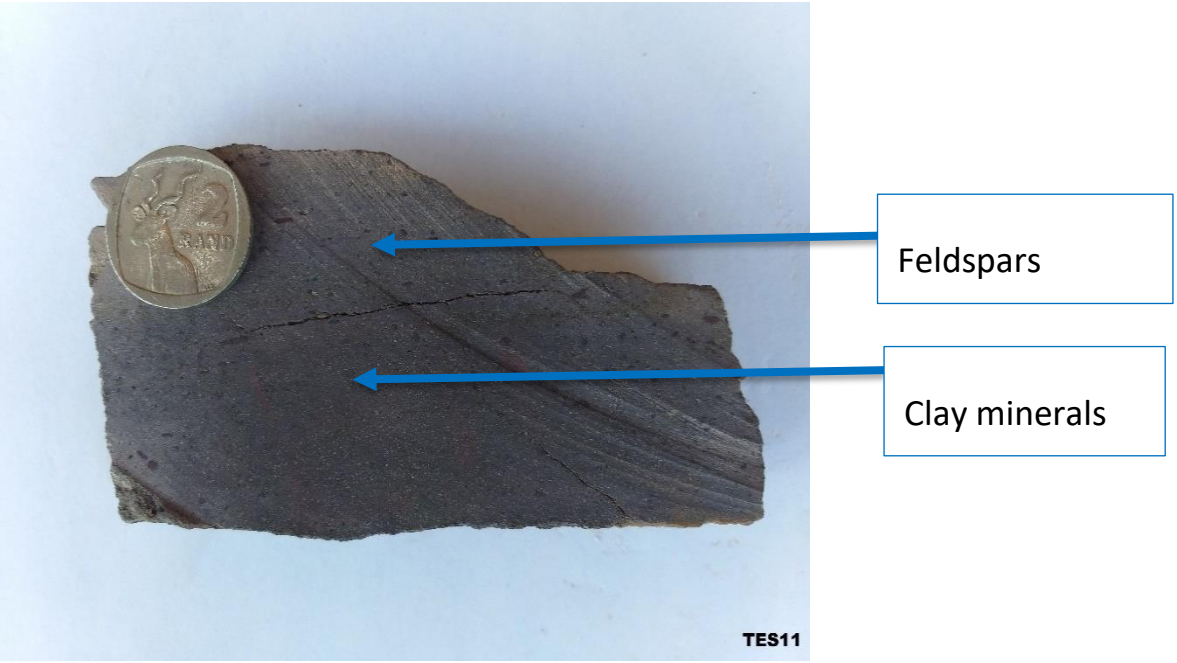

Plate 4.7: Grey mudstone specimen showing clay sized grains.

In thin section, the rock sample showed different minerals including; clay minerals, small quartz grains and muscovite. Clay minerals were dominant with very fine texture. Muscovite displayed colour variation of green, pink and blue colours (Fig. 4.25).

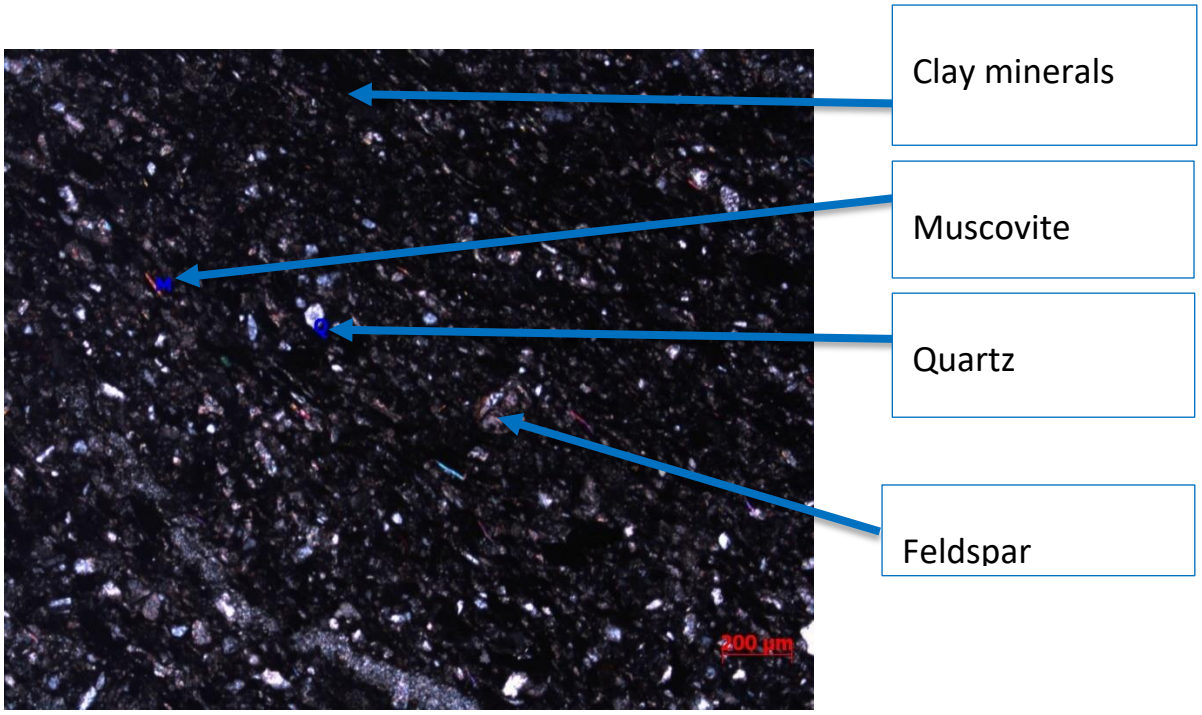

Figure 4.25: Photomicrograph of grey mudstone in thin section with fine grain texture.

Quartz vein

The sample was white in colour with interlocked grains and the white colour was caused by the presence of milky quartz. Mica occurred as shiny flickering biotite with no foliation. It was highly competent without any evidence of weathering (Plate 4.8).

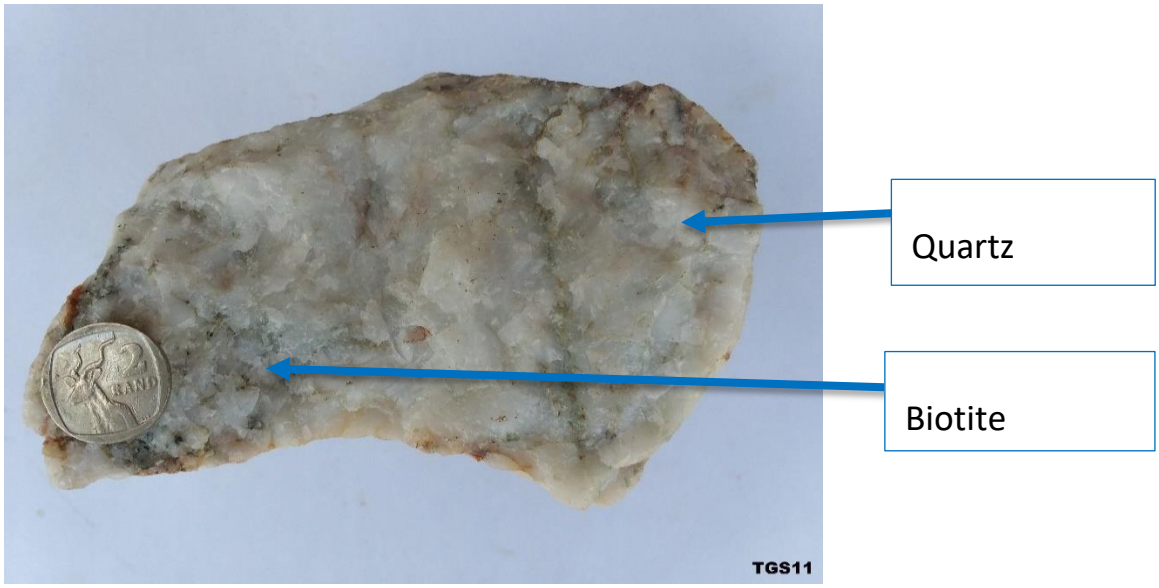

Plate 4.8 Quartz vein specimen with inclusion of biotite.

In thin section, the sample was comprised of quartz that makes up most of the rock sample. Quartz displayed white to grey crystal, with greyish crystals exhibiting extinction as the stage was rotated. The grain sizes were ranging from 325.24 µm to 1000 µm. Biotite was scattered in between quartz grains and it appeared to be a greenish to brown in colour with grain sizes less than 150 µm (Fig. 4.26).

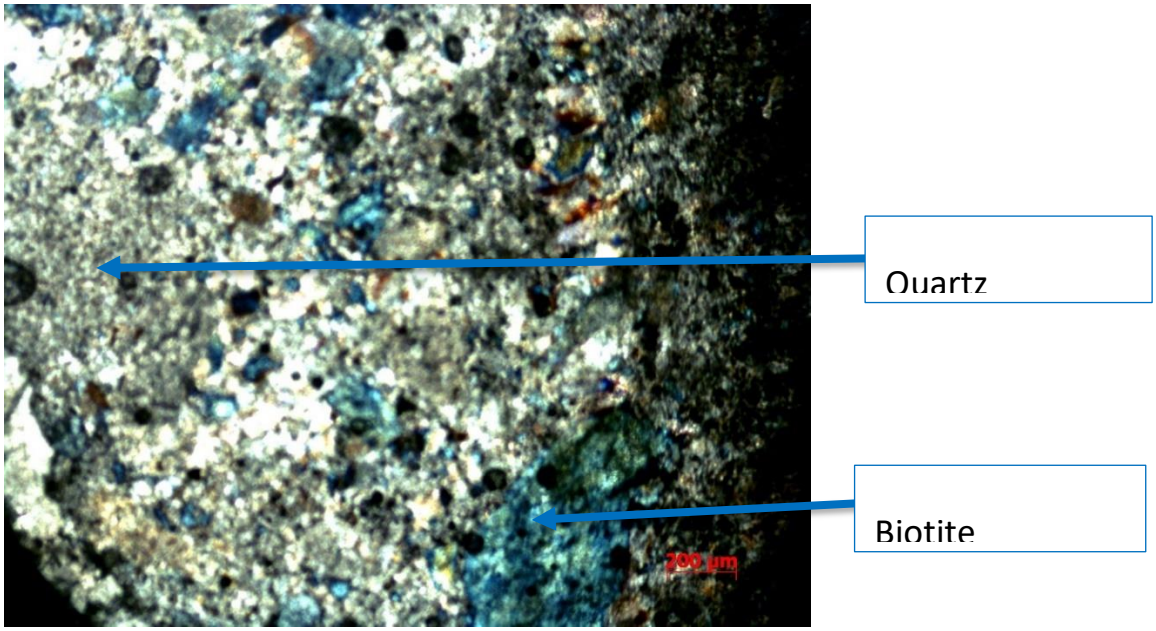

Figure 4.26: Photomicrograph of quartz vein in thin section with skeletal quartz grains.

Quartz Arenite

The sample was brown in colour and coarse grained. It was made of sand sized grains of which the quartz gains were dominant. Sandstone was dominated with quartz with some shiny mica minerals that might be biotite as well as feldspars. The gains were well rounded and sorted which makes it to be texturally matured. It was also mineralogical matured as it was dominated with quartz (Plate 4.9).

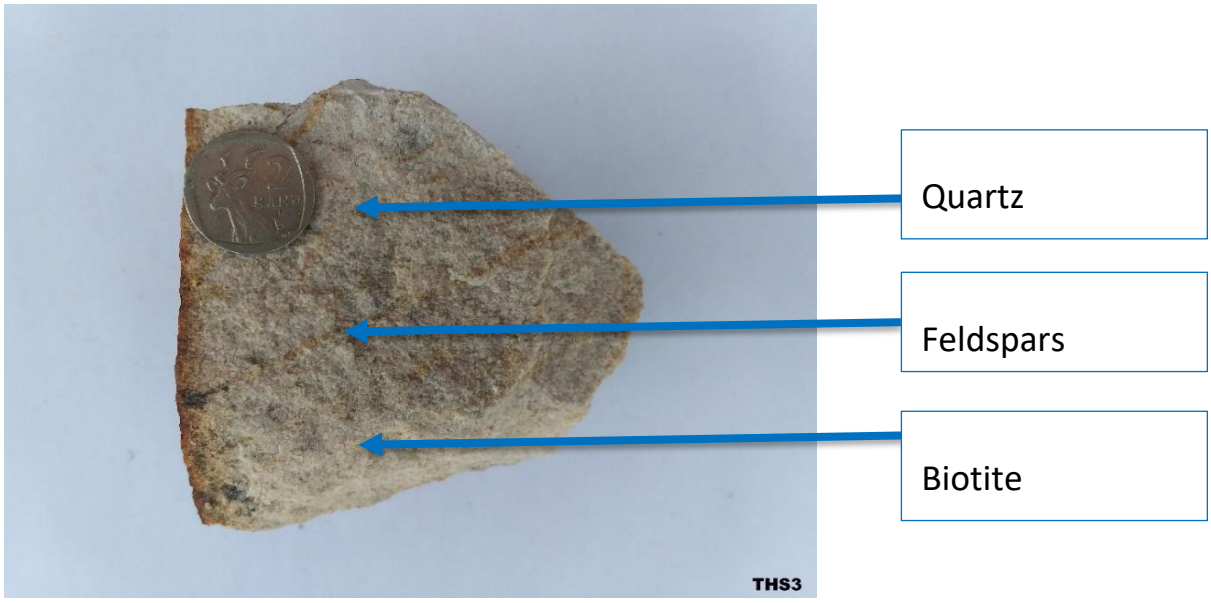

Plate 4.9: Quartz arenite specimen showing fine sand sized grains.

In thin section, the rock was found to be dominantly composed of quartz grains which were recognized by low relief, low birefringence and first order colour interference. Plagioclase feldspar showed and albite twinning in between quartz grains. The quartz grains were more rounded in shape and grain sizes were ranging between 255.32 µm and 947.34 µm. Biotite was in small quantity with dark brown colour (Fig. 4.27).

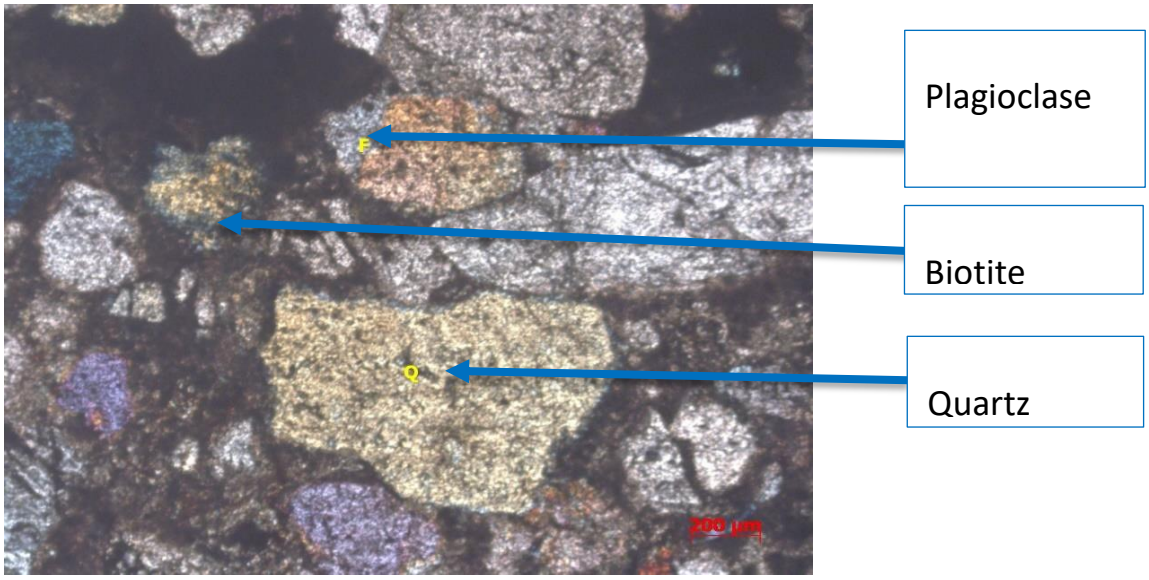

Figure 4.27: Photomicrograph of quartz arenite in thin section showing quartz, plagioclase and biotite.

Dolerite

Dolerite was massive and greenish in colour with medium to coarse grained texture. It was composed of dark minerals which are mafic minerals such as pyroxene and plagioclase. It was also exhibiting some shiny particles which may be biotite. The outcrop was localized and highly weathered as there were lots of cracks (Plate 4.10).

Plate 4.10: Dolerite specimen showing mafic minerals.

In thin section, the rock sample showed large fracture phenocrystals of olivine with grain size of about 420.40 µm. It also showed high birefringence, distinctive fracturing, lack of cleavage and alteration products. Some grains of plagioclase showed a simple twinning while other grains did not display twinning. Orthopyroxene showed low interference of colours with some grains exhibiting extinction compared to clinopyroxene which was brownish yellow with two cleavage at 90° (Fig. 4.28).

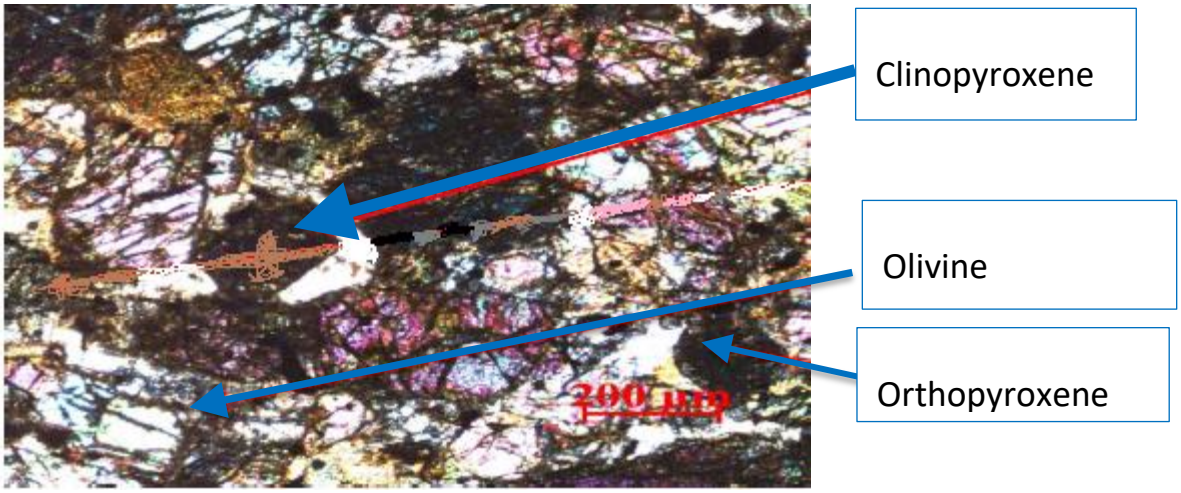

Figure 4.28: Photomicrograph of dolerite in thin section showing mafic minerals.

4.4 Mineralogical analysis of rocks

Mineralogical analysis was done using both physical and optical properties of minerals. Rock description of samples from section 4.3 was used to summarize the mineralogical characteristics of each rock (Table 4.6). The analysis was done to identify and classify rocks hosting the Mushithe coal occurrence.

Quartz was the most dominant mineral in most of the rock samples because is widespread occurrence in the earth crust. In quartzite, quartz occurred in the form of mudstones and shale veins as well as distinct crystals while in quartz rock it occurred as very large crystals of milky quartz. Under the microscope quartz was identified as angular, whitish in colour and showed extinction when the stage was rotated about 360°.

Felspar was identified in sandstones, mudstones and shale, thin section during microscopic analysis. In Sandstone and Dolerite plagioclase showed an excellent albite twinning. Plagioclase feldspar twinning was not clearly visible under the microscope in. Biotite was found in quartzite, quartz vein and sandstones as a minor mineral.

Petrographic study showed that dolerite was rich in olivine and pyroxene. Olivine showed bluish colour with high relief and distinctive irregular fracture pattern while

pyroxene also showed bluish colour with subhedral crystal shape and two cleavages at 90°. olivine and pyroxene were only observed in dolerite sample.

Mudstones and shale samples were rich in clay minerals when studied under a microscope. The clay minerals identified were kaolinite and serpentine. They were dark in colour ranging from reddish to black with low relief and birefringence. Ironstone was composed of oxides minerals which include limonite, hematite and magnetite with some quartz grains. Calcrete was composed of calcite as the major mineral.

Table 4.6: Mineralogical analysis of rocks mapped around Mushithe Coal occurrence

Rock name	**Major minerals**	**Minor minerals**	**Degree of alteration**
Mudstone	Clay minerals, Feldspar	Serpentine	Low
Quartzite	Quartz	Biotite	Low
Calcrete	Calcite	Carbonate minerals	Medium
Sandstone	Quartz, Feldspar	Biotite	Medium
Shale	Clay minerals	Feldspar	Low
Dolerite	Olivine, Pyroxene	Plagioclase	High
Ironstone	Hematite, Magnetite	Limonite	Medium
Mudstone	Clay minerals, Feldspar	Serpentine	Low
Quartz vein	Quartz	Biotite	Low
Quartz arenite	Quartz, Feldspar	Biotite	Medium

4.5 Textural and grain size analysis

Rock samples studied in section 4.3 above showed a range of texture ranging from coarse, medium to fine grained (Table 4.7). Grain sizes were analyzed under the

microscope. This was done to characterize and classify rocks on the basis of their texture and grain size. All the analysed samples were predominately composed of rock forming minerals with the notable exception of ironstone.

Quartz arenite sandstone exhibited a coarse texture with quartz grain sizes ranging between 255.32 µm and 947.34 µm when studied under the microscope. Arkose sandstone also showed coarse texture with quartz grain sizes ranging between 153.30 µm to 744.64 µm (Table 4.7). Quartz arenite was texturally mature as the individual grains were more rounded and well sorted while arkose sandstone was texturally immature because of the angular grains. Quartzite showed coarse texture with vein and grain sizes ranging between 254.22 µm and 1000 µm (Table 4.9). Quartz vein showed a fine texture with quartz grain size ranging between 325.24 µm and 1000 µm.

All mudstone samples and Shale a very fine texture with grain sizes of less than 75 µm (Table 4.7). The fine texture in these rock samples was due to the abundance of clay minerals. Shale was fissile showing a strong tendency of breaking in thin layers. Calcrete was also very fine grained texturally. This was may be due the precipitation of carbonate minerals during the formation of the rock. The fined texture was also observed in Ironstone. Ironstone also exhibited opaque mineralogy likely hematite which were difficult to see under both polarized and non-polarised light.

Dolerite showed intermediate texture with different sizes of crystals comprised of mafic minerals during thin section analysis. It had phenocrysts of olivine with grain sizes reaching up to 420.40 µm. It was also composed of subhedral pyroxene crystals and anhedral plagioclase with no quartz crystals present.

Table 4.7: Textural and grain analysis of rocks mapped around Mushithe Coal occurrence

Rock name	Colour	Grain size (μm)	Texture	Structure
Mudstone	Red	<75	Very fine	Non-foliated
Quartzite	Brown	256.22-1000	Medium-coarse	Quartz Vein
Calcrete	White	<75	Very fine	None
Arkose	Brown	153.30-744.64	Coarse	Layered
Shale	Grey	<75	Very fine	Fissility
Dolerite	Green	420.40	Medium-coarse	None
Ironstone	Red	<75	Very fine	None
Mudstone	Grey	<75	Very fine	Non-foliated
Quartz vein	White	325.24-1000	Coarse	None
Quartz arenite	Brown	255.32-947.34	Coarse	Poor layering

4.6 Whole rock geochemical analysis

Whole rock geochemical analysis was done in order to determine the concentrations of major element oxides and trace elements of host rock samples within the study area (appendix B.2.) Average data from Upper Continental Crust (UCC) was used for comparison using the following formula (Taylor and McLennan, 1985):

$$Enrichment = \frac{\text{Value from study}}{\text{value from UCC}}$$

wherein a value greater than 1 indicated enrichment whereas values below 1 indicated depletion

4.6.1 Major oxides analysis

Major elements are useful for the classification of rocks. Major elements concentrations from major oxide data from appendix B.1 were plotted using histogram. Histograms (Fig. 4.29 and Fig. 4.30) are useful in interpreting the whole rock geochemical data for easier classification of rock samples.

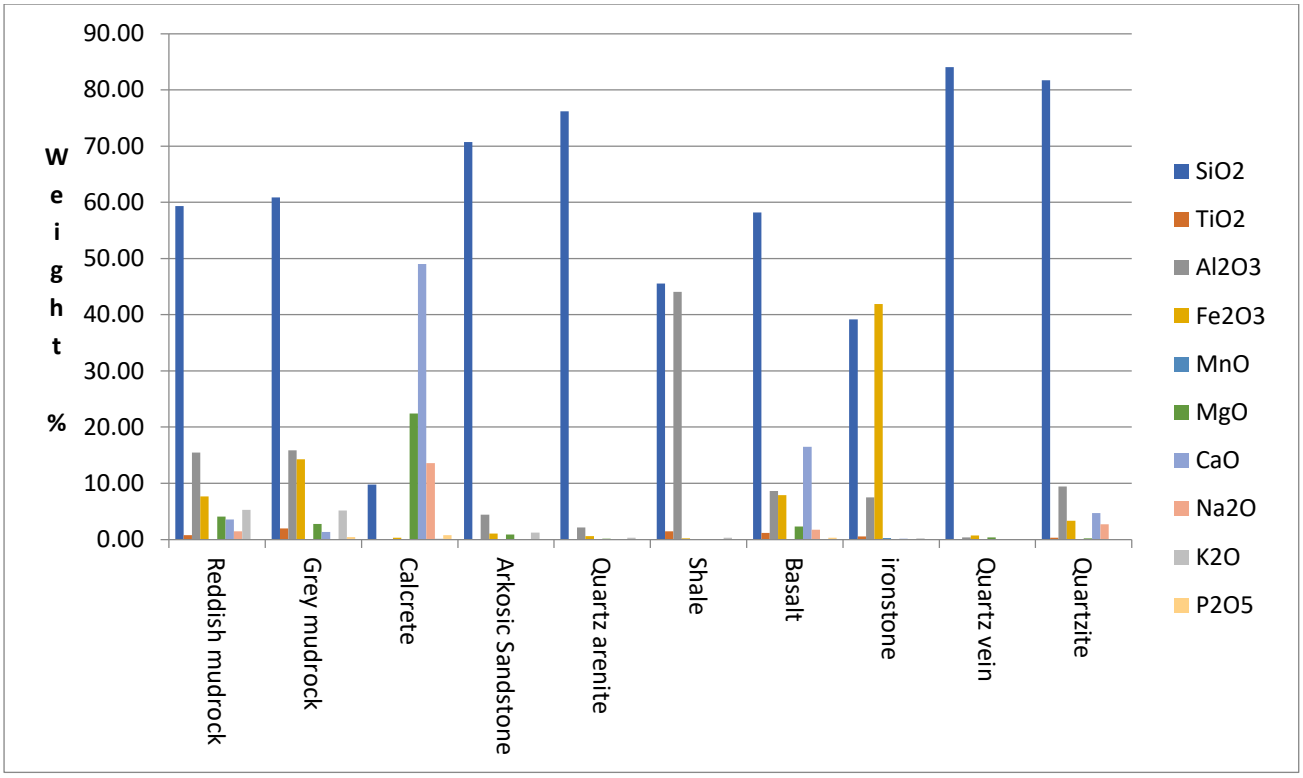

Figure 4.29: Major oxides in rock samples.

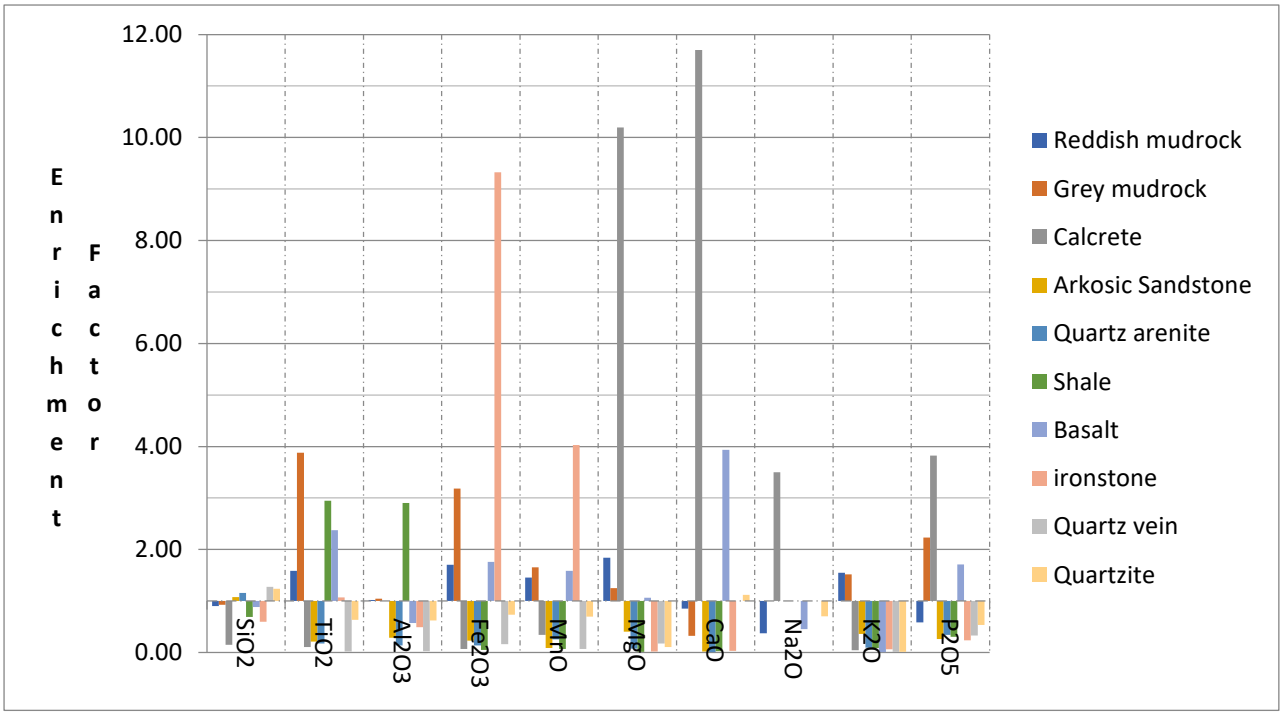

Figure 4.30: Major oxides enrichment relative to UCC in host rock samples.

The Major oxide chemistry of the studied samples varied based on their mineralogy. The bar graph (Fig. 4.29) indicated variations of major elements Si, Ti, Al, Fe, Mn, Mg, Ca, Na, K and P. The most dominant major oxides are SiO_2, Al_2O_3, Fe_2O_3 and CaO. SiO_2 is the most dominant with an average concentration of 58.56 wt%, ranging from 9.75 wt% to 84.06 wt% with calcrete having the lowest Silica content at 9.75 wt% and quartz vein with the highest concentration at 84.06 wt%. The second dominant major oxide is Al_2O_3 with 10.78 wt% average concentration and range of 44.09 wt%. Calcrete had no Al_2O_3 concentration and the highest was recorded in shale with 44.09 wt%. Fe_2O_3 is the third most dominant oxide with an average concentration of 7.80 wt% ranging from 0.23 wt% to 41.88 wt% with least concentration recorded shale and the highest concentration of recorded in Ironstone. The CaO had an average concentration of 7.55 wt% and range of 49.02 wt%. Quartz vein had no CaO concentration and the highest concentration was recorded in calcrete (Fig 4.29).

Other major oxides include TiO_2, MnO, MgO, Na_2O, K_2O and P_2O_5 (Fig. 4.13). The TiO_2 concentration values range from 0.01 wt% to 1.94 wt%, with the lowest concentration recorded in calcrete and the highest value recorded in mudstone. The average concentration of TiO_2 was found to be 0.65 wt%. In MnO the range is from 0.01 wt% to 0.28 wt% and the average of 0,07 wt% with the least concentration recorded in shale whereas ironstone had the highest concentration. The MgO concentration ranges from 0.02 wt% to 22.42 wt% and an average of 3.33 wt% (Fig 4.29).

Shale had the lowest MgO concentration with 0.02 wt% whereas calcrete has the highest MgO concentration with 22.42 wt%. The range of Na_2O concentration is equal to calcrete concentration of 13.61 wt%, with no Na_2O concentration in arkose, quartz arenite, shale, ironstone, mudstone, and quartz vein and an average of 1.95 wt%. The concentration of K_2O ranges from 0.02 wt% to 5.26 wt% with an average of 1.27 wt%. Dolerite had the least K_2O concentration with 0.02 wt% and the highest of 5.26 wt% in mudstone. Lastly P_2O_5 concentration ranges from 0.05 wt% to 0.77 wt% and an average of 0.21 wt %. Arkose had the lowest P_2O_5 concentration with 0.05 wt% and the highest of 0.77 wt% in calcrete (Fig.4.29)

The rock quartz samples had the highest SiO_2 content followed by the quartzite and sandstone samples respectively. The mudstone and shale samples had the highest Al_2O_3 content. The Ironstone and calcrete had the highest Fe_2O_3 and CaO content respectively.

In the selected samples sandstone, quartz vein and quartzite are enriched in SiO_2. The enrichment of SiO_2 in these samples indicates the prominence of quartz as well as silicates (Fig. 4.30) The sandstone enriched in TiO_2 and Al_2O_3 which indicates the prominence of feldspar and clay minerals, a similar enrichment is noted in the mudrocks. The reddish mudstone is enriched in Fe_2O_3 whereas the darker one is depleted. Fe_2O_3 is also enriched in ironstone (Fig 4.30).

Dolerite is enriched in both Fe_2O_3 and MgO which is indicative of ferromagnesian mineralogy in sample (Fig 4.30).

4.6.2 Trace element analysis

Geochemical data from appendix B.2 was used to graphically illustrate the concentration of elements Trace elements were sub-divided into the following groups (Taylor and McLennan, 1985) to allow for more efficient analysis: large ion lithophile elements (Fig. 4.31), high-field strength elements (Fig. 4.32) Transition elements (Fig. 4.33), and rare earth elements (Fig 4.34)

Large-ion Lithophile Elements (LILE)

Trace elements classified in this group are Ba, Rb, Sr, Th and U (Fig. 4.31). They are also known as the alkali and alkaline earth elements. They are relatively soluble in aqueous solutions due to low ionic potential. They are mobile during metamorphism and weathering.

Ba was the most abundant element in rock types with concentration ranging between 65.8 ppm and 1506.2 ppm with an average concentration of 541.48 ppm compared to 550 ppm for UCC. The Ba concentration in arkose and quartz arenite were 137.8 ppm and 102.8 respectively thus showing depletion whereas in mudstone and shale with concentrations 1506.2 ppm, 650.1 ppm and 1157.5 ppm respectively Ba was enriched. The least concentrations of Ba 65.8 ppm and 97.5 ppm were noted in

quartz vein and calcrete respectively as a result representing depletion. The abundance of Ba in mudstone and shale may be attributed to the presence of mica and clay minerals (Rollinson, 1993).

Sr concentration ranged between 8.3 ppm and 643.3 ppm with an average concentration of 219.03 ppm compared to 350 ppm of UCC. Arkose, quartz arenite, mudstone and shale are depleted in Sr while calcrete, dolerite and quartzite showing Sr enrichment. The smallest Sr concentration was noted in quartz arenite and the highest was recorded in dolerite. Depletion of Sr may be due to leaching during weathering (Best, 2003).

Rb concentration ranged from 2.40 ppm to 125.70 ppm with an average concentration of 40.02 ppm compared to 112 ppm for UCC. Rb was depleted in quartz arenite and mudstone with the exclusion of mudstone having Rb abundance which was slightly greater than that of UCC, with concentration of 125.7 ppm. The depletion of Rb may be attributed to washing away of Biotite in the rock samples which in turn indicate the presence of fine grained Siliclastic materials (Rollinson, 1993).

Generally, the concentration of Th was low in all rock types. Th concentration ranges from 4.10 ppm to 35.30 ppm with an average concentration of 16.78 ppm compared to 10.7 ppm for UCC. Th was depleted in quartz arenite, mudstone (6.40 ppm), calcrete (0 ppm), quartz vein (6.20 ppm), dolerite (4.10 ppm) and quartzite (4.40 ppm). Conversely, it was enriched in arkose (31 ppm), Mudstone (15.80 ppm), shale (31 ppm) and Ironstone (35.30 ppm). Concentration of U ranged between 5.0 ppm and 59.80 ppm with an average of 16.42 ppm. Ironstone has the highest concentration of both Th (35.30 ppm) and U (59.80 ppm) respectively. This suggests that Ironstone contains some felsic minerals since the enrichment of Th and U is an indication that the source rock composition was felsic (Winter, 2014).

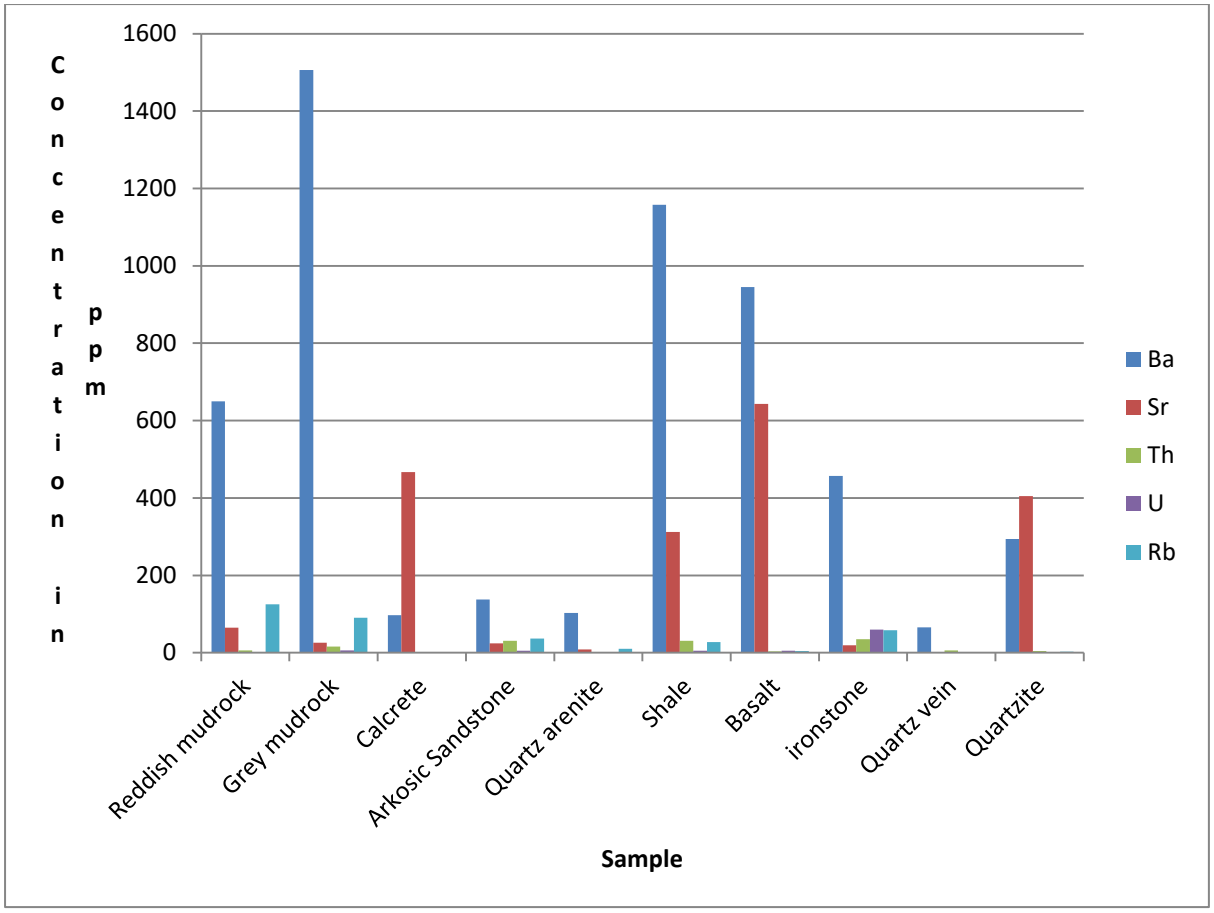

Figure 4.31: Bar graph showing concentrations of Large-ion Lithophile Elements (ppm).

High Field Strength Elements (HFSE)

The trace elements classified in this group are Y, Zr, Nb and Hf (Fig. 4.32). HFSE elements are enriched in felsic rather than mafic rocks. They are predominantly insoluble which is credited to their high ionic potential and ionic charge to ionic radius ratios and as a result making them immobile in the course of weathering and metamorphism (Best, 2003). Zr was the most dominant in all rock types with Y being the second most dominant. Nb and Hf were noted in low concentration and in a small number of rock types.

Zr concentration ranged from 6.50 ppm to 679.70 ppm with an average concentration of 189.11 ppm compared to 190 ppm for UCC. The highest concentration of Zr was noted in shale whereas the lowest was noted in quartz vein. Zr was only enriched in mudstone and shale with concentrations 340.3 ppm and

679.70 ppm respectively. The enrichment may be a consequence of the presence of diagenetic clay minerals and also the abundance of clinopyroxene, amphibole and mica minerals in trace concentrations (Winter, 2014).

Concentration of Y ranged between 3.0 ppm and 56.70 ppm with the lowest concentration noted in ironstone whereas the highest concentration was noted in mudstone and the average concentration was 20.94 ppm compared to 22 ppm for UCC. Y was depleted in all rock samples except mudstones and shale which are enriched with concentrations 32.2 ppm, 56.7 ppm and 34.1 ppm respectively. The Y concentration is enriched by the grain size fractionation during transportation as HFSE elements are immobile during sedimentary processes (Winter, 2014). Its abundance can also be associated with presence of Biotite, Feldspar and Pyroxene as an accessory element.

The concentration of Nb ranges from 1.50 ppm recorded in quartz arenite to 36.60 ppm recorded in shale and the average concentration of 9.30 ppm compared to the 12 ppm of UCC. Nb was enriched in mudstone and Shale with concentrations 18.1 ppm and 36.6 ppm respectively.

Hf concentration ranged between 3.40 ppm and 20.90 ppm with an average concentration of 14.03 ppm compared to 5.80 ppm of UCC. The lowest concentration of Hf was recorded in quartzite while the highest concentration was recorded in quartz vein. Hf was enriched in mudstone, arkose, quartz arenite, shale and dolerite with concentrations 20.9 ppm, 20.7 ppm, 6.2 ppm, 20.7 ppm and 20.6 ppm respectively. The abundance of this concentration of Hf indicates the presence of felsic minerals in source rock (Rollinson, 1993).

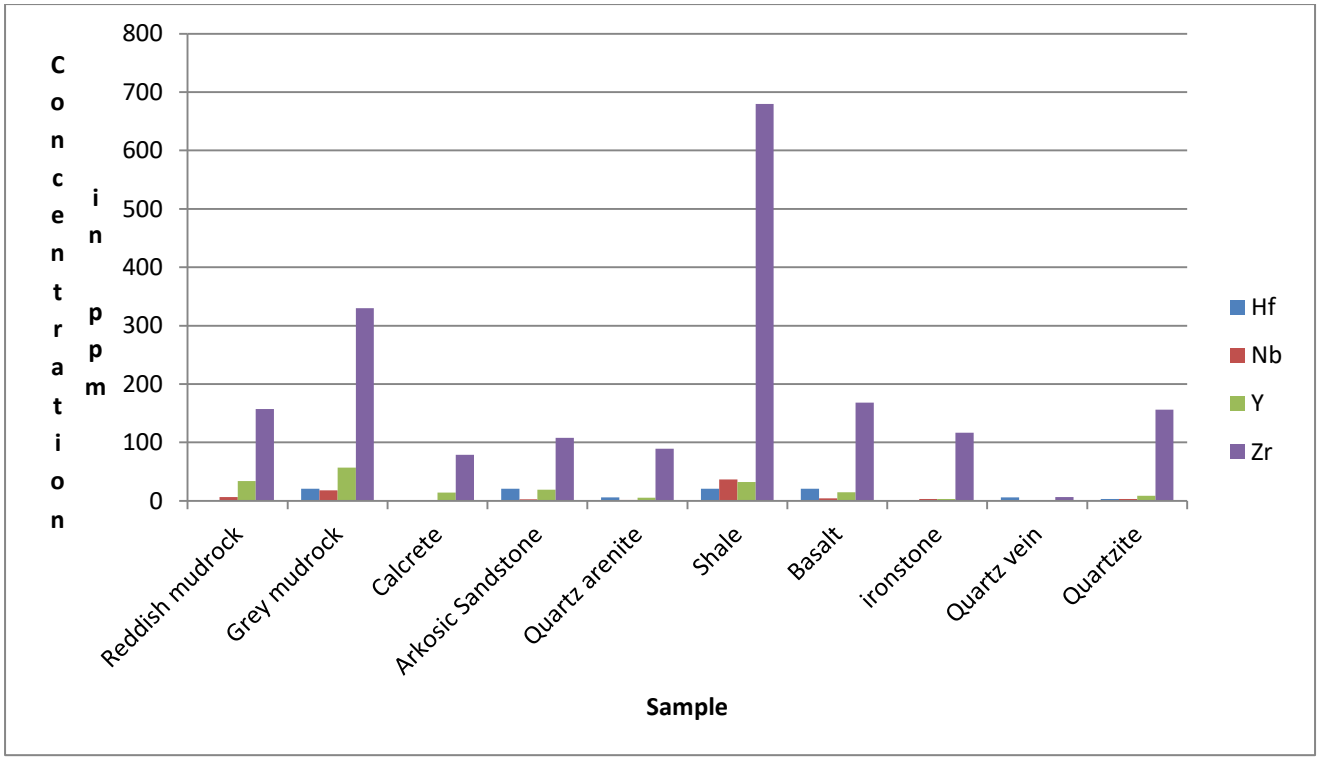

Figure 4.32: Bar graph showing concentrations of High Field Strength Elements (ppm).

Transition Trace Elements (TTE)

This group comprises of trace elements such as V, Co, Cu, Ni and Sc (Fig. 4.33). The solubility of transition metals is quite variable and depends upon valence state and availability of anions with which they can form soluble coordination complexes. They range from moderately incompatible (Ti, Cu and Zn) to very compatible (Cr, Ni and Co). High concentrations of the highly compatible elements (Cr, Ni and Co) indicate a mantle source or crystal accumulation (Best, 2003).

V concentration ranges from 11.90 ppm to 395.60 ppm with an average concentration of 167.66 ppm compared to the 107 ppm of UCC. V was enrichment in mudstones, shale, dolerite and ironstone while depletion occurred in arkose, quartz arenite, calcrete, quartz vein and quartzite. The enrichment of highly compatible Co has occurred in mudstones, dolerite and ironstone with depletion in calcrete, arkose, quartz arenite, shale, quartz vein and quartzite. The average concentration of Co was 21.46 ppm as compared to the UCC content of 17 ppm, ranging from 1.50 ppm to 88.60 ppm.

The moderately incompatible Cu had an average concentration of 49.84 ppm compared to 25 ppm for UCC and ranged between 5.80 ppm and 147.50 ppm. Concentration of Ni ranged between 2.40 ppm and 115.70 ppm with an average concentration of 39.82 ppm as compared to 44 ppm for UCC. Arkose exhibited a remarkable depletion in both Cu and Ni. In general, all TTE were depleted in both quartz vein and quartzite. Sc was depleted in all rock types and it was below the detection limit except in calcrete with concentration 4.4 ppm. High concentrations of the highly compatible elements (Cr, Ni and Co) indicate a mantle source or crystal accumulation (Best, 2003).

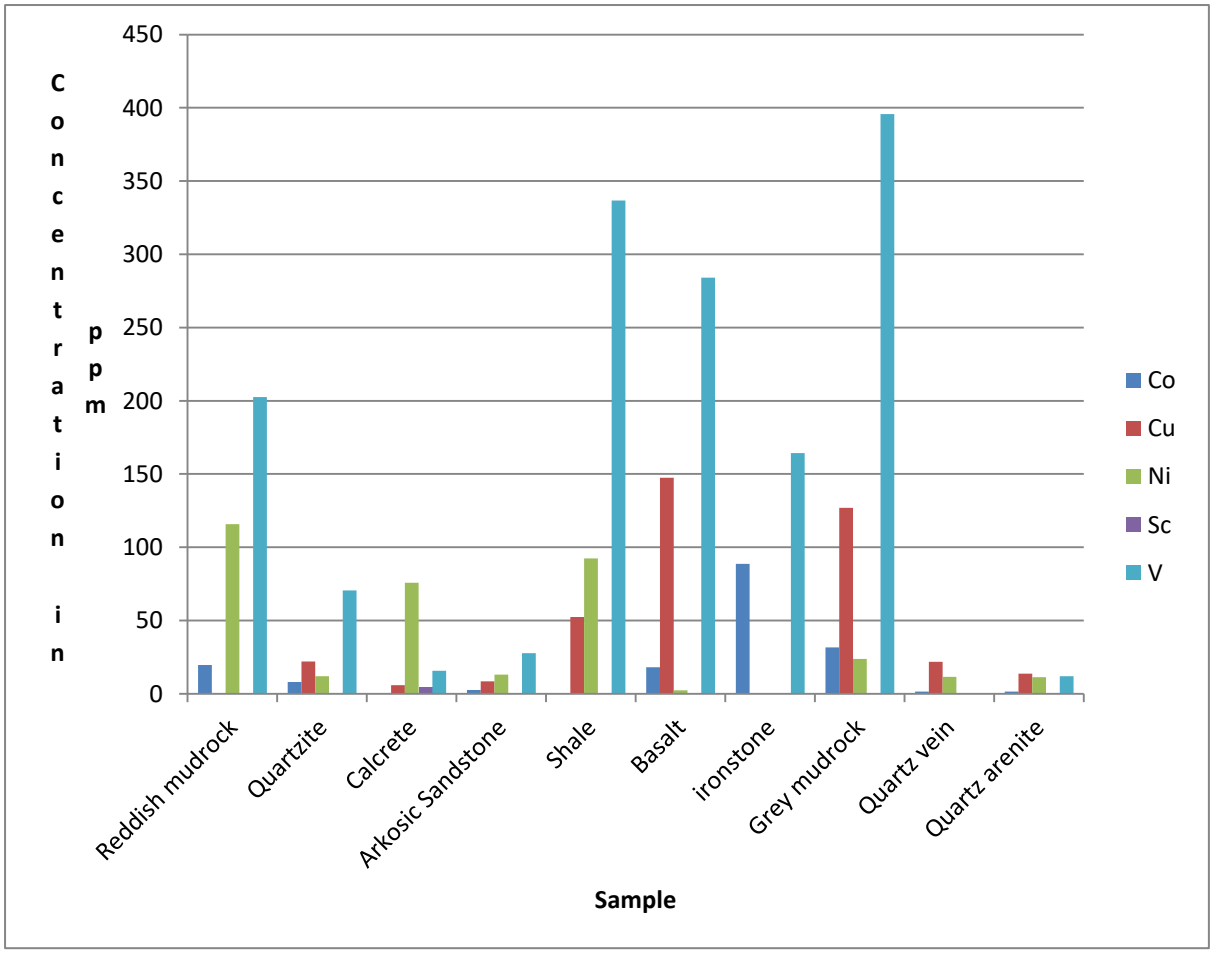

Figure 4.33: Bar graph showing concentrations of Transition Trace Elements in (ppm).

Rare Earth Elements (REE)

The REE include trace elements such as La, Ce, Pr, Nd, Sm, Eu, Gd, Tb, Dy, Ho, Er, Tm, Yb and Lu (Hanson, 1980). They are strongly electropositive and have electronegativity of 1.2 or less. They are relatively insoluble in aqueous solution as a consequence of their higher charge and high ionic potential. They are regarded as incompatible elements because of their large ionic charge and large ionic radii (Best, 2003). Degree of incompatibilities varies due to the ionic radii.

The REE's are useful in studying altered or weathered rocks as they are highly insoluble and immobile with their patterns often remain unchanged during metamorphism. The study revealed the occurrence of REE; Ce, La, Dy, Sm and Yb (Fig. 4.34). Ce was the most abundant in all rock types. Dy and Sm were also present in moderate concentration in most of the rock types. Yb and La were found in low concentration and in few rock types.

Ce had average concentration of 268.71 ppm ranging from 10.90 ppm to 692.90 ppm with the least concentration recorded in calcrete with the highest concentration in arkose and shale. The concentration of La ranged from 10.30 ppm to 477.20 ppm with an average concentration of 132.36 ppm. Dy concentration ranged from 0.70 ppm to 133.10 ppm with an average concentration of 26.27 ppm. The highest concentrations of La and Dy were recorded in arkose while the lowest were recorded in ironstone. Sm had an average concentration 143.10 ppm and ranged from 55.40 ppm in mudstone to 230.80 ppm in ironstone. Yb concentration ranged from 8.80 ppm to 50.80 ppm with an average concentration of 25.39 ppm. The highest concentration of Yb was noted in mudstone and the lowest was recorded in quartzite.

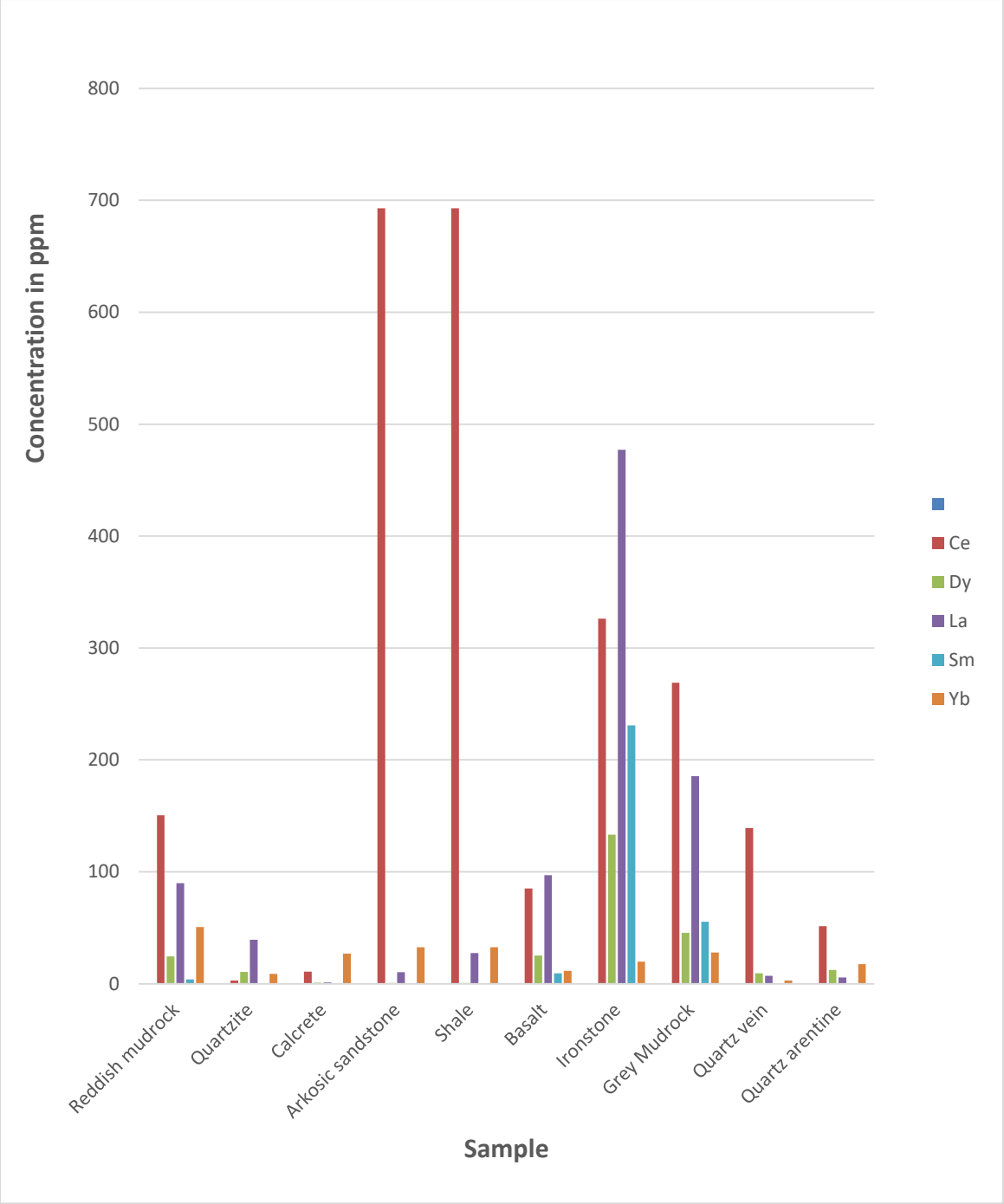

Figure 4.34: Bar graph showing concentrations of Rare Earth Elements (ppm).

CHAPTER 5: CONCLUSIONS AND RECOMMENDATIONS

The current study came up with a number of conclusions and recommendations that are presented below.

5.1 Conclusions

a) A detailed geological map of Mushithe coal occurrence was produced and the following rocks are associated with coal; sandstone, quartzite, ironstone, quartz vein, mudrock, calcrete and dolerite. These rocks strike to the north-east. These rocks as well as coal are intruded by dolerite dyke that resulted in the devolatilization of coal in this area.

b) Coal at Mushithe was formed in a wet swamp in overflowing water environment. This is further corroborated by the presence of rocks associated with marine environment such as calcrete and ironstone as well mudstone which formed when tiny particles settle in water. Malaza (2013) classified the depositional environment of the Soutpansberg Coalfield as fluvial likewise Mphaphuli (2017) also indicated the environment of formation as a wet swamp.

c) Coal at Mushithe has the following properties:

- Calorific value of coal ranging between 4.66 MJ/Kg and 20.99 MJ/Kg with average 14.26 MJ/Kg. The average calorific value of Mushithe Coal is less than 28.24 MJ/Kg at Tshikondeni Deposit (east) but greater than 12.99 MJ/Kg at Waterberg Coalfield (west). This corresponds with the increase in coal quality from west to east noted by Sparrow (2012).
- Low sulphur content ranging from 0.11% to 0.32% with average value of 0.29% which is an indication that sulphur came from plant material amalgamation during peat accumulation (Chou, 2012).
- High ash content ranging from 9.10% to 66.40% with average value of 27.90%). The ash content is controlled by intercalation with shale partings (Wood et al, 1983).

- Low carbon ranging between 14.21% and 57.19% with average value of 41.02%, the low carbon can be attributed to devolatilization by dolerite dyke (Thomas, 2013).
- The coal at Mushithe is enriched in TiO2 and Fe2O3 which is attributed to the prevalence of clay minerals and pyrite as pointed out by petrographic study which showed clay minerals being the most prevalent mineral matter followed by pyrite.
- Elemental composition of coal is controlled by organic matter, silicates, carbonates and sulphides. This is evident in the mineral matter of coal as well as low sulphur which is characteristic of plant material accumulation.
- Random vitrinite reflectance ranged between 0.94 %ROV to 1 %ROV which is lower than 1.23% at Tshikondeni Deposit (Mphaphuli, 2017). This is consistent with Sparrow (2012) and Hancox and Gotz (2014) who noted that coal rank decreases from east to west across the Soutpansberg coalfield.

d) Coal at Mushithe is rich in vitrinite but low in Inertinite and devoid of Liptinite. Vitrinite in coal ranged between 70.20 vol% and 82 vol% with average value of 77.75 vol%. Inertinite in coal ranged between 18 vol% and 29.8 vol% with average value of 22.25 vol%. The most common vitrinite maceral is collotelinite whereas pseudovitrinite is absent thus making Mushithe good for coking.

e) According to UNECE (1988) coal classification based on vitrinite reflectance and calorific value,the Mushithe coal is classified as medium B-C rank bituminous coal, with Coal 2A ranking medium rank B, whereas Coal 1B and 2C ranked medium rank C bituminous. Coal 2A had the highest calorific value of 20.99 MJ/kg and Vitrinite reflectance ranging between 0.912 ROV% and 1.172 ROV%. This is lower than Tshikondeni Coal but higher than that of Waterberg Coalfield. This confirms a decrease in coal rank from east to west as was stated by sparrow (2012).

f) According to Steyn and Minnitt (2012) grading of coal, the Mushithe coal is graded below D as the calorific value is below 24.5 MJ/kg however the coal at Mushithe has qualities typical of higher graded coals; Mushithe has sulphur content typical of grade A coal. Furthermore, Coal 2A has ash content characteristic of Grade A coals.

5.2 Recommendations

- Future exploration in the area should be conducted to fully establish the extent of coal occurrence in this area. Further exploration should incorporate geophysical work and exploratory drilling; this should lead to resource evaluation as the current study did not establish the extent of coal occurrence and its resource evaluation.
- Further studies should be carried out to determine the extent of dyke devolatilization of coal.
- Palynological studies should be done to comprehensively reconstruct the paleoclimate and paleoenvironment in the area. The study of palynology coupled with petrography will provide better interpretation of the depositional environment of coal.

REFERENCES

Akinyemi, S.A. (2011). Geochemical and Mineralogical Evaluation of Toxic Contaminants Mobility in Weathered Coal Fly Ash: As a Case Study, Tutuka Dump Site, South Africa, University of Western Cape, Bellville, Unpublished dissertation, 346 pp.

Arcgis.com (2018). ArcGIS online. [online] Available at: https://www.arcgis.com/home/signin.html [Accessed 26 Feb. 2018].

Best, M.G. (2003). Igneous and Metamorphic Petrology. Second Edition. Blackwell Science Ltd; 108 Crowley Road, Oxford OX4 1JF, UK. 729 pp.

Bordy, E.M. (2006) Sedimentological Investigation of the Lower Karoo in the Chapudi Coal Project Area (Tshipise Basin, Limpopo Province, South Africa). Unpublished Research Report, 28 pp.

Brandl, G. (1986). The Geology of the Pietersburg Area. Explanation Sheet Geological Survey of South Africa, Council for Geoscience, 43 pp.

Brandl, G. (1999). Soutpansberg Group. Catalogue of South African Lithostratigraphic Units, SA Committee for Stratigraphy, Council for Geoscience, pp. 6-41.

Brandl, G. (2002). The Geology of the Alldays Area. Explanation sheet 2228, Alldays. Geological Survey South Africa, 71 pp.

Catuneanu, O., Wopfner, H., Eriksson, P.G., Cairncross, B., Rubidge, B.S., Smith, R.M.H., Hancox, P.J. (2005). The Karoo Basins of South-Central Africa, Journal of African Earth Sciences, 43, 211 253.

Chou, C.L. (2012). Sulphur in coals: A Review of Geochemistry and Origins. Int. J. Coal. Geol. 12, pp. 1 - 13.

Coetzee, S. (2015). The Caking and Swelling of South African Large Coal Particles. [online] Hdl.handle.net. Available at: http://hdl.handle.net/10394/15167 [Accessed 26 Feb. 2019].

De Jager, F.S.J., (1986) Coal occurrences of the central, north-western, northern and eastern Transvaal. In: Anhaeusser, C.R., Maske, S. (Eds.), Mineral Deposits of Southern Africa. Geological Society of South Africa, pp. 2047–2055.

Diessel C.F.K. (1986). The Correlation Between Coal Facies and Depositional Environments : Advances in the Study of the Sydney Basin. Proc. 20th Symp. University Newcastle, pp.19-22.

ESKOM (2018). Eskom Home. [online] Available at: http://www.eskom.co.za/ [Accessed 15 Feb. 2018].

Falcon, R. (2013). Coal petrography. The Coal Handbook: Towards Cleaner Production, pp.53-79.

Geng, H., Brandl, G., Sun, M., Wong, J. and Kröner, A. (2014). Zircon ages defining deposition of the Palaeoproterozoic Soutpansberg Group and further evidence for Eoarchaean crust in South Africa. Precambrian Research, 249, pp.247-262.

Google Earth. (2018). Google Earth – Google Earth. [online] Available at: https://www.google.com/earth/ [Accessed 15 Feb. 2018].

Gore, J., James, D., Zengeni, T. and Gwavava, O. (2009). Crustal structure of the Zimbabwe craton and the Limpopo belt of southern Africa: New Constraints From Seismic Data and Implications for Its Evolution. South African Journal of Geology, 112 (3-4), pp. 213-228.

Hancox,P.J., and Gotz, E., (2014). South Africa's Coalfields – A 2014 Perspective. International Journal of Coal Geology, 132, pp. 170 – 254.

Hardie, A., Dynes, J., Kozak, L. and Huang, P. (2009). The Role of Glucose in Abiotic Humification Pathways As Catalyzed By Birnessite. Journal of Molecular Catalysis A: Chemical, 308(1-2), pp.114-126.

Horrocks, P.C. B., (1981). The Precambrian Geology of an Area Between Messina And Tshipise Limpopo Mobile Belt, University of Johannesburg, Johannesburg, Unpublished, 385 pp.

Jeffrey, L.S. (2005). Characterization of the Coal Resources of South Africa. Journal of the Southern African Institute of Mining and Metallurgy, *105*(2), pp.95-102.

Jones, J. (2010). The nature of macerals. Fuel, 89(7), 1743 pp.

Kabanda, T.A. (2004). Climate. [ebook] Thohoyandou: Institute of Conservation and Natural History of the Soutpansberg, pp.10 - 11. Available at: http://www.soutpansberg.com/workshop/pdf_files/climate.pdf [Accessed 21 Feb. 2018].

Kruszewska, K.J. (2003). Fluorescing Macerals in South African Coals. International Journal of Coal Geology, 54, pp. 79-94.

Le Blanc Smith, G. (1980) Genetic Stratigraphy of the Witbank Coalfield. Transactions Geological Society of South Africa 83(3), pp. 313–326.

Mahanyele, P.J. (2010). Interpretation of Airborne Magnetic Data Over Selected Areas of Witbank Coalfield, South Africa: An Aid To Mine Planning, University of Pretoria, Pretoria, Unpublished dissertation, 118 pp.

Malaza, M. (2013). Basin Analysis of the Soutpansberg and Tuli Coalfields, Limpopo Province of South Africa, University of Fort Hare, Alice, Unpublished dissertation, 270 pp.

Maphala, T. (2012). Effects Of Carbon Dioxide Storage In Coal On The Physical And Chemical Properties Of Coal, University of Witwatersrand, Johannesburg, Unpublished, 214 pp.

McCourt, S., Brandl, G.,(1980) A Lithostratigraphic Subdivision of the Karoo Sequence in the North-Eastern Transvaal. Ann. Geol. Surv. S. Afr. 14, 51–56.

Meyers, R. and Attar, A. (1982). Coal Structure. New York: Academic Press. 340 pp.

Mphaphuli M. (2017). Petrographic Consideration of the Impact of the Tshipise Fault on Coal Quality in the Soutpansberg Coalfield, South Africa, University of Johannesburg, Johannesburg, Unpublished dissertation, 143 pp.

Msomi, T.K.B. (2014) Influence of an Igneous Intrusion on the Surrounding Coal Body, University of Pretoria, Pretoria, Unpublished dissertation, 114 pp.

Osborne, D. (2013). The Coal Handbook: Towards Cleaner Production. Cambridge: Woodhead Publishing Ltd. 576 pp.

Phupheli, M.R. (2007). Purifying Coal for the Production of Nuclear Graphite. Unpublished Master's Dissertation, University of Pretoria, pp. 6-18.

Pierce, B.S., and Dennen, K.O. (2009). The National Coal Resource Assessment Overview: U.S. Geological Survey Professional Paper 1625–F, 402 pp.

Rigby, M., Basson, I., Kramers, J., Gräser, P. and Mavimbela, P. (2011). The structural, metamorphic and temporal evolution of the country rocks surrounding Venetia Mine, Limpopo Belt, South Africa: Evidence for a single palaeoproterozoic tectono-metamorphic event with implications for a tectonic model. Precambrian Research, 186(1-4), pp.51-69.

Rollinson, H.R. (1993). A Terrane Interpretation of the Archaean Limpopo Belt. Geological Magazine, 130, pp. 755–765.

Rollinson, H.R. (2003). Using Geochemical Data: Evaluation, Presentation, Interpretation. Longman Group UK Limited. 352 pp.

Rollinson, H.R. and Blenkinsop, T. (1995). The Magmatic, Metamorphic and Tectonic Evolution of the Northern Marginal Zone of the Limpopo Belt in Zimbabwe. Journal of the Geological Society of London, 152, pp. 65–75.

Scheetz, B. and Earle, R. (1998). Utilization of Fly Ash. Current Opinion in Solid State and Materials Science, 3(5), pp. 510-520.

Schobert, H. H. (1995). Lignites of North America (Vol. 23). Elsevier. pp 679.

Schweinfurth, S.P. (2009). An Introduction to Coal Quality. In: Pierce, B.S., Dennen, K.O. (Eds.). the National Coal Resource Assessment Overview: U.S. Geological Survey Professional Paper 1625-F, Chapter C, 16 pp.

Scott, A. (2002). Coal Petrology and the Origin of Coal Macerals: A Way Ahead?. International Journal of Coal Geology, 50 (1-4), pp. 119-134.

Shibaoka, M. (1978). Micrinite and Exudatinite in Some Australian Coals, and their relation to the generation of petroleum. Fuel, 57(2), pp.73-78.

Silva, L., Ward, C., Hower, J., Izquierdo, M., Waanders, F., Oliveira, M., Li, Z., Hatch, R. and Querol, X. (2010). Mineralogy and Leaching Characteristics of Coal Ash from a Major Brazilian Power Plant. CCGP, 2(1), pp. 51-65.

Spackman, W. (1958). Section of Geology and Mineralogy: The Maceral Concept and the Study of Modern Environments as a Means of Understanding The Nature Of Coal. Transactions of the New York Academy of Sciences, 20(5 Series II), pp. 411-423.

Sparrow, J. (2012). The Soutpansberg Coalfield “The Forgotten Basin”. Presentation at the Inaugural Fossil Fuel Foundation Limpopo Conference, Conference Abstract.

Speight, J. (2005). Handbook of Coal Analysis. 1st ed. Hoboken, N.J.: Wiley-Interscience. 227pp.

Stach E., Mackowsky M., Teichmüller M., Taylor G.H., Chandra D. and Teichmüller R. 1982). Coal Petrology. Gebrüder, 535 pp.

Steyn, M. and Minnitt, R.C.A. (2010). Thermal Coal Products in South Africa. Journal of the Southern African Institute of Mining and Metallurgy, 110(10), pp.593-599.

Studer, A. (2008). Trace Elements in Miocene Subbituminous Coals from the Swiss Molasse Basin with Special Attention to Uranium and its Mode of Occurrence. Unpublished Master’s Thesis, Swiss Federal Institute of Technology (ETH) Zurich, pp. 12-15.

Sullivan, J.H., (1995). The Geology of the Coal-bearing Rocks of the Karoo Sequence in the Tshikondeni Mine Area, Northern Transvaal. Unpublished MSc Thesis, University of Pretoria, Pretoria. 195 pp.

Swaine, D.J. (1990).Trace Elements in Coal. London, Butterworths, 278 pp.

Taylor, G.H., Teichmuller, M., Davis, A., Diessel, C.F.K., Littke, R. and Robert, p. (1998). Organic Petrology. Gebrüder Bomtraeger. Berlin. 704 pp.

Taylor, S.R. and McLennan, S.M. (1985). The Continental Crust: Its Composition and Evolution. Blackwell Scientific Publications, 312 pp.

Thabo, F.E., Sullivan, J.H. (2000) The Geotechnical Aspects of Tshikondeni coal Mine. J. Afr.Earth Sci. 31 (1A), 78–79.

Thomas, L. (2013). Coal Geology. 2nd ed. West Sussex: Wiley-Blackwell. 444pp.

UNECE (1988). International Coalification System for Medium- and High-Rank Coals. ECE/COAL115. United Nations Economic Commission for Europe, Geneva, 26 pp.

Van Der Walt, B. (2012). The Petrology, Petrography and Geochemistry of Anomalous Borehole Core Sequences: A Case Study of Diatreme Activity. University of Johannesburg, Johannesburg, Unpublished MSc dissertation, 319 pp.

Venmyn Deloitte (2016). Independent Competent Persons Report on Coal of Africa Limited's Greater Soutpansberg Project Prepared for Coal of Africa Limited and Peel Hunt LLP. [online] Venmyn Deloitte. Available at: http://www.coalofafrica.com/our-business/technical-reports [Accessed 27 Nov. 2017]

Walker, S. (2000). Major Coalfields of the World, Coal Research, International Energy Agency, Vienna, 126 pp.

Ward, C. (2016). Analysis, Origin and Significance of Mineral Matter in Coal: An Updated Review. International Journal of Coal Geology, 165, pp. 1 – 27.

Watkeys, M.K. (1984). The Precambrian Geology of the Limpopo Belt North and West of Musina, University of Witwatersrand, Johannesburg, Unpublished, 349 pp.

Wheeler, A.T. (2015). Palaeoenvironmental and Palaeoclimatic Reconstruction of the Witbank Coal Deposits (Karoo Basin South Africa), University of Pretoria, Pretoria, Unpublished MSc dissertation, 96 pp.

White, R. (2015). Changes in Chemical and Physical Properties of South African Caking Coals During Pyrolysis. [ebook] Potchestroom: North West University, pp.40 - 75. Available at: White, R. (2019). Changes in Chemical and Physical Properties of South African Caking Coals During Pyrolysis. [ebook] Potchestroom. Available at: https://dspace.nwu.ac.za/bitstream/handle/10394/15818/White_R_2015.pdf?sequence=1 [Accessed 18 Feb. 2019]. [Accessed 18 Feb. 2019].

Williams, A., Pourkashanian, M., Jones, J.M. and Skorupska, N. (2000). Combustion and Gasification of Coal. Applied energy technology series. USA. 336 pp.

Winter, J.D. (2014). Principles of Igneous and Metamorphic Petrology Second Edition. Pearson Education Limited. 738 pp.

Wood, G.H., Kehn, T.M., Carter, M.D. and Culbertson, W.C.(1983). Coal resource Classification System of the US Geological Survey. US Department of the Interior, Geological Survey. pp.106-118

World Coal Association (2015). Home. [online] Available at: https://www.worldcoal.org/ [Accessed 26 Feb. 2018].

Xie, K. (2015). Structure and Reactivity of Coal. Berlin, Heidelberg: Springer Berlin Heidelberg. 413pp.

Zaccone, C., Plaza, C., Ciavatta, C., Miano, T. and Shotyk, W. (2018). Advances in the Determination of Humification Degree in Peat Since Achard (1786): Applications in Geochemical and Paleoenvironmental Studies. Earth-Science Reviews, 185, pp.163-178.

APPENDICES

Appendix A

Petrographic study of coal

CLIENT:		Sedzani Mukatuni					
PROJECT:		MSc, Soutpansberg					
DATE:		9-Nov-18					
JOB / SAMPLE NUMBERS:							
ANALYST:		Prof NJ Wagner					
ICCP ACCREDITATION:		ICCP/SCAP-056/AB ; ICCP/CBAP/056; DOMVR 056					
Table 1: MACERAL GROUP ANALYSIS (% BY VOLUME)							
THESE RESULTS RELATE ONLY TO THE SAMPLES ANALYSED							
Sample no:		1886		1887		1888	
Sample identification:		Coal 1B		Coal 2A		Coal 3C	
		inc. mm	mmf	inc. mm	mmf	inc. mm	Mmf
MACERAL GROUP	MACERAL (vol%)	vol%	vol%	vol%	vol%	vol%	vol%
Vitrinite	Telinite	9.9	10.9	0.0	0.0	15.3	18.6
	Collotelinite	49.4	54.3	32.8	34.3	40.4	49.1
	vitrodetrinite	0.0	0.0	0.0	0.0	0.0	0.0
	collodetrinite	15.2	16.7	34.3	35.9	11.1	13.5
	corpogelinite	0.0	0.0	0.0	0.0	0.0	0.0
	Gelinite	0.0	0.0	0.0	0.0	0.0	0.0
	pseudovitrinite	0.0	0.0	0.0	0.0	0.0	0.0
Inertinite	Fusinite	6.7	7.3	16.3	17.0	7.1	8.7
	reactive semifusinite	0.0	0.0	0.0	0.0	0.0	0.0
	inert semifusinite	8.3	9.1	11.0	11.5	7.4	9.0

	Micrinite	0.4	0.4	0.0	0.0	0.0	0.0
	Macrinite	0.0	0.0	0.0	0.0	0.0	0.0
	Secretinite	0.8	0.9	0.0	0.0	1.0	1.2
	Funginite	0.2	0.2	0.0	0.0	0.0	0.0
	inertodetrinite R	0.0	0.0	0.0	0.0	0.0	0.0
	inertodetrinite I	0.0	0.0	1.3	1.3	0.0	0.0
Liptinite	Sporinite	0.0	0.0	0.0	0.0	0.0	0.0
	Cutinite	0.0	0.0	0.0	0.0	0.0	0.0
	Resinite	0.0	0.0	0.0	0.0	0.0	0.0
	Alginate	0.0	0.0	0.0	0.0	0.0	0.0
	liptodetrinite	0.0	0.0	0.0	0.0	0.0	0.0
	Suberinite	0.0	0.0	0.0	0.0	0.0	0.0
	exsudatinite	0.0	0.0	0.0	0.0	0.0	0.0
Mineral matter	Clay	6.9		3.8		14.0	
	Quartz	0.2		0.3		0.5	
	Pyrite	2.0		0.5		2.2	
	Carbonate	0.0		0.0		0.2	
	Other	0		0.0		0.7	
SUMMARY TABLE							
MACERAL GROUP	VITRINITE	74.5	82.0	67.0	70.2	66.7	81.1
TOTALS (vol%)	INERTINITE	16.4	18.0	28.5	29.8	15.5	18.9
	LIPTINITE	0.0	0.0	0.0	0.0	0.0	0.0
	MINERAL MATTER	9.1		4.5		17.7	
	TOTAL INERTINITE	16.4	18.0	28.5	29.8	15.5	18.9
	TOTAL REACTIVE	74.5	82.0	67.0	70.2	66.7	81.1

	MACERALS						
TABLE 2: VITRINITE REFLECTANCE ANALYSIS (RoV%)							
Sample no:		1886		1887		1888	
Sample identification:		Coal 1 A		Coal 2B		Coal 3C	
Vitrinite reflectance	Random vitrinite reflectance	0.94		1.00		0.95	
(%RoVmr)	standard deviation	0.047		0.049		0.081	
	# points	99		99		100	
	Range	0.836 - 1.064		0.912 - 1.172		0.738 - 1.118	
	RANK CATEGORY	Med Rank C bituminous		Med Rank B bituminous		Med Rank C bituminous	

Appendix B

Whole rock geochemistry of samples

B.1. Whole rock geochemistry of coal samples

	COAL 1-A	COAL 1-B	COAL 1-C	COAL 2-A	COAL 2-B	COAL 2-C	COAL 3-A	COAL 3-B	COAL 3-C
SiO2 (%)	24.77	36.4	18.8	25.2	16.49	46.65	16.36	18.81	13.96
TiO2(%)	0.895	0.887	0.508	0.907	0.477	1.111	1.363	0.705	0.751
Al2O3(%)	9.89	17.12	7.69	12.65	5.9	22.37	6.64	7.18	4.51
Fe2O3(%)	4.2	5.33	1.93	1.66	4.8	7.93	3.62	3.03	8.72
MnO(%)	0.011	0.12	0.006	0	0.011	0.067	0.002	0.019	0.015
MgO (%)	3.0161	3.5162	2.6154	0	2.6567	1.2803	0.1356	4.668	0.3211
CaO (%)	4.96	6.22	3.48	0.32	4.43	1.38	0.89	10.39	1.13
Na2O (%)	0.882	0.593	2.156	0.803	1.533	0.411	1.755	3.738	1.632
K2O(%)	0.33	0.36	0.25	0.23	0.32	0.58	0.19	0.13	0.39
P2O5 (%)	0.188	0.28	0.109	0.179	0.123	0.257	0.317	0.393	0.099
Sc (PPM)	0.4	0.4	0.3	0	0.6	0.1	0.1	1	0.1
V (PPM)	213.2	206.5	162.6	206.9	200.8	257.8	315	175.8	282.3
Cr (PPM)	102.6	120.8	68.1	45.3	91.1	108	98.9	62.1	212

Co (PPM)	9.9	11.7	5.4	4	12.4	18.8	8.6	7	25.3
Ni (PPM)	202.3	559	558.5	216.5	310.8	305	198.4	251.6	196.6
Cu (PPM)	93.4	77.2	63	101.9	74.8	86.5	231.4	129.1	176.7
Zn (PPM)	248.3	588.8	557.5	59.4	746.5	725	57.5	199.6	84.4
Ga (PPM)	93.9	130.5	135.5	42.6	64.8	46.9	137.3	147.4	95.4
Ge (PPM)	7.6	4.6	6.3	1.7	3.6	3.1	4.6	4.2	2.6
As (PPM)	13.5	8	7.7	9.4	16.6	21.4	15.9	12.3	15.9
Rb (PPM)	31.9	23.2	66.8	35.8	34.5	34.3	52.5	53.1	25.3
Sr (PPM)	678.2	264.6	466.6	550.4	822.6	455.5	870.2	1424.7	191.6
Y (PPM)	95.4	69	99.7	38.2	100.9	71.6	42.7	48.5	43.6
Zr (PPM)	314.1	133.5	193.4	296.2	347.6	386.7	387.3	394.2	282.2
Nb (PPM)	18.9	7.8	9.6	14.3	20	16.1	22.6	14.2	15
Mo (PPM)	0.9	0.5	0.8	0.9	0.2	1	3.5	0.9	1
Ag (PPM)	1.7	1.2	1.1	2.3	0.6	0.2	1.1	0.9	0.7
Cd (PPM)	0.1	0.1	0.1	0.1	0.1	0.1	0.1	0.1	0.1
Sn (PPM)	3.8	3.5	3.4	3.7	2.7	3	3.2	3.3	3.8
Sb	0.2	0	0	0	0.4	0.4	0	0	0.6

(PPM)									
Cs (PPM)	5.4	5.4	5.4	5.4	5.4	5.4	5.4	5.4	5.4
Ba (PPM)	726	414.3	437.5	734.8	719.7	556.4	1075.5	584.5	618.9
La (PPM)	55.8	54.1	23.1	29.1	69.8	98.7	61.2	38.8	95.3
W (PPM)	10.9	37.2	31.3	0	19	1.2	7.4	0	0
Ta (PPM)	1.3	1.2	1	1.4	1.1	1.3	2.8	1.7	2.2
Hf (PPM)	0	5.5	0	16.1	10	8.8	25.3	14.2	27.7
Tl (PPM)	2.7	5.8	5.8	0	2.8	1.9	5.7	6.8	4.2
Pb (PPM)	128	74.1	71.6	87.7	154.4	199.6	147.9	114.9	147.8
Bi (PPM)	0.4	0.4	0.4	0.5	0.4	0.5	0.6	0.5	0.4
Ce (PPM)	139.1	124.7	323	171	404	162.7	646.6	350.8	165
Sm (PPM)	0	0	0	0	0	2.7	0	0	0
Eu (PPM)	0.1	0.1	0.1	0	1.2	0.7	0	0.2	0.2
Gd (PPM)	6.9	7.9	0.6	0	15.9	21.7	3	5.4	20.4
Tb (PPM)	1.3	1.5	0.6	0.5	1.6	2.4	1.1	0.9	3.5
Dy (PPM)	13.3	15.3	6.1	5.3	17	25.2	11.5	9.6	27.7
Er (PPM)	2.2	2.5	1.1	0.9	2.8	4.1	1.9	1.6	21

Yb (PPM)	76.3	201.5	197.5	77.8	115.7	117.2	74.1	91.9	80.5
Th (PPM)	9.3	0	7.7	12	14.3	15.1	10.4	10.1	18.7
U (PPM)	11.9	2.9	6	8.9	6	7.6	12.3	33.3	2.6
S (PPM)	1628.1	2973.5	2543.5	2169.5	744.5	519.3	2983.2	1847.2	3892.7

B.2. Whole rock geochemistry of host rock

Sample	T_AS_2	T_BS_{10}	T_BS_{12}	T_CS_3	T_CS_6	T_ES_5	T_ES_{11}	T_BS_6	T_CS_2	T_HS_3	T_GS_{11}
SiO2	59.33	60.88	9.75	65.51	70.73	76.18	45.54	58.20	39.18	84.06	81.74
TiO2	0.79	1.94	0.05	0.58	0.11	0.09	1.47	1.19	0.54	0.01	0.32
Al2O3	15.49	15.84	<0.01	24.17	4.39	2.13	44.09	8.66	7.51	0.39	9.42
Fe2O3	7.66	14.29	0.30	7.26	1.05	0.62	0.23	7.89	41.88	0.73	3.31
MnO	0.10	0.12	0.02	0.02	0.01	0.02	0.01	0.11	0.28	0.01	0.05
MgO	4.05	2.75	22.42	0.13	0.90	0.17	0.02	2.34	0.05	0.38	0.23
CaO	3.57	1.35	49.02	0.06	0.07	0.03	0.10	16.50	0.13	<0.01	4.70
Na2O	1.46	<0.01	13.61	<0.01	<0.01	<0.01	<0.01	1.77	<0.01	<0.01	2.73
K2O	5.26	5.14	0.15	0.68	1.23	0.32	0.29	0.02	0.21	0.04	0.04
P2O5	0.12	0.45	0.77	0.03	0.05	0.07	0.06	0.34	0.05	0.07	0.11

Sample	A2	E11	B10	B12	C2	H3	C3	C6	E5	G11	B6
Ag	0.2	0.2	0.4	0.5	0.9	1	0.5	0.2	0.2	0.8	0.4
As	<4	<4	<4	<4	<4	<4	13.2	<4	<4	<4	4.1
Ba	650.1	1506.2	97.5	492.5	137.8	102.8	1157.5	945.2	457.4	65.8	294.5
Bi	<3	<3	<3	<3	<3	<3	<3	<3	<3	<3	<3
Ce	150.6	269	10.9	37.9	692.9	51.5	692.9	85.1	326.3	139.2	<10
Co	19.6	31.6	<1	17.7	2.6	1.5	<1	18.2	88.6	1.6	8
Cr	52.9	76.3	8.5	59.2	2.2	9.3	101.1	27.2	284.8	6.6	22.3
Cs	5.4	5.4	5.4	5.4	5.4	5.4	9.7	5.4	67.4	5.4	5.4
Cu	<2	126.9	5.8	18.3	8.4	13.7	52.5	147.5	<2	21.8	22.1
Dy	24.4	45.4	1	23.1	0.7	12.4	0.7	25.1	133.1	9.4	10.5
Er	4.3	7	0.2	3.9	0.1	2.3	0.1	4	19.7	1.7	1.8
Eu	1	1.2	0.2	0.2	0	0.4	0	1.1	2.9	0.3	0.5
Ga	17.5	17.1	2.3	16.3	4.4	3	79.7	17.4	5	<1	14.3
Gd	22.8	51.4	0	19.1	0.3	9.5	0.3	23.8	162.1	7.6	8.6
Ge	1.2	1.2	1.2	1.4	1.2	1.3	1.7	1.3	1.2	1.2	1.4
Hf	<3	20.9	<3	3.2	20.7	6.2	20.7	20.6	<3	5.7	3.4
La	89.8	185.6	<10	82.8	10.3	<10	27.3	97.1	477.2	<10	39.2
Mo	2	<2	<2	4.4	<2	<2	<2	<2	<2	<2	<2
Nb	6.6	18.1	<1	6.9	2.9	1.5	36.6	4.4	3.4	<1	3.3
Ni	115.7	23.8	75.9	<1	13	11.4	92.5	2.4	<1	11.6	12.1
Pb	17.2	19.9	5.6	29.5	123.2	13.6	123.2	6.8	21.4	19	38.3
Rb	125.7	90.2	<2	22.7	37.1	10.3	27.8	4.9	58.6	2.4	3.2
S	6.5	0	137.5	13.3	37.9	0	37.9	31.1	47.9	0	15.9
Sc	<3	<3	4.4	<3	<3	<3	<3	<3	<3	<3	<3
Sm	<10	55.4	<10	<10	<10	<10	<10	<10	230.8	<10	<10
Sn	2.3	2.1	2.3	2.4	2.9	2.6	3.5	1.9	0.9	3.2	2.8
Sr	64.9	26.3	466.8	25.1	24.2	8.3	312.6	643.3	19.6	<4	405.3
Ta	<2	<2	<2	<2	<2	<2	<2	<2	<2	<2	<2
Tb	2.6	4.1	0.1	2.4	0.1	1.4	0.1	2.4	12.2	1	1.1
Th	6.4	15.8	<3	22.2	31	<3	31	4.1	35.3	6.2	4.4
Tl	<3	<3	<3	<3	4.7	<3	4.7	4.7	<3	<3	<3
U	<2	6.1	<2	<2	5.6	<2	5.6	5	59.8	<2	<2
V	202.5	395.6	15.7	130.1	27.7	11.9	336.8	284	164.2	<1	70.5
W	<3	<3	<3	<3	<3	<3	<3	<3	<3	<3	<3
Y	34.1	56.7	14.2	7.4	19.1	5.5	32.2	14.8	3	<1	8.9
Yb	50.8	27.9	26.9	8.8	32.6	17.6	32.6	11.6	19.7	<3	8.8
Zn	124.8	136	33.1	28.7	12.1	5.2	15.4	37.1	94.6	<2	11.9
Zr	157.4	329.9	79	340.3	108	89.2	679.7	168.5	116.5	6.5	156.4

Appendix C

Geological field mapping field data

Sample	Latitude	Longitude	Elevation (m)	Surrounding Environment	Mineral Composition	Colour and Texture	Strike Direction	Dip Direction	Rock Name
A1	22° 30' 45.73"S	30° 48' 06.80"E	390	Light red soil, poor vegetation and interbedding sandstone.	Clay minerals and Feldspars	Dark brown soil. Very fine texture.	188° SE	N 78° E	Mudstone
A2	22° 30' 46.05"S	30° 48' 06.10"E	391	Brown soil, poor vegetation and very competent outcrop.	Clay minerals and Feldspars	Brown soil. Very fine texture.	95° NE	N 83° E	Mudstone
A3	22° 30' 49.5"S	30° 48' 05.80"E	392	Dark brown soil, poor vegetation and competent outcrop.	Mafic minerals, Feldspars	Dark green.			Dolerite
A4	22° 30' 51.9"S	30° 48' 07.80"E	393	Dark greenish boulders around and competent outcrop.	Quartz and mica	Brown with, fine Interlocked grans.	75° NE	N 23° W	Quartzite
A5	22° 30' 55.2	30° 48' 07.7	386	Floats of Quartz, competent outcrop with	Quartz, Mafic minerals,	Dark green.			Dolerite

	"S	0"E		Quartz vein.	Feldspars				
A 6	22° 30' 57.8 "S	30° 48' 08.7 0"E	390	Brownish soil poor vegetation and competent Quartz vein outcrop.	Quartz, Feldspars and Mica	Brown, Fine texture.			Qu artz vein
A 7	22° 31' 01.6 0"S	30° 48' 08.4 0"E	380	Light brown soil, Sandstone floats and competent outcrop.	Quartz and Feldspars	Brown. Fine texture.	89° NE	S 22° E	Qu artz ite
A 8	22° 31' 19.4 0"S	30° 48' 07" E	406	Light brown soil, dispersed vegetation and distinct outcrop	Quartz and Feldspars	Brown, course grained.	41° NE	S 62° E	San dst one
A 9	22° 31' 13" S	30° 48' 07" E	396	Quartzite floats, dispersed vegetation and competent outcrop.	Quartz and mica	Brown with, fine Interlocke d grans.	45° NE	N 22° W	Qu artz ite
B 1	22° 30' 46.0 8"S	30° 48' 01.0 7"E	395	Dark brown soil, poor vegetation and distinct outcrop.	Quartz and Feldspars	Brown and coarse texture.	95° SE	N 15° E	San dst one
B 2	22° 30' 47.4	30° 48' 01.2	394	Quartzite floats, brownish soil and distinct outcrop.	Quartz and Feldspars	Brown and visible Course	118 ° SE	N 61° E	San dst one

	0"S	0"E				grains.			
B 3	22° 30' 48.10"S	30° 48' 0.70"E	390	Reddish soil, poor vegetation and distinct outcrop.	Clay minerals and Feldspars	Dark brown. Very fine texture.	92° SE	N 49° E	Mudstone
B 4	22° 30' 48.40"S	30° 47' 58"E	372	Reddish sandy soil, interbedding mudstone, distinct outcrop.	Quartz and Feldspars	Brown and medium texture.	91° SE	S 46° W	Sandstone
B 5	22° 30' 50"S	30° 47' 57.6"E	390	Dark reddish soil, dense vegetation igneous outcrop.	Mafic minerals, Feldspars	Dark green.			Dolerite
B 6	22° 30' 51"S	30° 47' 58"E	385	Floats of Quartz and outcrop with interlocked grains.	Quartz and Feldspars	Brown with fine texture.	106° SE	S 63° W	Quartzite
B 7	22° 30' 56"S	30° 47' 57"E	383	Floats of Quartz, brownish soil and competent outcrop with vein.	Quartz, Mafic minerals, Feldspars	Dark green.			Dolerite
B 8	22° 30' 58"S	30° 47' 55"E	385	Dark reddish soil, dense vegetation and igneous outcrop.	Mafic, greenish minerals.	Green with fine texture.			Dolerite

B 9	22° 31' 03.70"S	30° 47' 53.70"E	390	Almost entirely Quartz floats and Quartzite outcrop.	Quartz and Feldspars	Brown with fine texture.	120° SE	N 44° E	Quartzite
B 10	22° 31' 04.10"S	30° 47' 53.60"E	387	White carbonaceous floats around distinct calcrete outcrop.	Carbonate and Quartz	White and fine texture.			Calcrete
B 11	22° 31' 07"S	30° 47' 54"E	381	Iron rich floats, dispersed vegetation around the outcrop.	Iron	Reddish with very fine grains.	82° NE	N 71° W	Ironstone
B 12	22° 31' 08.30"S	30° 47' 55"E	377	Dispersed vegetation and highly weathered outcrop.	Quartz and Feldspars	Brown, fine visible grains.	78° NE	S 44° E	Sandstone
B 13	22° 31' 11"S	30° 47' 56"E	371	Light brown sandy soil, lamination and outcrop near the stream.	Quartz and Feldspars	Brown, course grained.	104° SE	N 31° E	Sandstone
B 14	22° 31' 15.10"S	30° 47' 57"E	390	Quartzite floats, dispersed vegetation and competent outcrop.	Quartz, Feldspars and Mica	Interlocked grans.	182° SE	N 78° E	Quartzite

B 1 5	22° 31' 23" S	30° 47' 58" E	404	Dark brown soil, Quartzite and Iron rich floats.	Quartz and Iron	Dark red with very fine grains.	76° NE	N 46° W	Iron stone
B 1 6	22° 31' 18.20"S	30° 47' 59" E	400	Brown soil, dispersed vegetation outcrop with visible grains.	Quartz and Feldspars	Brown and visible Course grains.	165° SE	N 37° E	Sandstone
C 1	22° 31' 13.40"S	30° 47' 45.50"E	398	Quartzite floats dispersed vegetation and competent outcrop.	Quartz and Feldspars	Brown with Interlocked grans.	71° NE	N 45° W	Quartzite
C 2	22° 31' 10.60"S	30° 47' 45.90"E	396	Light brown soil, poor vegetation and outcrop with lamination.	Quartz and Feldspars	Brown and visible Course grains.	102° SE	N 51° E	Sandstone
C 3	22° 31' 09.10"S	30° 47' 46.80"E	395	Brown soil, fissility and less competent outcrop.	Clay minerals	Black and fine texture.	53° NE	S 18° E	Shale
C 4	22° 31' 01.90"S	30° 47' 50.10"E	394	Reddish soil, Iron rich floats and distinct outcrop.	Iron	Red and very fine texture.	102° SE	N 17° E	Iron stone

C 5	22° 31' 01.10"S	30° 47' 50.60"E	396	Dark brown soil, highly weathered igneous localised outcrop.	Mafic minerals, Feldspars	Dark green.			Dolerite
C 6	22° 30' 55.50"S	30° 47' 48.60"E	388	Reddish soil, dense vegetation with quartz vein on the outcrop.	Quartz, Mafic minerals, Feldspars	Dark green.			Dolerite
C 7	22° 30' 51.10"S	30° 47' 51.30"E	391	Soil is slightly red, Quartzite floats, igneous boulders around outcrop.	Quartz, Mafic minerals, Feldspars	Greenish, fine texture.			Dolerite
C 8	22° 30' 44.10"S	30° 47' 46.60"E	405	Reddish soil, Iron rich floats and dispersed vegetation near outcrop.	Iron	Red. Fine texture.	96° NE	S 42° E	Ironstone
C 9	22° 30' 42.50"S	30° 47' 47.30"E	410	Brown soil, dispersed vegetation and sandstone floats near outcrop.	Quartz and Feldspars	Brown and coarse texture.	81° NE	S 58° E	Sandstone
C 10	22° 30' 45.10"S	30° 47' 46.90"E	398	Brown soil, sandstone floats and distinct outcrop.	Quartz and Feldspars	Brown and coarse texture.	97° NE	S 12° E	Sandstone

D 1	22° 31' 00.30"S	30° 47' 43.70"E	378	Reddish soil, dispersed vegetation and highly weathered outcrop.	Quartz, Feldspars and Mica	Interlocked grains with fine texture.	107° SE	N 15° E	Quartzite
D 2	22° 31' 00.90"S	30° 47' 42.80"E	397	Brown soil and competent outcrop with quartz vein.	Quartz, Feldspars and Mica	Brown, Fine texture.			Quartz vein
D 3	22° 31' 22"S	30° 47' 43.20"E	396	Dispersed vegetation with sandstone floats around outcrop.	Quartz and Feldspars	Brown with Coarse texture.	83° NE	S 54° E	Sandstone
D 4	22° 30' 38.30"S	30° 47' 38.10"E	398	Light brown soil, poor vegetation and outcrop with lamination.	Quartz and Feldspars	Brown with Coarse texture.	305° NW	S 64° W	Sandstone
D 5	22° 30' 42.90"S	30° 47' 42"E	414	Dark brown, dispersed vegetation and distinct outcrop.	Clay minerals and Feldspars	Dark brown. Fine texture.	41° NE	S 62° E	Mudstone
D 6	22° 30' 48"S	30° 47' 42"E	398	Light brown, Quartzite float and competent outcrop.	Quartz, Feldspars and Mica	Brown. Fine texture.	103° SE	S 23° W	Quartzite
D	22°	30°	404	Light reddish soil,	Mafic,	Dark			Dol

7	30' 51.10"S	47' 41" E		dense vegetation and igneous outcrop.	greenish minerals, Feldspars	green.			erite
D 8	22° 30' 52.80"S	30° 47' 42" E	403	Dark brown, dispersed vegetation and competent outcrop.	Clay minerals and Feldspars	Dark brown. Very fine texture.	133° SE	N 81° E	Mudstone
D 9	22° 30' 55.50"S	30° 47' 44.60"E	394	Quartz float, dispersed vegetation and competent outcrop.	Quartz	White, Interlocked grains. Fine texture.			Quartz vein
E 1	22° 31' 25.90"S	30° 47' 34.40"E	407	Brown soil, dispersed vegetation and lamination.	Quartz and Feldspars	Brown. Coarse texture.	78° NE	S 24° E	Sandstone
E 2	22° 31' 13.80"S	30° 47' 33.70"E	392	Dark brown soil, highly eroded and weathered outcrop.	Clay minerals, Felspars	Dark brown. Very fine texture	78° NE	S 54° E	Mudstone
E 3	22° 31' 11" S	30° 47' 32.60"E	389	Brown soil, fissility and less competent outcrop.	Clay minerals	Black and very fine texture.	117° SE	N 36° E	Shale
E	22° 30'	30° 47'	390	Reddish soil, dense vegetation	Mafic, greenish	Green with fine			Dolerit

4	58.70"S	35.40"E		localised igneous outcrop.	minerals.	texture.			e
E5	22° 30' 55.80"S	30° 47' 34.30"E	400	Reddish soil, dense vegetation, Iron rich floats.	Iron	Red. Very fine texture.	92° NE	S 41° E	Iron stone
E6	22° 30' 53.50"S	30° 47' 34.50"E	405	Sandstone floats, poor vegetation and distinct outcrop.	Quartz and Feldspars	Dark brown. Coarse texture	78° NE	S 44° E	Sandstone
E7	22° 30' 52.50"S	30° 47' 34.40"E	406	Brown soil, dispersed vegetation and outcrop with vein	Quartz and Feldspars	Light brown. Fine, Interlocked grains.	75° NE	N 23° W	Quartzite
E8	22° 30' 47.50"S	30° 47' 33.70"E	408	Dark brown soil, interbedding with reddish layers.	Quartz, Iron and Feldspars	Dark brown. Coarse texture.	54° NE	N 41° W	Sandstone
E9	22° 30' 44.50"S	30° 47' 32"E	397	Brown soil, poor vegetation and competent outcrop.	Clay minerals and Feldspars	Dark brown soil. Very fine texture.	106° SE	N 47° E	Mudstone
E1	22° 30' 42.5	30° 47' 30.7	397	Brown soil, dispersed vegetation and	Quartz and	Light brown. Fine,	54° NE	N 41°	Quartz

0	0"S	0"E		very competent outcrop	Feldspars	Interlocked grains.		W	ite
E11	22° 30' 41.60"S	30° 47' 30.90"E	395	Brown soil, poor vegetation and competent outcrop.	Clay minerals and Feldspars	Dark brown soil. Very fine texture.	112° SE	N 48° E	Mudstone
E12	22° 30' 38.40"S	30° 47' 30.30"E	391	Sandstone floats, poor vegetation and distinct outcrop.	Quartz and Feldspars	Dark brown. Coarse texture	72° NE	S 40° E	Sandstone
F1	22° 30' 37.70"S	30° 47' 28" E	390	Light brown soil, poor vegetation and outcrop with lamination.	Quartz and Feldspars	Brown and visible Course grains.	67° NE	N 71° W	Sandstone
F2	22° 30' 43.60"S	30° 47' 27.10"E	397	Dark brown, dispersed vegetation and competent outcrop.	Clay minerals, Felspars	Dark brown. Very fine texture	102° SE	N 82° E	Mudstone
F3	22° 30' 47.80"S	30° 47' 26.40"E	406	Brown soil, mudstone and sandstone floats, lamination.	Quartz and Feldspars	Brown and visible Course grains.	128° SE	N 34° E	Sandstone

F 4	22° 30' 57.40"S	30° 47' 25.70"E	391	Poor vegetation interbedding of sandstone and mudstone.	Quartz and Feldspars	Brown and medium texture.	94° NE	S 42° E	Sandstone
F 5	22° 30' 59.50"S	30° 47' 25.80"E	389	Floats with clay sized particles, very competent outcrop.	Clay minerals	Brown. Very fine texture	106° SE	N 88° E	Mudstone
F 6	22° 31' 12.60"S	30° 47' 25.90"E	388	Brown soil, fissility and less competent outcrop.	Clay minerals and dark minerals	Black and very fine texture.	54° NE	N 21° W	Shale
H 1	22° 31' 21.20"S	30° 48' 16.80"E	424	Light brown soil, dispersed vegetation and distinct outcrop	Quartz and Feldspars	Brown, course grained.	41° NE	S 62° E	Sandstone
H 2	22° 31' 15.10"S	30° 48' 14.30"E	403	Quartzite floats, dispersed vegetation and competent outcrop.	Quartz and mica	Brown with, fine Interlocked grans.	75° NE	N 23° W	Quartzite
H 3	22° 31' 02.10"S	30° 48' 15.30"E	392	Brown soil, highly eroded and weathered outcrop.	Quartz and Feldspars	Brown, course grained.	45° NE	N 22° W	Sandstone
H	22°	30°	378	Brown soil,	Clay	Black and	118	N	Sha

4	31' 01.70"S	48' 07.80"E		fissility and less competent outcrop.	minerals and dark minerals	very fine texture.	° SE	34° E	le
H 5	22° 30' 58.80"S	30° 48' 08.70"E	390	Quartz float, dispersed vegetation and competent outcrop.	Quartz	White, Interlocked grains. Fine texture.			Quartz Rock
H 6	22° 30' 56.10"S	30° 48' 16.90"E	380	Soil is slightly red, Quartzite floats, igneous boulders around outcrop.	Quartz, Mafic minerals, Feldspars	Dark green.			Dolerite
H 7	22° 30' 54.10"S	30° 48' 17.70"E	390	Reddish soil, dense vegetation with quartz vein on the outcrop.	Quartz, Mafic minerals, Feldspars	Greenish, fine texture.			Dolerite
H 8	22° 30' 44.70"S	30° 48' 13"E	403	Floats with clay sized particles, interbedding Sandstone.	Clay minerals and Feldspars	Brown. Very fine texture	72° NE	N 38° W	Mudstone
H 9	22° 30' 43.30"S	30° 48' 12"E	408	Dark brown, dispersed vegetation and competent outcrop.	Clay minerals and Feldspars	Brown. Very fine texture	76° NE	N 42° W	Mudstone
H 1	22° 30'	30° 48'	414	Quartzite floats and competent	Quartz and	Brown with	104 °	N 24°	Quartz

0	41.90"S	11.30"E		outcrop with Quartz vein.	Feldspars	Interlocked grans.	SE	E	ite
H11	22° 30' 39.40"S	30° 48' 09" E	413	Dark brown, dispersed vegetation and competent outcrop.	Clay minerals, Felspars	Dark brown. Very fine texture	104° SE	N 18° E	Mudstone
H12	22° 30' 37.60"S	30° 48' 08.30"E	414	Quartzite floats dispersed vegetation and competent outcrop.	Quartz and Feldspars	Brown with Interlocked grans.	74° NE	S 42° E	Quartzite
H13	22° 30' 37.20"S	30° 48' 05.60"E	415	Floats with clay sized particles, interbedding Sandstone.	Clay minerals and Feldspars	Brown. Very fine texture	68° NE	N 72° W	Mudstone
H14	22° 30' 31.60"S	30° 48' 05.40"E	412	Brown soil, dispersed vegetation and lamination.	Quartz and Feldspars	Brown. Coarse texture.	78° NE	S 24° E	Sandstone
H15	22° 30' 27.80"S	30° 48' 07.40"E	410	Sandstone floats, poor vegetation and distinct outcrop.	Quartz and Feldspars	Dark brown. Coarse texture	165° SE	N 37° E	Sandstone
H1	22° 30' 31.1	30° 48' 10.9	409	Quartzite and Sandstone floats, poor vegetation,	Quartz and	Dark brown. Coarse	104°	N 31°	Sandst

6	0 "S	0 "E		distinct outcrop.	Feldspars	texture	SE	E	one
H17	22° 30' 18.50 "S	30° 48' 10.10 "E	405	Brown soil, very competent outcrop with Quartz vein.	Quartz and Feldspars	Brown with Interlocked grans.	259° SW	S 51° E	Quartzite
H18	22° 30' 18.40 "S	30° 48' 10.10 "E	403	Brown soil, Quartzite floats and outcrop with Quartz vein.	Quartz and Feldspars	Brown with fine texture.	110° SE	N 22° E	Quartzite
H19	22° 30' 15.80 "S	30° 48' 10 " E	400	Light brown soil, poor vegetation and competent outcrop.	Quartz and Feldspars	Brown. Fine texture.	76° NE	N 24° W	Quartzite
H20	22° 30' 10.30 "S	30° 48' 10.50 "E	393	Floats with clay sized particles, very competent outcrop.	Clay minerals	Brown. Very fine texture	249° SW	N 42° E	Mudstone
I1	22° 30' 25.70 "S	30° 47' 50.30 "E	388	Light brown, Quartzite float and competent outcrop.	Quartz, Feldspars and Mica	Brown. Fine texture.	270° SW	S 27° W	Quartzite
I2	22° 30' 29.30 "S	30° 47' 45.40 "E	400	Dark brown, dispersed vegetation and competent outcrop.	Clay minerals, Felspars	Dark brown. Very fine texture	188° SE	N 78° E	Mudstone

I3	22° 30' 29.90"S	30° 47' 43.90"E	402	Sandstone floats, poor vegetation and distinct outcrop.	Quartz and Feldspars	Brown. Coarse texture	78° NE	S 52° E	Sandstone
I4	22° 30' 33.30"S	30° 47' 43.20"E	405	Quartzite floats dispersed vegetation and competent outcrop.	Quartz and Feldspars	Brown with fine texture.	78° NE	S 44° E	Quartzite
I5	22° 30' 34.20"S	30° 47' 43.90"E	399	Clay size particles floats, competent outcrop with lamination.	Clay minerals, Feldspars	Brown. Very fine texture	78° NE	S 54° E	Mudstone
J1	22° 30' 43.20"S	30° 47' 27.70"E	396	Dark brown, dispersed vegetation and competent outcrop.	Clay minerals, Felspars	Dark brown. Very fine texture	54° NE	S 21° E	Mudstone
J2	22° 30' 41.20"S	30° 47' 27.10"E	393	Floats with clay sized particles, very competent outcrop.	Clay minerals	Brown. Very fine texture	82° NE	S 71° E	Mudstone
J3	22° 30' 31.50"S	30° 47' 24.40"E	391	Brown soil, dispersed vegetation and very competent	Quartz and Feldspars	Light brown. Fine, Interlocke	108° SE	N 18° E	Quartzite

				outcrop		d grains.			
J4	22° 30' 18.10"S	30° 47' 22.20"E	388	Light brown soil, dispersed vegetation and distinct outcrop	Quartz and Feldspars	Brown, course grained texture.	78° NE	S 44° E	Sandstone
J5	22° 30' 11.70"S	30° 47' 43.10"E	376	Brown soil, dispersed vegetation and distinct outcrop	Quartz and Feldspars	Brown, course grained.	41° NE	S 62° E	Sandstone